AUTOLOGOUS BONE MARROW-DERIVED MESENCHYMAL STEM CELL TRANSPLANTATION AS A THERAPY FOR NEURONAL CEROID LIPOFUSCINOSIS

A Dissertation presented to
the Faculty of the Graduate School
University of Missouri, Columbia

In partial fulfillment
of the requirements for the degree

Doctor of Philosophy

---

by

DOUGLAS N. SANDERS

Dr. Martin L. Katz Dissertation Supervisor

AUGUST 2007

The undersigned, appointed by the dean of the Graduate School, have examined the Dissertation entitled:

AUTOLOGOUS BONE MARROW-DERIVED MESENCHYMAL STEM CELL TRANSPLANTATION AS A THERAPY FOR NEURONAL CEROID LIPOFUSCINOSIS

presented by Douglas N. Sanders,

a candidate for the degree of Doctor of Philosophy

and hereby certify that, in their opinion, it is worthy of acceptance.

Dr. Martin L. Katz

_____

Dr. Gary S. Johnson

_____

Dr. Mark D. Kirk

_____

Dr. Joel Maruniak

_____

Dr. Bimal K. Ray

_____

“...I can't do this all on my own.
No. I know, I'm no Superman.
I'm no Superman.”

Thanks Ang!

ACKNOWLEDGEMENTS

I would like to take this opportunity to thank Dr. Katz for giving me the chance to learn from him and contribute to the interesting and important work in his laboratory. I would also like to thank the members of my committee, especially Dr. Johnson and Dr. Kirk who provided constructive criticism and helpful advice in the areas of their expertise as they pertained to this research. The members of Dr. Kirk's laboratory (Chris Pierret, Jason Morrison, Kathleen Spears and Prakash Rath) have also been invaluable collaborators in this work, who generously donated both their time and expertise to make these experiments happen. Finally, the staff of the University of Missouri Cytology and Cell & Immunology core facilities have been instrumental in performing many of these experiments. I would especially like to recognize Joyce Carafa at the CIC facility for her assistance with all manner of FACS-related experiments, which were central to the completion of this work. Thank you all for helping me to get to this point.

AUTOLOGOUS BONE MARROW-DERIVED MESENCHYMAL STEM CELL TRANSPLANTATION AS A THERAPY FOR NEURONAL CEROID LIPOFUSCINOSIS

Douglas N. Sanders
Dr. Martin L. Katz Dissertation Supervisor

ABSTRACT

The Neuronal Ceroid Lipofuscinoses (NCLs) are a group of rare genetic diseases characterized by neurodegeneration and accumulation of autofluorescent lysosomal storage bodies in certain cells. There is currently no effective clinical treatment for the NCLs, though research indicates that stem cell transplant may be efficacious. The bone marrow stroma is composed of a heterogeneous population of cells including endothelial cells, fibroblasts, adipocytes, osteocytes and two types of multipotent adult stem cells. Mesenchymal stem cells (MSCs) are stroma-derived adult stem cells which are known to give rise to cells of mesodermal origin including bone, cartilage, fat, tendon, muscle and possibly germ cells. MSCs may also be capable of differentiating into cells of a non-mesodermal origin, including neural cells. We have isolated a population of untransformed, self-renewing, multipotent, stroma-derived cells from both murine and canine bone marrow. These cells express protein markers associated with MSCs, grows quickly in culture, with a doubling time of 24-36 hours, and murine cells have been expanded in culture for more than 150 population doublings without evidence of senescence or loss of differentiation potential. Upon differentiation, these MSCs express appropriate protein and RNA markers and display histochemical features consistent with terminally differentiated cells.

Using a suicide gene knockout model, we demonstrate genetic modification of our MSC isolate through small fragment homologous replacement (SFHR) as a precursor to repairing NCL-specific genes in autologous cells. Intraocular injection of eGFP expressing murine MSCs into the eye of a murine model of human infantile NCL (INCL) show that transplanted MSCs are capable of surviving in the eye of an allogeneic host for up to 5 weeks. Withing 2 weeks after injection, cells were observed to form close associations with the retinal tissue and at 5 weeks, MSCs had integrated into host tissue with no obvious signs of immune rejection. We also report that MSCs transplanted onto brain slices cultured from NCL-affected mice are able to reduce the amount of autofluorescent storage material in surrounding cells through enzymatic cross-

correction. Isolation of canine MSCs and characterization of several models of canine NCL lay the foundation for similar experiments in canine models.

Our characterization of these cells indicates they may be ideal candidates for studying autologous adult stem cell transplants as a therapy in patients with neurodegenerative disease. Further experiments in animal model systems will help to determine the most effective method of implantation, the potential for cellular replacement and survival time of donor cells after transplant. Because of their multipotent phenotype, ease of isolation and growth in culture, ready ability to engraft in a multitude of tissues and susceptibility to genetic manipulation, autologous MSCs offer many advantages over other potential therapies as a treatment for NCLs. Development of a standardized approach to using autologous MSC transplant as a therapy could lead to vast improvements in clinical outcome not just for NCLs but for numerous other diseases including common ailments such as heart disease, stroke, diabetes and Parkinson's as well as other rare inherited genetic disorders.

LIST OF FIGURES

TABLE OF CONTENTS

Chapter I

Introduction

1. The Neuronal Ceroid Lipofuscinoses

The neuronal ceroid lipofuscinoses (NCLs) are a group of autosomal-recessive, inherited diseases characterized by neurodegeneration and the accumulation of yellow-emitting autofluorescent lysosomal storage material (i.e. – ceroid lipofuscin) in the retina, brain, liver and other tissues. [1] Several forms of the disease exist and are classified by age of onset, which can range from early infancy to late adolescence, by rate of disease progression, and by the specific pattern of symptoms. Diagnosis of the disease is based on clinical symptoms, the presence of autofluorescent storage material in biopsied tissues and, when possible, genetic testing of the known *CLN* genes for defective alleles. [2][3] Clinical symptoms associated with the disease include blindness, seizures, ataxia, dementia, coma and ultimately death.

Ten forms of NCL have been described in humans, 8 of which are associated with a known gene or genes. The *CLN1* form is designated as infantile, with an age of onset between birth and 2 years of age. Four other forms, CLN2, 5, 6 and 7 are designated as late-infantile, with an age of onset between 2 and 7 years. Specific genes have been linked to the CLN2, 5 and 6 forms. The CLN7 grouping has recently been found to be heterogeneous, including patients with mutations in the *CLN6*, *CLN8*, and *MFSD8* genes. [179] Mutations in the *Cathepsin D*, *CLN3* and *CLN8* genes cause the juvenile form, with an age of onset between 4 and 10 years. [180] Another form of juvenile onset NCL, CLN9, does not yet have an associated gene, though functional assays indicate it may be a regulator of dihydroceramide synthase. [181] The CLN4 form is associated with onset at the late juvenile to adult stages, between 11 and 50 years. No gene has yet been associated with this form of NCL either. Of the 8 known gene products, 7 have been characterized to some extent. Cathepsin D, CLN1 and CLN2 are known to be soluble lysosomal enzymes. Cathepsin D is a ubiquitiously expressed lysosomal protease involved in proteolytic degradation, cell invasion and apoptosis. [180] CLN1 possesses a palymitoyl protein

thioesterase activity and is predicted to play a role in degredation of membrane-associated proteins. CLN2 has been shown to possess tripeptidyl peptidase activity which is pepstatin insensitive. [132] CLN3, CLN5 and MFSD8 are lysosomal integral membrane proteins. Sequence analysis of the MFSD8 protein indicates that it may belong to the major facilitator superfamily of transporter proteins, but no definite enzymatic activity has been attributed to any of these three proteins. [132][179] CLN6 and CLN8 are transmembrane proteins resident in the endoplasmic reticulum in neuronal cells. No specific enzymatic functions have been reported for either protein. [182][183][184]

In addition to the morphology observed under electron microscopic analyses, NCLs can also be classified by the accumulation of specific proteins as the major hydrophilic constituents of their storage material. All forms of human NCL tested so far (except CLN1) accumulate subunit C of mitochondrial ATP synthase as the major protein component of their lysosomal storage material. The CLN1 form is associated with the lysosomal accumulation of saposins A and D. [1][3] Currently, there is no thorough understanding of the relationship between storage material accumulation, which proteins are accumulated and the progression of the disease. While neurodegeneration occurs primarily in tissues which also accumulate large amounts of storage material, it is not know whether there is a cause and effect relationship between the two. In 2006, Kim et al. reported that in humans, the CLN1 form of NCL causes endoplasmic reticulum stress-induced activation of unfolded protein response (UPR) which, in turn, mediates activation of caspase-4 and caspase-3. [176] Activation of ER caspases is a known induction signal for apoptotic cell death. The same experiments also showed that NCL-affected brains contain high levels of growth-associated protein 43 (GAP-43) which is post-translationally palmitoylated and appears to be abnormally localized in the ER of affected cells. Inhibition of caspase-4 activity protected NCL-affected cells from undergoing apoptosis. [176] Whether the accumulation of autofluorescent lysosomal granules is part of the process that activates apoptosis or is merely a side-effect of the defects which lead to induction of UPR and downstream apoptotic signals will require further experiments to determine.

In addition to humans, NCLs are known to occur in a number of other mammals, including mice, dogs, cats, sheep, cattle and goats. [4][5][6][7][8][9][10] Some of these animals have been well characterized and developed as models of human NCL. These animal models have proven useful for delineating the genetic basis for several forms of human NCL as well as understanding the biochemical pathways leading to onset of the disease.

Although NCLs have been characterized for more than a century, there are currently no clinical therapies available for treating patients with NCL. Several approaches for treating this group of diseases have been explored including enzyme replacement therapy, gene therapy, bone marrow transplant, antioxidant therapy and stem cell transplant. [11][12][13][14] None of these methods has met with enough success to become available as a treatment to the general public as yet, although the stem cell and gene therapy trials are in their early stages. By carefully characterizing the existing animal models and using them as a basis for testing potential therapies, progress toward a cure can be made.

The purpose of this research is to determine the feasibility and effectiveness of using autologous mesenchymal stem cells (MSCs) as a cellular therapy for the NCLs. We chose this therapy because we believe it offers significant promise while avoiding some of the problems presented by other potential therapies. In order for cellular therapy to be practical, it must be possible to isolate appropriate cells consistently and in a timely manner, modify the cells efficiently (if necessary), transplant the cells to an appropriate tissue and have them survive long term and the transplanted cells must be able to ameliorate the disease. This work describes the results of our experiments which begin to address these criteria in relation to adult, bone marrow-derived MSCs. We describe the isolation of bone marrow-derived mesenchymal stem cells from murine and canine sources, characterization of the isolated cells, modification of those cells by means of small fragment homologous replacement (SFHR) and treatment of one of the disease symptoms by transplantation onto an *in vitro* model of diseased neural tissue. These data lay the foundation for future experiments which will test the efficacy of these cells as a treatment for NCL in several animal models available to our lab.

2. Location and Origins of Adult Mesenchymal Stem Cells

During embryonic and fetal development, pluripotent embryonic stem cells differentiate through several levels of specification to generate all the tissues of the adult body. This process requires intricate biomolecular regulation which is orchestrated by a variety of cellular factors including transcriptional activators, transcriptional inhibitors, siRNAs, chromatin remodeling, protein gradients and intercellular signaling cascades. For many years it was believed that this process culminated in the production of a fully formed adult body composed entirely of terminally differentiated cells of limited self-renewal capacity. The discovery of tissue-specific stem cells in many organs of the adult body has overturned this previous viewpoint. Of particular interest has been the revelation that many cells of the body which were previously believed to be irreplaceable once lost, such as brain neurons, cardiac myocytes and ovarian eggs are, in fact, replaced through a natural process of turnover by adult stem cells resident in surrounding tissue. [15][16][17] This revelation has led to speculation that these adult stem cells, which are naturally capable of replacing certain cells at a steady rate, might be coaxed into healing large areas of tissue damage through physical and biochemical manipulation. MSCs have been an area of great interest in the adult stem cell field because they are easily isolated from live donors and appear to have the ability to differentiate into numerous tissues which might benefit from therapeutic intervention.

Mesenchymal stem cells are actually a broad class of adult stem cells found in many organs and tissues throughout the body. The adult mesenchyme is something of a catch-all phrase applied to tissues of mesodermal origin which constitute the connective tissues, vasculature, blood and lymphatic systems of an organism. As a result, the term “mesenchymal” stem cell can be confusing if not defined properly. In the context of this work, “mesenchymal stem cells” or “MSCs” will be used to refer specifically to bone marrow-derived mesenchymal stem cells which are not of haematopoietic or endothelial lineage. Other adult stem cells which might technically be referred to as mesenchymal stem cells as well, such as skeletal muscle satellite cells, brown

adipose tissue-derived stem cells and cardiac stem cells, will be referred to specifically by their tissue of origin.

Even though it is sometimes useful for purposes of discussion to separate these cells by their organ or tissue of origin, such distinctions may not be as significant as once believed. When tissue-specific adult stem cells were originally discovered it was assumed that these cells developed during embryogenesis as part of the tissue in which they reside and as such had already specified a developmental fate. So, while experimental results showed that adult stem cells could proliferate and differentiate in much the same way as embryonic stem cells, they were believed to lack the pluripotent differentiation potential of embryonic stem cells. This was soon called into question, however, as experiments showed that adult stem cells (and MSCs in particular) displayed a much higher degree of plasticity than expected both in culture and after transplantation *in vivo*. [18]

Although evaluation of cell differentiation *in vitro* is often quite rigorous, the accepted standard for determining whether a cell can assume a specific developmental fate is to test whether it will do so after transplant *in vivo*. In the case of embryonic stem cells, this is usually tested by the cell's ability to form a teratoma (a tumor containing cells which have their origin in all three embryonic germ layers). Since MSCs do not form teratomas, transplant into specific tissues and tracking the fate of transplanted cells is the usual means of determining a cell's potential plasticity. Using these methods, MSCs have been shown to differentiate *in vivo* into bone, cartilage, fat, liver, kidney, skeletal muscle, smooth muscle, vascular endothelium, cardiomyocytes, melanocytes, keratinocytes, neurons, glia, Schwann cells, photoreceptors, retinal pigment epithelium and other cell types. [18] Many of these tissues are vastly different in function and biochemical properties than the cells MSCs usually give rise to in the bone marrow compartment; some are even derived from non-mesodermal germ layer cells, something which was at one time considered impossible under normal circumstances.

The act of a stem cell derived from a tissue of one germ layer origin transforming into a cell of another germ layer is referred to as transdifferentiation. The concept of transdifferentiation has

met with much skepticism within the scientific community since it was first reported in 1999 that adult neural stem cells were able to produce haematopoietic lineage cells after transplantation into irradiated host animals. [19] However, further research seems to indicate that such transformations are not only possible, but may actually occur as a part of normal physiology throughout the life of an organism. Using the differentiation of MSCs into neural cell types as an example, it has recently been demonstrated that MSCs express several proteins (Nestin, βIII-tubulin, tyrosine hydroxylase, MAP2 and GFAP) that were previously thought to be confined to cells of neural origin, without any specific induction or apparent loss of mesenchymal differentiation ability. [20] In addition, Pacary et al. found that MSCs exposed to conditions which promote neural differentiation in cerebral progenitors *in vivo* (induction of HIF1 activity and inhibition of Rho kinase activity) also act to promote neurodifferentiation of MSCs *in vitro*, suggesting that MSCs already have the cellular machinery in place to respond to cerebral differentiation signals and undergo neurodifferentiation as part of their natural physiology. [21] Perhaps even more telling are the results of an experiment in which four female patients who received sex mismatched bone marrow transplants for various haematopoietic diseases were examined post-mortem for evidence of donor cells in their brain tissue. [22] All subjects were found to have Y chromosome positive cells in the brain (primarily in neocortical and hippocampal tissues) which labelled positive for NeuN and Kv2.1 (a neuron specific ion channel). Measurements of Y-positive cells adjusted for brain volume suggest that the number of marrow-derived neurons in these subjects may have been as high as 1 in 2,000-4,000 cells. Longer post-transplant survival time also correlated with an increase in the number of marrow-derived cells in the brain tissue. It was unclear whether the cells were of mesenchymal or haematopoietic origin. These and other results support the hypothesis that cells of bone marrow origin leave the stromal compartment, circulate through the bloodstream and contribute to the regeneration or growth of multiple tissues as part of their natural biological function.

An alternative explanation for the transdifferentiation phenomenon has been proposed recently by several groups. [23][24][25] During development, a structure called the neural crest develops at the interface between the non-neural ectoderm and the dorsal region of the neural plate.

Experiments tracing the lineage of cells giving rise to the neural crest indicate that they are drawn from both the neuroepithelium and surface ectoderm regions. During development, neural crest cells are induced to undergo an epithelial-to-mesenchymal conversion which, among other things, down regulates several adhesion molecules and facilitates their exit from the neural plate and migration throughout the body of the developing organism. These cells appear to follow specific, highly-conserved pathways which segregate them into four distinct axial populations (the cranial, cardiac, vagal and trunk populations) each of which contributes to a distinct set of tissues along the neuraxis. Among the many cell types that have been documented to arise from migratory neural crest cells are sensory, cholinergic and adrenergic neurons, glial cells, Schwann cells, chromaffin cells, parafollicular cells, melanocytes, chondroblasts, chondrocytes, odontoblasts, osteoblasts, osteocytes, fibroblasts, striated myoblasts, smooth myoblasts, adipocytes and other connective tissue cells. [26] In other words, neural crest cells are capable of differentiating down many of the same lineages as adult MSCs and, during embryogenesis (and despite the fact that they are ectodermal in origin), contribute to almost all of the tissues in which adult mesenchymal stem cells are to be found. This leads to the interesting possibility that adult stem cells are not, as has been proposed, tissue-specific stem cells derived during embryogenesis from fate-determined cells of the organ in which they reside, but adult remnants of a population of cells which already demonstrates, during development, the ability to form cells of all three germ layers. If this is the case, then the term transdifferentiation may be misapplied when it is used to describe the behavior of MSCs, as it implies a change from one determined fate to another. If MSCs arise from a population of cells which have not yet specified a developmental fate, as this hypothesis predicts, then their nature transcends the concept of transdifferentiation.

3. Function of Bone Marrow-derived Mesenchymal Stem Cells

The primary function of the bone marrow is the production of blood cells (erythrocytes, lymphocytes and thrombocytes) and the maintenance of the surrounding bone tissue. Two classes of adult stem cell are responsible for these functions. Haematopoietic stem cells (HSCs), which are responsible for haematopoiesis, and mesenchymal stem cells, which give rise to the bone-forming and stromal cells of the marrow. The bone marrow stroma is an intricate network of

support cells that surrounds the machinery of the haematopoietic system. The interaction between the haematopoietic and stromal compartments of the marrow has been examined extensively and has been shown to play an important role in regulation of HSC activity. Of particular importance seem to be a subset of stromal cells which reside along the endosteal surface of bones, termed SNO (Spindle-shaped, N-cadherin^{+}, CD45^{-}, Osteoblastic) cells, which interact directly with HSCs through expression of N-cadherin, fibronectin and various integrins. These stromal cells provide signals through the Wnt/BMP regulatory pathways which modulate the balance between HSC quiescence, self-renewal and differentiation. [27] In addition, specialized stromal cells such as osteoblasts, osteoclasts and reticular cells contribute to formation of the niche environment. All such cells are descended from the tissue-resident mesenchymal stem cells and control of stromal composition (a key part of regulating haematopoietic activity) is dependent upon MSC fate choices. [28][29]

Unlike their well-characterized haematopoietic counterparts, the location and exact nature of MSCs in the marrow compartment is still only vaguely understood. This is partly due to the fact that haematopoietic stem cells in the marrow outnumber mesenchymal stem cells by approximately 100 to 1. [30] In addition, it has been very difficult to identify and study mesenchymal stem cells *in situ* because no definitive marker of MSC identity (other than differentiation potential) has been identified. Although MSCs are known to be positive or negative for any number of protein markers, no single marker (or even panel of markers) has been shown to identify a completely homogeneous population of cells either *in vitro* or *in vivo*. Since it has proven so difficult to identify MSCs in their niche, elucidation of their interaction with other cells of the stroma and the haematopoietic apparatus has been limited. While it is known that MSCs give rise to the osteoblasts that create new bone and, stromal cells that support differentiation and migration of HSCs and other specialized cells, it is not known where they reside within the stroma and what cells, signalling molecules and adhesion proteins make up the MSC niche.

In the past, localization of a stem cell within its niche has proven very important in understanding the nature of the stem cell and the process by which it gives rise to various progeny. The unique

structure of the intestinal crypt for intestinal stem cells and the follicular bulge for dermal stem cells are two examples of adult stem cells that are localized to a specific region within a structurally defined “pouch”. The anatomic localization of these stem cells was a great advantage in defining the activities of those particular niches because the transition from stem cell through progenitor to progeny could be tracked spatially. [31][32] If such a spatial arrangement exists for MSCs in marrow stroma, it has not yet been discovered.

In addition to acting as a continuous source of marrow stromal cells, MSCs may also play a role in replenishment of cellular progenitors or repair of damaged tissue in many areas of an organism. Experiments seeking a means of acquiring MSCs other than bone marrow biopsy (a safe but invasive procedure) have demonstrated the presence of rare, circulating cells that appear to have the same characteristics as bone marrow-derived MSCs and may originate from that source as well as others. [33] In 2001, Kuznetsov et al. isolated plastic adherent clonal cells from adult peripheral blood which were $CD45^-$, $CD14^-$, $CD105^-$, and $CD34^-$ (all markers of cells of haematopoietic or vascular origin) and positive for many characteristic MSC proteins such as collagens I and III, fibronectin, osteonectin, α-smooth muscle actin, CD44, VCAM1 and β_1 integrin. [34] These cells were able to generate bone and fat when transplanted *in vivo*. Similar cells, isolated by the same method, demonstrate an ability to migrate to areas of damage or inflammation and contribute to wound healing. MSCs derived from bone marrow stroma possess the same ability to seek and repair tissue damage when infused systemically. [35]

4. Isolation and Molecular Characteristics of Mesenchymal Stem Cells

The first description of the clonogenic nature of bone marrow stromal cells was published in *Nature* in 1963. [36] Friedenstein et al., in 1974, went on to describe a method of isolating “colony forming unit – fibroblast” cells from whole marrow by adherence to a plastic substrate. [37] Much of what we know about MSCs today is still based on the same isolation techniques. MSCs are generally defined as clonogenic, mononuclear, plastic-adherent cells with a fibroblast-like spindle shape and the ability to become adipocytes, osteocytes and chondrocytes under specified conditions *in vitro*.

This method of isolation is entirely adequate for most purposes and is the method used for deriving the cells described in this work. However, there can be no question that the plastic adherence method does not yield a fully homogeneous population of cells. The variability of cells within this population suggests that in addition to MSCs it may contain a mixture of stromal and epithelial cell precursors as well as adherent cells of haematopoietic origin. [38] Cells obtained by plastic adherence are invariably less than 100% clonogenic and many clonogenic cells show limited potentiality (being able to differentiate into only one or two mesenchymal lineages). In addition, plastic adherent populations are very rarely homogeneous in their expression of cell surface proteins which identify different subsets of stromal and haematopoietic cells. Clonal cells which truly meet the definition of "mesenchymal stem cell" outlined above make up only a fraction of the isolated cells. In addition, the amount of heterogeneity in clonality, multipotentiality and surface antigen expression varies significantly between different isolations. Thus, while useful, this method is not optimal for acquiring pure populations of adult MSCs for study or transplant.

Since their initial characterization, numerous methods for isolating populations of MSCs directly from bone marrow have been tested, either in conjunction with or separate from their ability to adhere to plastic. Many of these have relied on cell surface antigen expression. As was mentioned in the previous section, these experiments have been hampered by the inability to find a truly definitive marker for MSCs which separates them from other cells resident in the bone marrow stroma. However, certain experiments have yielded illuminating results which have advanced our knowledge of MSC characteristics.

Some researchers have modified the plastic adherence method to improve selection for true MSCs. Pochampally et al. used plastic-adherence and survival in serum-free culture to derive a population of putative MSCs which expressed Oct4 and displayed telomere lengths significantly longer than those of other characterized MSCs. [39] While these cells were clonogenic and multipotent, they were only able to divide approximately 10 times in culture before senescing. While this lack of self-renewal suggests that the cells may have been progenitors rather than true stem cells, it is also possible that the lack of growth factors in the serum-free medium induced

early apoptosis or differentiation. Battula et al. used a similar method but grew the cells in gelatin-coated flasks and supplied basic fibroblast growth factor in the MSC culture medium. [40] From this isolation procedure they derived multipotent MSCs which were positive for self-renewal and pluripotency associated molecules such as the frizzled 9 cell surface receptor and the transcription factors Oct4 and nanog. The cells were also able to proliferate 4-5 times faster than cells selected by the conventional, plastic adherence method. Unlike Pochampally's group, these cells were able to grow indefinitely in culture.

Numerous attempts have been made to use cell surface antigens as a target for isolating a pure population of MSCs. Several antibodies, such as SH2, SH3, Stro1 and SCA1, have been generated which, in whole bone marrow extracts, ostensibly label MSCs specifically. These antibodies were generated by creating a pool of antibodies against whole, adherence-purified MSCs then negatively selecting for antibodies which react with normal stromal cells and cells of haematopoietic origin. The SH2 and SH3 antibodies (which target different sections of the CD73 antigen) have been used extensively to identify MSCs. The Stro1 antibody (stromal antigen 1) has also been used alone or in conjunction with other markers to purify MSCs. However, several groups have described instances of these antibodies reacting with non-MSC cells from bone marrow, indicating that they are indicative but not definitive for MSC identity. [41] In 2003, Gronthos et al. used a positive selection protocol involving magnetic cell sorting of bone marrow mononuclear cells (BMMNCs) positive for Stro1 and vascular cell adhesion molecule (VCAM or CD106) to isolate MSCs from bone marrow. [38] These cells constituted a small portion (1.4%) of BMMNCs but showed high levels of clonogenicity and multipotency. Colony forming unit – fibroblast (CFU-F) assays indicated that this method purified over 90% of the CFU-Fs contained in whole bone marrow. In addition, these cells were quiescent (no Ki-67 activity) but expressed telomerase and were highly proliferative after several days of *in vitro* culture. While this method appears to be useful in deriving a relatively pure population of CFU-F^+ cells, whether this translates to a pure population of MSCs remains questionable. It has been observed that a portion of CFU-F^+ cells in bone marrow are actually haematopoietic in nature. [41] It is unclear whether the cells isolated by this method include these contaminating haematopoietic CFU-Fs.

Others have used cell surface antigens possibly associated with more primitive progenitor cells to positively select for MSCs. In 2005, Tondreau et al. used positive staining for CD133 as a criteria for isolating MSC from peripheral and cord blood. [33] While the initial sort yielded a heterogeneous population contaminated with numerous haematopoietic cells, plastic adherent culture in MSC conditioned medium yielded a culture of MSCs positive for MSC markers SH2, SH3, CD105 and CD44 but largely negative for markers of haematopoietic origin such as CD14, CD34 and CD45. These cells were clonogenic and expressed Oct4. More recently, Gang et al. used positive selection for the SSEA4 antigen (stage-specific embryonic antigen 4) to isolate what they propose to be a pure culture of primitive MSCs. The expression of this embryonic antigen on adult stem cells is unusual because SSEA4 is a globo-series glycolipid molecule whose expression was thought to be restricted to preimplantation embryos and certain very specific somatic cells such as erythrocytes. A switch from globo-series to lacto-series glycolipids (identified by SSEA1) occurs after implantation and the globo-series ganglioside synthesis pathway is not retained by most embryonic tissues. The authors found that the $SSEA4^+$ population was completely free of contaminating $CD45^+$ (haematopoietic) cells, was highly clonogenic and individually cloned cells were 76.5% multipotent (based on the ability of individual clones to undergo adipogenic, osteogenic and chondrogenic differentiation), a large improvement over MSCs isolated by plastic adherence alone, which have been reported to be between 17-30% multipotent. [42]

Another popular method for isolating MSCs has been negative selection for antigens specific to common contaminating elements such as vascular and haematopoietic cells. At least three groups have used negative selection for $CD45^+$ and glycophorin A^+ cells as an initial step for purifying MSCs. [43][44][45] Catherine Verfaillie's group combined immunodepletion methodology with plastic adherence and survival in serum-free medium supplemented with EGF and PDGF-BB. [45] They described the resulting multipotent adult progenitor cells as a subset of mesenchymal stem cells despite a cell surface antigen expression profile which showed the cells to be positive for several antigens normally associated with haematopoietic rather than

mesenchymal cells. Lagar'kova et al., on the other hand, used the same immunodepletion step but cultured their plastic adherent cells in high serum (20%) medium. [44] The cells they obtained were positive for many MSC markers such as vimentin, desmin, CD105, CD90 and CD13. A small fraction also expressed detectable levels of SSEA4 antigen. In addition, they showed that, unlike MAPCs, their cells were negative for markers of endothelial and haematopoietic origin such as CD34, CD11b and CD117. Other groups have used alternate immunodepletion criteria such as Schrepfer et al., who selected for plastic adherent $CD11b^-$ cells. [46] This method yielded a pure population of CD44, CD90, CD105, SCA1 positive cells which showed no contamination by cells of haematopoeitic origin, but only after 10 passages in culture. A more restrictive immunodepletion by Baddoo et al., isolated adherent cells which were negative for CD11b, CD34 and CD45, were clonogenic and displayed typical MSC markers but were not more multipotent than many other selection methods. [47] When clonal progeny were tested, only 20-50% were able to differentiate into adipocytes and, of those, only a portion were also able to differentiate into other mesenchymal cells such as osteocytes and chondrocytes, possibly indicating that the culture was contaminated with more highly specified precursor cells.

These varied methodologies and results illustrate some of the difficulties surrounding the isolation of a pure population of MSCs. Although some markers are indicative of MSCs, none of the ones listed here seem to be definitive for a completely homogeneous population. In addition, the assays used to estimate purity may, themselves, be flawed. It appears that some of these protocols are capable of producing a population of cells that is more homogeneous than plastic adherence alone, but variance in culture conditions and assay criteria may ultimately play as much of a role as purification procedure in determining the perceived purity of a culture. A population of cells which is homogeneous at isolation may not remain so after days or even hours in culture. The bone marrow stroma is a complex tissue, composed of many varied cells which appear to form a highly orchestrated series of cytokine and growth factor gradients controlling haematopoietic and osteochondral genesis. In the absence of appropriate culture conditions, it is likely that even homogeneous MSCs undergo some form of specification and differentiation over time in an attempt to recreate their natural stromal environment. A better understanding of the

nature of MSCs and their niche will be needed before purification procedures can be modified to isolate a completely homogeneous population that can be maintained as such in culture.

5. Mesenchymal Stem Cells as a Source of Cellular Therapy.

Despite the hurdles still to be overcome in understanding the nature of MSCs, the promise of a readily accessible, easily renewable source of potentially regenerative cells has prompted many researchers to move forward with experiments to evaluate their therapeutic potential. MSCs have been evaluated for their ability to treat cerebral, spinal, renal, gastrointestinal and cardiac ischemia, osteogenesis imperfecta, diabetes, retinal injury and numerous genetically inhereted neurodegenerative diseases such as Niemann-Pick, Parkinson's, mucopolysaccharidosis and the NCLs. In general, MSCs used in these experiments show a strong propensity to migrate to sites of injury or degeneration and often provide therapeutic benefits.

One of the first clinical uses of MSCs was in the treatment of osteogenesis imperfecta (OI). Previous studies, done with whole bone marrow transplant, yielded limited improvement. In a 1999 clinical trial, Horwitz et al. showed that intravenous infusion of allogenic bone marrow increased bone density, bone mineralization and growth velocity while simultaneously decreasing the incidence of bone fracture in several patients with severe OI. [48] In 2002, the same group repeated those experiments with IV-infused, plastic adherence-purified MSCs. [49] Treated patients showed improvements in the disease phenotype that outstripped the results for whole bone marrow infusion, indicating that MSCs were the component of the BMT responsible for the improvements seen in the original experiments and that higher doses of purified MSCs are more therapeutic. Even though donor cell engraftment did not appear to exceed 1% in any of the patients, the production of clinically recognizable improvements in disease phenotype indicates that MSC infusion is a viable treatment for such diseases.

MSCs have also been tested for their ability to treat diseases of other mesodermal tissues. They have proven effective in replacing lost cells and contributing to healing in a number of medically significant disease models affecting the liver, kidney and the heart. In the U.S. alone, approximately 6,500 liver transplants were performed on patients with chronic liver failure in

2005 and the number has been increasing steadily for the last 15 years. [50] Renail failure, including costs of dialysis, tissue matching and transplants, costs the U.S. healthcare system an estimated $20-28 billion dollars per year. [51] Cardiovascular disease is the leading cause of morbidity and mortality in most developed countries, costing the U.S. healthcare system an estimated $431 billion dollars per year to treat. [52] Research shows that adult MSCs are able to engraft in these organs and promote tissue repair. In 2004, for example, Morigi et al., using a cisplatin-injury model of renal failure, established that IV infused MSCs can engraft in renal tubules and become tubular epithelial cells. MSC treatment markedly accelerated tubular proliferation and contributed to restoration of renal structure and function as measured by serum BUN and creatine levels. Untreated or HSC treated controls showed no engraftment or accelerated healing. [53] Numerous studies have been conducted establishing the contribution of transplanted or indigenous MSCs to repair of myocardial tissue after acute infarction. Transplants have been introduced by IV infusion, direct myocardial injection, surgical implantation of cellular sheets on fibrin matrix patches and direct attachment of pre-differentiated, beating cardiomyocyte tissue. [54][55][56] Often, MSCs are pre-treated with 5-azacytidine, a potent demethylase which inactivates gene silencing caused by DNA methylation, or extracellular matrix components to promote their differentiation into myocardial tissue. Results from several laboratories indicate that MSCs transplanted by various methods are capable of engrafting into injured myocardial tissue and taking on physiological and morphological indicators of myocardial differentiation such as multi-nucleated myotubes, spontaneous, isoproterenol-dependent beating, sarcomeric organization, gap junctions with neighboring myocytes and expression of cardiomyocyte specific proteins such as desmin, myosin, actinin, troponin I, phospholamban, adrenergic and muscarinic receptors. [56] Endogenous MSCs have also proven capable of contributing to myocardial repair. Fukuda et al. demonstrated that eGFP labeled MSCs implanted into the bone marrow of recipient mice could be mobilized to peripheral blood circulation by granulocyte colony stimulating factor (G-CSF) and contributed to repair of damaged myocardium after acute infarction. [57] The use of autologous or allogeneic MSCs may be able to reduce our

dependence on invasive surgery and organ transplants to treat these prevalent and costly diseases.

Perhaps the most exciting prospect for MSCs in clinical therapy, however, is their potential for treating neural injury and neurodegenerative diseases. The discovery that MSCs appear to contain the components of biochemical pathways which are essential for neural differentiation in normal development and are capable of undergoing neural differentiation both *in vitro* and *in vivo* has prompted research into their ability to treat neural injury and disease. One of the focuses of this research, repair of damaged peripheral and spinal nerves, has met with some success in animal models. In 2001, Sasaki et al. used whole bone marrow stromal cells to treat demyelinated spinal cord injuries in rats. [58] The dorsal funiculus of the spinal cord was demyelinated by irradiation followed by injection of ethidium bromide. This treatment results in specific loss of myelinating glial cells while preserving axons in the affected region. Microinjection of both cultured Schwann cells and whole bone marrow stroma into the injured region resulted in remyelination (remyelination by stromal cells resulted in a predominantly peripheral pattern, including myelinating cells surrounding multple axons in several instances observed). Many cells in the stromal transplant group were observed to express markers of glial (GFAP) and neural (NSE) differentiation. Since the whole bone marrow transplant contained both MSCs and HSCs, purified HSCs were also injected as a control and showed survival but no remyelination effects, indicating that MSCs were responsible for the results observed. Further work has also been done in models of spinal cord and peripheral nerve injury with purified MSCs. In 2004, Tohill et al. used plastic-adherent MSCs purified through 5 passages *in vitro* to regenerate severed sciatic nerve in a rat model. [59] Some MSCs were exposed to glial growth factor (GGF) prior to transplantation. Both treated and untreated MSCs were able to enhance regeneration and remyelination of the severed nerve and displayed indicators (GFAP and S100) of glial differentiation. Cells treated with GGF were more effective than untreated cells and were nearly equivalent to transplanted Schwann cells in their promotion of axonal growth. Coronel et al. showed that MSCs administered at a site distal to an injured axon specifically home to and engraft areas containing corresponding cell bodies. In their model, the sciatic nerve was injured

by constriction in an ipsilateral, bilateral or contralateral manner and undifferentiated MSCs were injected directly into the right lumbar-4 dorsal root ganglion (L4-DRG). [60] MSCs preferentially engrafted in DRGs hosting primary sensory neurons affected by a lesion of their peripheral branches. MSCs injected in a bilateral or contralateral injury subject migrated to left lumbar dorsal root ganglia in an injury-specific fashion. MSCs transplanted into uninjured rats survived, but no migration was observed. Homing to ganglia hosting injured neurons was found to be dependent on fractalkine and SDF1. Taken together, these findings demonstrate that MSCs are able to sense nerve damage, engraft specifically in injured tissues and contribute to repair of affected peripheral nerves.

Perhaps even more daunting than repair of peripheral or spinal nerves is repair of cranial neural tissue. MSCs have been tested for their ability to contribute to repair of both traumatic brain injury and neurodegenerative diseases of the brain. It is known that MSCs infused into embryonic brain are able to engraft and form functional neuronal tissue without disrupting the brain architecture or function. In work done by Munoz-Elias et al., MSCs infused into the ventricles of embryonic rats behave in a manner very similar to embryonic neural stem cells. [61] Transplanted MSCs were able to migrate along radial glial processes, home to periventricular germinal zones, express progenitor vimentin and nestin and form both migratory neurons and guiding radial glia. By postnatal day 3, transplanted MSCs populated areas distant from the site of injection including neocortices, hippocampi, the rostral migratory stream and olfactory bulbs. Whereas donor cells in the subventricular region continued to express nestin, cells located in neocortex and midbrain expressed mature neuronal markers such as NeuN. Recipients showed high levels of engraftment and no neurologic deficits at 2 months post-natal (the longest timepoint tested). While not definitive, such results suggest that MSCs may be able to undergo similar engraftment and differentiation in adult tissues.

In models of traumatic brain injury, MSCs have demonstrated the ability to home to sites of damage and contribute to healing in a manner similar to their behavior in peripheral nerve injury. In a blunt force trauma model of brain injury, Lu et al. demonstrated that MSCs injected into the

tail vein of injured rats were able to cross the blood-brain barrier and home to sites of brain injury. [62] Animals which received MSC treatment had reduced motor and neurological deficits at 4, 7 and 14 days after injury. Some transplanted cells in the injured area expressed either GFAP or NeuN when examined at day 14. Using a ligation-induced cerebral ischemia model, Chen et al. produced similar results. MSCs derived from 5-fluorouracil treated animals and infused intravenously either 1 or 7 days after injury improved somatosensory behavior and neurological severity scores in treated rats. Transplanted cells were shown to preferentially localize to the site of cerebral injury and some cells in the injured area expressed markers of glial or neuronal tissue. In a more detailed study, Zhao et al. showed similar results with a ligation model of ischemic injury using $CD45^-$, $GlyA^-$ plastic-adherent cells transplanted directly into the cerebral ventricles. [63] They also observed that transplanted cells migrated to injured areas (even crossing the corpus callosum in subjects with a contralateral injury) and reduced neurological deficits but not infarct size in treated animals. Although they also observed some donor cells at the site of injury producing glial and neuronal proteins, the transplanted cells did not morphologically resemble differentiated cells. Their results led them to predict that neurological benefits were predominantly due to production of extracellular matrix components and neurotrophic factors by the transplanted cells.

In addition to treatments for traumatic injury, MSCs have been tested for their ability to delay or correct deficits caused by neurodegenerative disorders. For example, extensive work has been done on the treatment of Niemann-Pick disease (a hereditary deficiency in acid sphingomyelinase activity) with autologous MSCs. In 2002, Jin et al. tested the ability of autologous MSCs (retrovirally transduced to express human acid sphyngomyelinase) to prevent neurodegeneration in a mouse model of Niemann-Pick disease. [64] They found that modified MSCs injected directly into the hippocampus and cerebellum of affected mice migrated away from the site of injection and engrafted in cerebral tissue for more than 7 months after transplant. This treatment reduced levels of cerebral sphingomyelin, extended the lifespan of transplant recipients, improved neuromotor function, maintained body weight at near normal levels and drastically reduced Purkinje cell loss compared to untreated controls despite low levels of engraftment in cerebral

tissue (possibly due to immunorejection of the xenogenic human ASM protein). They went on to show that a combination of intracerebral and intravenous infusion of the same cells increased the beneficial outcome over intracerebral infusion alone. [65] The neuroprotective effects of treatment and the drastic reductions in Purkinje cell loss appear to have been mediated at least partially by fusion of transplanted cells with native Purkinje cells. The incidence of cell fusion seems to be directly correlated to the severity of the neurodegeneration present at the time of treatment. [66] Intracerebral transplant of MSCs has also been shown to improve cognitive and motor function and decrease cell loss in rodent models of mucopolysaccharidosis type VIII (β-glucoronidase deficiency) and in 6-hydroxydopamine-lesioned rodents (a model of Parkinson's disease). [67][68] In both cases, transplanted cells migrated toward and preferentially engrafted in areas undergoing significant degeneration. Much of the therapeutic benefit seen from MSCs in these studies is due to the release of soluble enzymes from the transplanted cells which are taken up by host cells deficient in that activity. Our proposed use of MSCs for treatment of NCLs depends upon a similar phenomenon. Several clinical trials using MSCs for just this purpose have already been approved and carried out. In one study, patients with Hurler Syndrome (mucopolysaccharidosis type-IH) and metachromatic leukodystrophy (MLD), diseases resulting from deficiencies in α-L-iduronidase and aryl-sulfatase A respectively (both soluble enzymes) showed improvement in bone mineralization and nerve conduction velocities after intravenous infusion of plastic-adherence purified MSCs from allogeneic donors. [69] Although engraftment in bone marrow was low or undetectable in all patients, therapeutic benefits of the treatment were observed longterm (up to 24 months after transplant). These studies demonstrate that even very low-level engraftment of transplanted cells in enzyme-replacement cellular therapy can produce observable therapeutic benefits in patients suffering from neurodegenerative disorders.

MSCs have also shown the ability to engraft in retinal tissues. This is significant, since NCLs affect not only the neural tissue of the brain, but that of the retina as well. Rat MSCs induced toward photoreceptor differentiation by the application of activin A, taurin and EGF were able to express photoreceptor-specific proteins such as rhodopsin, opsin and recoverin *in vitro*. The same cells, when injected into the sub-retinal space of RCS rats, were observed to engraft in the

retina for up to 6 months and, in the majority of cases, take on the morphology of photoreceptor cells and express rhodopsin. A few cells were observed to take on the stellate morphology of amacrine cells and expressed CRABP1 (an amacrine marker). [70] Another study, using a mechanical injury model of retinal damage, demonstrated that MSCs isolated from 5-fluorouracile-treated animals were able to engraft at the site of damage and take on the characteristics of cells in the outer nuclear layer when injected intravitreally. [71]

6. Modification of Autologous Cells by Small Fragment Homologous Replacement

Although unmodified autologous cells are useful as therapies for organ damage such as cardiac and cerebral ischemia, the treatment of inherited diseases by enzyme replacement cellular therapy requires that transplanted autologous cells be modified to produce the protein missing in the affected patient. Traditionally, the preferred method of correcting a genetic deficiency has been to insert a novel copy of the gene driven by a non-native promoter in a random portion of the host genome. This approach has several drawbacks. It allows ectopic and unregulated expression of the gene product, which could potentially cause complications after treatment. It also leaves open the possibility that the inserted gene will interrupt important genetic elements in the host genome, causing cell death or, even worse, tumorigenic transformation of the cell. [72] These modifications also regularly rely on viral vectors for introducing the large DNA molecules necessary to encode a novel gene. Though viral vectors have been used for many years and are potentially very beneficial as a tool for gene therapy both *in vitro* and *in vivo* they still carry with them some risk of infection or detrimental immune responses. [73]

An alternative to the insertion of a novel gene cassette is repair of one or more copies of the endogenous, defective gene. One method for accomplishing such a repair is small fragment homologous replacement (SFHR). SFHR relies on the hybridization of small fragments of single-stranded or double-stranded DNA to their complementary sequence in the genome, creating a recombination joint structure with one or more mismatched base pairs. DNA mismatch repair processes then resolve the junction using the modified DNA molecule as a template. This results in the exchange of genetic information from the small DNA fragment to the native gene. [74]

Small fragment homologous replacement has been successfully used to introduce small genetic changes in genes in several *in vivo* and *in vitro* systems. Using a defective zeocin antibiotic resistance gene as a selectable marker, Colosimo et al. demonstrated the ability to introduce a single nucleotide replacement at an efficiency of 4% in cultured human airway epithelial cells. [75] Using a hygromycin resistance-GFP fusion gene as an indicator of recombination efficiency, Tsuchiya et al. showed that using a 606nt ssDNA fragment matching the sense strand increased recombination events 10-fold over that for dsDNA fragments in their model. They attributed this improved efficiency to isolation of the sense strand and to adenine methylation of the DNA fragment (a by-product of the phagemid DNA replication process in *E. coli* used to generate the ssDNA molecule). [76] SFHR has also been used to correct defective genes directly related to inherited genetic diseases. Low level (1%) correction was demonstrated for the ΔF508 cystic fibrosis transmembrane conductance regulator mutant in cultured human and rodent airway epithelial cells. [77] Correction was also demonstrated for this mutation in a murine *in vivo* model, but at 10-fold lower efficiencies than with cultured cells. [78] In a model of spinal muscular atrophy (SMA) in which the primary defect in the *SMN1* gene is refractory to treatment by SFHR due to its size, activation of the *SMN2* gene (a paralog of the defective SMN1 gene, which is also has a single nucleotide defect causing inactivation through alternate splicing) by SFHR was used to correct the disease in cultured human trophoblast cells. A two-fold increase in wild-type SMN protein was seen in targeted cells. [79] Very efficient recombination (~20%) was achieved in experiments by Zayed et al. in which the genetic defect responsible for severe combined immune deficiency syndrome of SCID mice (a single nucleotide polymorphism in the DNA-dependent protein kinase catalytic subunit gene) was corrected by SFHR in cultured T cells, with selection of corrected cells by survival of radiation exposure. [80] Perhaps most significantly for our research, Kapsa et al. demonstrated that bone marrow stromal cells obtained from *mdx* mice (a murine model of muscular dystrophy containing a dystrophin gene rendered dysfunctional by a single nucleotide mutation) could be corrected for their genetic defect at an efficiency of 15% by SFHR and, when transplanted back into affected mice, contributed to remodeling of skeletal muscle and improvement in disease symptoms. [81]

7. Summary

The neuronal ceroid lipofuscinoses are a set of inherited metabolic diseases which result in accumulation of autofluorescent storage material and neurodegeneration in affected individuals. Using animal models of NCL we propose to test the hypothesis that autologous MSCs can have disease-specific defective genes repaired by SFHR and that such cells, once repaired, can replace missing enzymatic activity and reduce neurodegeneration when transplanted back into the affected donor. The use of autologous cells overcomes some technical issues associated with other forms of gene or cell therapy, such as immune rejection of transplants. MSCs are an easily accessible source of renewable, host cells and previous research indicates that they are capable of engrafting in and contributing to repair of many tissues affected by NCL-related degeneration. In fact, tissue degeneration seems to enhance engraftment and differentiation of MSCs in many *in vivo* models. Autologous cells must be genetically repaired at the site responsible for NCL phenotype in order to be effective therapeutic tools. SFHR can repair defective genes while leaving them under the control of their native promoter and other regulatory elements and has been used successfully in the past to modify cultured cells at an efficiency which is adequate for clinical use. The following research details our isolation and characterization of MSCs from murine and canine bone marrow, evaluation of their ability to correct NCL phenotypes in live animal and tissue culture models and testing of SFHR efficiency in modifying a marker gene within the MSC genome.

Chapter II

Isolation and Growth Characteristics of Murine Mesenchymal Stem Cells

1. Introduction

The first step towards treatment of NCLs with autologous MSCs is the development of protocols for consistently and efficiently isolating and culturing cells from patients which meet the requirements for successful therapy. These requirements include the ability of the cells to be grown and expanded in culture, undergo successful genetic modification, engraft into appropriate tissues, survive after transplant, and produce a therapeutic substance in vivo. In addition, the process should be as inexpensive and simple as possible in order to make treatment easily accessible to patients and their physicians. Although various options (as outlined in Chapter 1) such as isolation based on protein surface markers and culture with various cytokines, growth factors and additives has been shown to produce, in some cases, a more homogeneous population of cells, maintenance of high levels of homogeneity in culture has not yet been achieved. In addition, such techniques require significantly more time and costly materials than plastic-adherent culture alone. When considered in the light of eventual application to human patients, the more specific isolation procedures do not seem to present an advantageous cost/benefit ratio vs. plastic adherence alone. In addition, much of the *in vivo* evidence supporting the usefulness of MSCs as therapeutic agents relies on whole bone marrow or plastic adherence-purified MSCs. It seems that a highly purified initial culture is not necessary for establishing an MSC line with useful therapeutic potential. Although future results (ours or those coming from other labs) may lead us to modify this technique, we chose to test whether the most accessible purification method would generate MSCs meeting the requirements for treatment of NCLs in our animal models first.

In this section we describe our isolation and culturing procedures for murine MSCs and report the growth characteristics of our isolated cells. The results establish that we can successfully and consistently isolate a population of plastic adherent cells from murine bone marrow which display the morphology and growth features characteristic of murine MSCs described by other researchers. Our results also indicate that our purification procedures produce a cell population which meets the first requirement for therapeutic cells, the ability to grow and expand in culture.

2. Materials and Methods

Isolation of Murine Bone Marrow-derived Mesenchymal Stem Cells

Bone marrow-derived murine mesenchymal stem cells (mMSCs) were isolated from the femurs of male adult C57BL/6-Tg(ACTB-EGFP)1Osb/J mice (Jackson Labs stock #003291) 4-8 weeks of age at the time of collection. These mice constituitively express eGFP in most cell types. Mice were euthanized by CO_2 inhalation according to our standard ACUC approved protocol (UMC ACUC protocol # 1701). Both hind limbs were shaved and the area sprayed with 70% ethanol prior to dissection. Femurs were isolated by removing the skin on the upper portion of the leg and hip area and bisecting the pelvis on either side of the hip joint with dissecting scissors. Muscle was cut away from the hip joint, femur and knee joint with a razor blade. The femur was isolated by carefully cutting through the cartilage and ligament at each joint. It was then scraped with the razor blade to remove the last of the muscle and connective tissue. The intact femur was immersed in 70% ethanol before being transferred into the cell culture hood for further dissection.

Whole marrow was collected by flushing the marrow cavity of both femurs with MSC growth medium. The ends of the femur were removed with a sharp razor blade, exposing the medullary cavity. These bone fragments were diced finely with a razor and placed into an empty 15ml conical tube. Whole marrow was flushed from the cavity by inserting a 20 gauge needle attached to a 5ml syringe into the proximal end of the femur and flushing with 3ml of media into the same 15ml conical tube. This process was repeated with another 3ml of media from the opposite (distal) end of the femur to wash out any remaining cells, yielding a total of 12ml of marrow cell

suspension. The tube was vortexed for 2 minutes to wash cells from the diced fragments. After allowing the bone fragments to settle to the bottom of the tube for 1 minute, the media and suspended cells were transferred by pipette to a fresh 15ml conical tube. Cells were pelleted by centrifugation in a clinical centrifuge at low speed and the supernatant decanted. The pellet was resuspended in 5ml of MSC culture medium and cells were transferred to a T-25 flask and allowed to adhere for 24 hours before growth medium was changed.

MSCs were maintained in culture in standard MSC growth medium consisting of Gibco ά-MEM (Invitrogen cat# 12561) + 20% FBS, 2mM L-Glutamine, 1% Penicillin/Streptomycin solution. Cells were maintained at between 50-90% confluency at all times. Medium was changed every 48 hours and fresh medium was made every 2 weeks. When cells were passaged, medium was aspirated by vacuum and replaced with 2ml of Gibco brand 0.05% Trypsin-EDTA (Invitrogen cat#25300) which was allowed to wash over the cells briefly before being aspirated. 1ml of Trypsin-EDTA was added back into the flask and cells were incubated at 37°C. After 3 minutes, flasks were struck vigorously against a solid surface 5 times to loosen cells and then placed back in the incubator for another 2 minutes. After incubation was complete, the Trypsin-EDTA was neutralized with 9ml of culture medium. Cells were pipetted up and down with a 10ml culture pipette 20 times to create a single-cell suspension. The 10ml of cell suspension was then divided into two T-25 flasks (5ml in each), which were immediately placed back into the incubator to allow cells to adhere.

Cryopreservation of Mesenchymal Stem Cells

Frozen aliquots of cells were prepared for long term storage from flasks near 100% confluency. Cells were treated with Trypsin-EDTA as described above and neutralized with 9ml of culture medium. The resulting cell suspension was transferred to a 15ml conical tube and cells were pelleted by centrifugation in a clinical centrifuge at low speed and the supernatant decanted. The cell pellet was resuspended in 4ml of freezing medium consisting of 90% culture medium + 10% dimethylsulfoxide (DMSO, Sigma-Aldrich St. Louis, MO cat#D-5879). The cell suspension was divided into 2ml aliquots which were slow-frozen in isopropyl alcohol freezing chambers at -70°C.

After 3 days in the freezing chambers, frozen aliquots were transferred to storage boxes and kept at -70°C until used.

To prepare cryopreserved samples for culture, frozen aliquots of cells were quickly thawed by immersion in 37°C water. The 2ml of cell suspension was then pipetted into 10ml of growth medium in a 15ml conical tube. The tube was inverted several times and then cells were pelleted by centrifugation in a clinical centrifuge at low speed and the supernatant decanted. The pellet was resuspended in fresh growth medium and the whole aliquot was transferred to a T-25 flask. Cells were incubated as above and medium was changed after 24 hours.

Growth Media Comparison

Initially, we experimented with 4 different culture media to determine which would support growth of mMSCs the best. Isolated cells were always plated initially in normal MSC growth medium. After 24 hours, medium was changed to normal MSC growth medium with or without LIF (Chemicon cat#ESG1106) or embryonic stem cell growth medium (ESGM) with or without LIF. ESGM consists of DMEM + 10% FBS, 10% Newborn Calf Serum (NCS), 0.3mM adenosine, 0.3mM guanosine, 0.3mM cytidine, 0.3mM uridine, 0.3mM thymidine, 1% Penicillin/Streptomycin mix and 0.02μM ß-mercaptoethanol. Cells were cultured for at least 20 passages and monitored for morphology, growth characteristics and longevity.

Assay of Clonogenicity

Clonogenicity was assayed in our cultured cells by the limiting dilution method. Cells at passage 8 and 22 were trypsinized as normal for passaging and replated at a concentrations of 10,000 cells/cm^2, 4,000 cells/cm^2 and 400 cells/cm^2 (corresponding to approximately 25%, 10% and 1% confluency respectively) in T-25 flasks in standard MSC growth medium. Medium was changed 4 hours after the initial plating to remove non-adherent cells from the culture. Evaluation of colony formation was conducted by light microscopy over a course 7 days.

Morphology Documentation

The cellular morphology of cultured MSCs was monitored and recorded by phase-contrast light microscopy. Growing cells were visualized on a Zeiss inverted microscope (Carl Zeiss Inc. Thornwood, NY) at 20X magnification. Images were captured with a QImaging Micropublisher 5.0 RTV digital camera running on QCapture software (QImaging Burnaby, BC).

3. Results

Isolation of Murine Bone Marrow-derived Mesenchymal Stem Cells

Murine mesenchymal stem cells (mMSCs) were isolated from femoral bone marrow and characterized for growth properties and morphology. Initial cultures exhibited a mixed population of cells with varying morphologies. (see Figure 2-1) For approximately the first 30 days of incubation cell numbers in the culture slowly declined. During this time period, the heterogeneity of the cells within the flask decreased, yielding a mixed culture primarily composed of three types of cells. The most abundant were fibroblast-like cells with a non-symmetrical geometry. The other two types of cells, small round cells and large, flattened, lymphocyte-like cells, comprised only a small fraction of the culture at 30 days. After this transition, cell numbers in the culture began to increase and cultures usually reached confluency around day 40-45. This mixed cell population continued through passage 4, after which spindle-shaped, fibroblast-like cells became predominant, lymphocyte-like cells disappeared and small round cells, though still present, made up a much smaller proportion of the population.

Measurements of doubling time were recorded after cultures were first passaged (p1). Doubling time for the first 5-6 passages was lengthy, usually 5-15 days. (see Figure 2-2) At p8, mMSCs were doubling every 36-48 hours and this rate remained steady for the culture thereafter. Murine MSCs frozen at p3 and thawed several months later displayed the same pattern of growth rate change as cells continuously cultured, with doubling times stabilizing at approximately 48 hours around p8. Cells frozen after p8 and beyond displayed no lag in growth and began doubling at around 48 hours immediately upon being thawed.

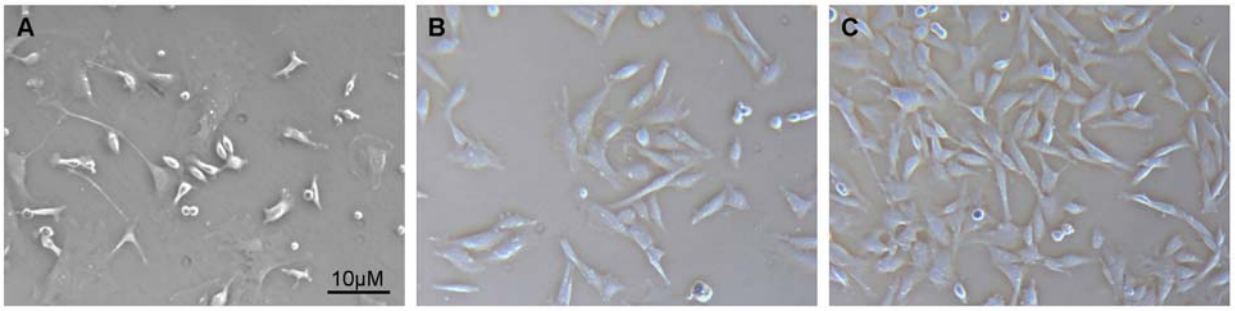

Figure 2-1: Murine MSCs at 24 hours after isolation (A), 30 days after isolation (B) and passage 12 (C). Newly isolated MSC cultures contained a mixed population of cells composed primarily of fibroblast-like cells, small round cells and flattened, lymphocyte-like cells. At 30 days (B), when cells were approaching the appropriate density for their first passage, the large flattened cells had disappeared and fibroblast-like cells were the main constituent of the population. After 12 passages (C), the MSC culture still contained a morphogenically heterogenous population, with fibroblast-like cells predominating.

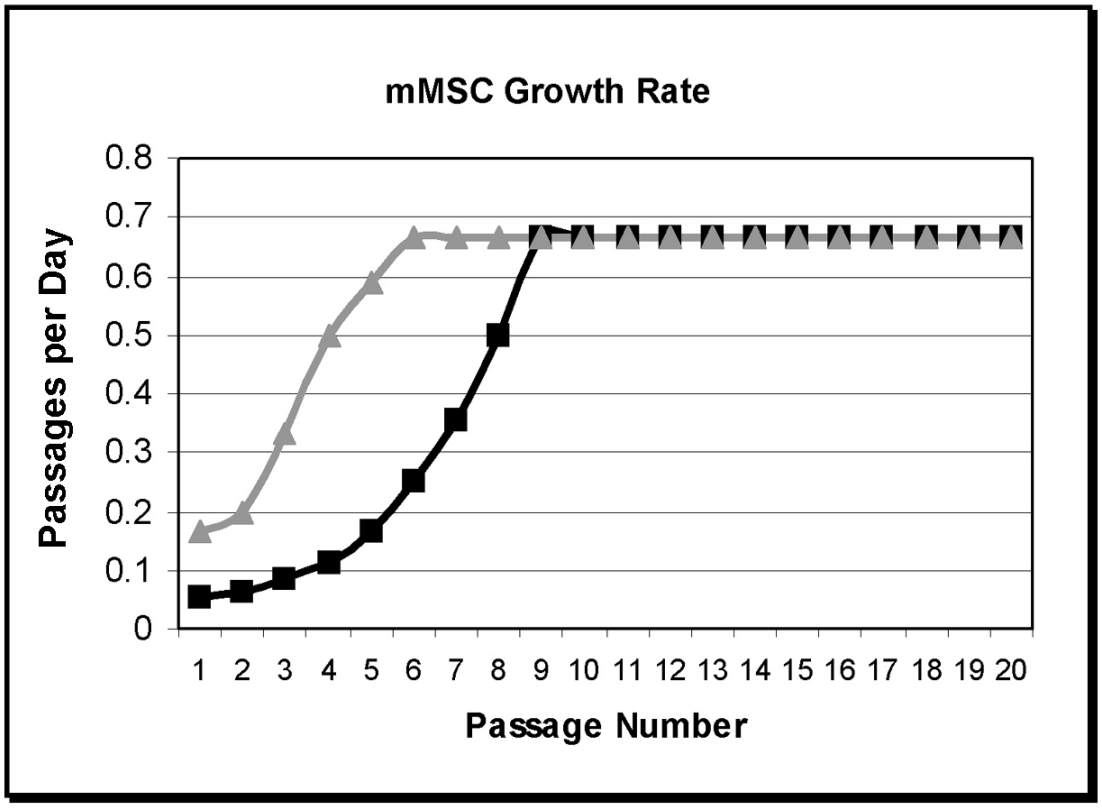

Figure 2-2: The growth rate of murine MSCs was measured for both freshly isolated cells (black squares) and frozen/thawed cells (grey triangles). Rate of doubling is measured in passages per day. Each population eventually reached a stable doubling rate of about 0.67 passages/day (about one doubling every 36 hours). Frozen/Thawed cells (which were frozen at passage 5) display a doubling rate immediately after thawing that is equivalent to that of a cell of the same passage which had never been frozen.

Murine MSCs were continuously cultured up to 300 passages. After p8, when doubling times stabilized at 36-48 hours, no discernible difference in cellular morphology, growth rate or culture characteristics were observed. Even at the highest passage numbers, the culture population remained mixed between fibroblastic, spindle-shaped cells and a very limited number of small, round cells. Whether these two populations represent similar populations in different stages of their growth cycle or phenotypically distinct cell lines has not been determined.

Growth Media Comparison

In our initial isolation of murine MSCs we were unsure which culture conditions would yield the best results for isolating a homogeneous population of multipotent, self-renewing cells quickly and with minimal manipulation. We hypothesized that growth factors and media which promote the primitive phenotype of murine embryonic stem cells (mESCs) such as leukemia inhibitory factor (LIF) might improve the yield of mMSCs in our cultures. To test this hypothesis we cultured whole bone marrow in four different media and compared the growth rate, cellular morphology and population characteristics of the cells in each. There was no discernible difference between the cell populations grown in MSC medium and ESC medium. Nearly identical growth rates, cell types and cell type proportions were observed for both conditions. Likewise, there was no discernible difference between the MSC+LIF and the ESC+LIF groups. Small differences were observed between the media with LIF and the media without LIF. In cultures containing LIF, the doubling time of the cells was slightly longer and the cells adhered less readily to the plastic (whereas in cultures with no LIF, cells were observed to adhere very strongly to the uncoated plastic culture flasks). No differences were detected between the LIF^+ and LIF^- conditions for cellular morphology or proportion of cell types within the population. After analysis of these data and comparison with the results for standard MSC medium, we determined that the alternate media did not contribute any significant advantage to growth rate or self-renewal capacity over standard MSC medium, which was used it in all further experiments.

Assay of Clonogenicity

Our MSC isolation and growth procedures call for our cultured cells to be maintained at a densities of 50% (~20,000 cells/cm^2) to 100% (~40,000 cells/cm^2) confluence after their initial passage. To test the clonogenicity of our cell population, MSCs at passage 8 and 22 were plated at limiting dilutions (10,000 cells/cm^2, 4,000 cells/cm^2 and 400 cells/cm^2 - corresponding to approximately 25%, 10% and 1% confluency respectively)and observed for their ability to form colonies. After 4 hours, when non-adherent cells were removed, the remaining MSCs were observed to be evenly distributed throughout the culture flask with the vast majority adhering as isolated, single cells in all samples.

Cells plated at a concentration of 10,000 cells/cm^2 grew very slowly over the course of 7 days, but were observed to proliferate and reached ~80% confluency by the end of observation. It could not be definitively established whether proliferating cells originated from a single-cell colony. Cells plated at 4,000 cells/cm^2 did not proliferate, but remained adhered as single cells during the course of observation. No significant cell death was observed for this group. Cells plated at 400 cells/cm^2 failed to proliferate and experienced significant cell death (observed as a decrease in adherent cells and an increase in floating cells) after 2 days in culture. No adherent cells could be detected in this group at the end of the 7 day observation period. There was no detectable difference between the passage 8 and the passage 22 groups.

4. Discussion

Stem Cell Identity

MSCs are bone marrow-derived adult stem cells. In order to establish that we have isolated MSCs we must demonstrate that the cells in our culture meet the definition of an adult stem cell. This definition is generally considered to include clonogenicity, self-renewal and the ability to differentiate into one or more cell types. In these experiments we have tested whether our isolated cells are clonogenic and self-renewing. While they have been demonstrated to self-renew by growing for more than 300 passages in culture, our assay of clonogenicity revealed that there was a density limitation on their proliferative ability. While cells plated at 10,000 cells/cm^2

were observed to adhere primarily as single cells, we cannot be certain that they began proliferation as single celled colonies due to the ability of MSCs to migrate along the plastic substrate in culture (see figure 7-6). The results for lower density platings suggest that the cells we have isolated are not completely clonogenic under our current culture conditions.

Some evidence suggests that MSCs secrete cytokines and growth factors such as fibroblast growth factor (FGF), vascular endothelial growth factor (VEGF) and interleukins as well as numerous extracellular matrix components. [82][83][84][29] It is probable that these factors contribute to the proliferative potential of MSCs *in vitro* and that a certain culture density which maintains these factors at a level conducive to proliferation is necessary for growth of our cells. We have not yet tested whether including such mitogenic factors affects the clonogenicity of our isolated MSCs.

It is also important to note that clonogenicity in culture may not be a useful measure of whether a cell qualifies as an adult stem cell. Haematopoietic stem cells which are clonal *in vivo* (i.e. – a single cell is capable of repopulating the entire haematopoietic system of a lethally irradiated animal) are frequently not clonal *in vitro*. MSCs which are clonal in one culture condition (high serum for example) might be non-clonal and even non-self-renewing in another culture condition. In addition, adult stem cells are never found as single cells in their natural state. MSCs are surrounded by supporting stromal cells and HSCs in the bone marrow. Intestinal crypt, neural and dermal stem cells are all surrounded in their native environment by specialized cells that create a specific microenvironmental niche that supports the maintenance of the resident stem cells undifferentiated state. It is likely that such cells work to reestablish similar micro-environments when they are grown *in vitro* and that cell density plays a part in this process in the absence of certain other factors in the medium. [85] In fact, we should probably consider whether clonal cells are even optimal for the treatment goals we have previously outlined. Clonal cells show a propensity to remain undifferentiated and proliferative even outside their normal stem cell niche. Is this a natural state or is it an abnormal state brought on by specific culture conditions and biochemical alterations in individual cells? Is clonality actually an indicator of tumorigenic

propensity? If clonality in adult stem cells represents the latter, then it is an undesirable trait for cells which will eventually be used in transplantation therapy. Once transplanted back into a living recipient, we do not want our isolated MSCs to maintain their stem cell status or continue to proliferate, we want them to incorporate as terminally differentiated, tissue-specific cells.

Thus, despite their reluctance to grow clonally with our standard culture conditions, we believe the cells we have isolated meet the required criteria for being characterized as MSCs. Although we do not consider clonogenicity to be required for our the success of MSC implantation therapy, it might be useful to be able to isolate clonal lines after performing genetic modifications on our MSCs. If necessary, we will carry out further experiments to determine which modifications to our standard culture medium will support clonal growth.

Laboratory to Clinic

The ultimate goal of this research is to develop autologous stem cells as a treatment for human neurodegenerative diseases. With that in mind, it is important to consider the transplantability of our methods from the laboratory to the clinic. One major issue involved in transferring these procedures to human clinical treatments is the use of animal products in culture medium. While issues of contamination with foreign viruses and prions have been recognized and dealt with, it is also known that cultured human cells are able to take up and express foreign sialic acid residues on their cell surface when exposed to them in culture. [86] The fetal bovine serum used in our culture medium contains such sialic acid residues and it is likely that our MSCs become contaminated with these during the culturing process. Since most humans are sensitive to these antigens, cells expressing them are likely to be targeted and attacked by the host immune system after transplant. This could render many of the benefits of using autologous stem cells moot.

Our use of bovine serum products for our current research is justified because we are already using allogeneic, rather than autologous cells for our murine transplant work. As a result, it is unlikely that sialic acid contamination renders the cells any more immunogenic than they would be otherwise. We are also performing transplants into an immunoprivileged site (the vitreous of the eye) which does not normally undergo inflammatory immune responses to foreign antigens.

However, transferring these techniques to human therapy will probably require modification of the culturing procedure. These modifications will likely take one of four forms.

- MSCs might be purified but not cultured before transplant. This method has been used before in some experiments and has the advantage of obtaining cells which are immunologically "clean" but has a very poor efficiency (requiring the extraction of large amounts of marrow from the donor) and is limited by the lack of definitive cell surface markers for MSCs.
- MSCs might be cultured in medium containing autologous serum. Experiments proving the effectiveness of this method have been carried out previously. [87] However, the technique is limited by the cost of acquiring sufficient quantities of serum and the inability of some patients to provide enough serum to adequately expand their own cells.
- MSCs might be cultured in serum free medium. Serum substitutes are available which readily support MSC expansion. [88] However, serum substitutes still contain some animal proteins, including small amounts of sialic acids. There is some evidence that sialic acid loading with serum substitutes is significantly less but it has not been established that serum substitutes render cultured cells free of foreign cell surface antigens. [89]
- The host might be rendered insensitive to specific foreign antigens by hyposensitization or induction of tolerance in the host immune system. It appears that MSCs already possess innate properties which induce T cell tolerance after transplant. [90] These properties may or may not render the presence of foreign surface antigens "invisible" to the host immune system. If the cell's natural ability to suppress an immune response is inadequate, the process could be strengthened by inducing certain factors in the donor cells prior to transplant that help them to avoid targeting by host T cells or by concurrent administration of another form of toleragenic treatment.

By thoroughly characterizing the cells we are using currently, we hope to be able to define features which will allow us to ensure that any modified culture procedure is still yielding the same population of cells.

Chapter III

Molecular Characterization of Isolated Murine Mesenchymal Stem Cells

1. Introduction

Extensive work has been done to characterize the molecular identity of bone marrow-derived MSCs. Although the body of work published on this subject is significant, there is little consensus as to the details. While nearly all MSC isolates share in common the basic features of plastic adherence, self-renewal, multipotentiality and high proliferative ability, analysis of the transcriptome and proteome of isolates disagrees in many cases. The Chemicon product catalog (www.chemicon.com) lists over 27 antibodies for cell surface markers associated with MSC identity. This number does not include some of the recently analyzed surface proteins mentioned in Chapter I, such as SSEA4 and *frizzled*. In order to track changes in MSC identity after implantation, it is important to know the molecular composition of our cultured cells *in vitro*. However, performing fluorescence activated cell sorting (FACS) analysis or immunohistochemistry (IHC) for every known or suspected marker of MSCs would be prohibitively expensive and time consuming. Many laboratories make use of transcript amplification through reverse transcriptase polymerase chain reaction (RT-PCR) or microarray chips to track the transcriptome of their cells before and after implantation or differentiation as an alternative to antibody labeling.

We chose to use a combination of protein and transcript-specific tests to establish the molecular identity of the MSCs isolated and used in this study. We limited analysis of cellular proteins to accomplish two goals. The first was to establish the identity of our cells as MSCs and to eliminate the possibility of HSC contamination in our cultures. The second was to examine undifferentiated and *in vitro* differentiated cells for indicators of proliferation, pluripotency and neural differentiation. We used RT-PCR to characterize expression of a wider range of genes that include indicators of pluripotency, self-renewal capacity and differentiation toward

adipogenic, osteogenic and neurogenic fates. We show that our isolated cells express some proteins and transcripts typical of murine MSCs. The data also reveal that some proteins that other groups have used as indicators of MSC identity are not present in our MSC population. Protein and RNA expression for differentiated cells also indicates that the MSCs we have isolated are able to undergo both adipogenic and neurogenic differentiation *in vitro*.

2. Materials and Methods

FACScan Analysis

Cells were trypsinized as described above, washed twice in ice-cold wash buffer (WB, 1x PBS + 5% heat-inactivated FBS) and resuspended in WB at a concentration of $1x10^6$ cells/ml. Antibody was added at the concentration called for by the manufacturer's instructions and incubated at room temperature with the cells for 45 minutes. Cells were washed once in WB to remove unattached antibody. For primary antibodies conjugated to fluorescent markers, cells were then washed once more with ice-cold 1xPBS (PBS) and finally resuspended in PBS. For unconjugated primary antibodies, cells were incubated with fluorophore conjugated secondary antibody in WB for an additional 30 minutes, washed once with WB, once with PBS and resuspended in PBS. Cells were kept on ice prior to FACScan analysis.

Cells were labeled with appropriate antibodies to determine expression levels of the cell surface antigens CD34 (Phycoerythrin (PE) conjugated rat α-mouse CD34, BD Pharmingen cat# 551387), CD44 (PE-Cy5 conjugated rat α-mouse CD44, BD Pharmingen cat#553135), CD73 (PE conjugated rat α-mouse CD73, BD Pharmingen cat#550741), CD105 (rat α-mouse CD105, unconjugated, BD Pharmingen cat#550546) and stem cell antigen 1 (SCA1, FITC conjugated rat α-mouse SCA1, BD Pharmingen cat#557405). Unconjugated antibodies were detected with an α-rat IgG secondary antibody (FITC conjugated goat α-rat IgG, Pierce Biotechnologies cat#31629). Cells were also labeled with Aldefluor which detects the bone marrow stem cell associated enzyme aldehyde dehydrogenase through the conversion of a substrate into a fluorophore. Cells were prepared as above and incubated with the substrate according to the manufacturer's instructions (Aldefluor Staining Kit, StemCo Biomedical Inc. Durham, NC).

Labeled cells were analyzed on a FACScan 488 Benchtop Analyzer (Becton Dickinson, Franklin Lakes, NJ) using CellQuest software.

Immunohistochemistry

MSCs were plated in 6-well plates as described in Chapter IV and examined by immunohistochemistry for expression of self-renewal, pluripotency, neurogenic precursor, neural and glial specific proteins. In addition to labeling undifferentiated cells of several passage numbers, a total of 10 plates were seeded for each neurogenic induction protocol. At 0, 2, 4, 6, 8, 12, 24, 48, 72, and 96 hours post-induction, medium was removed and cells were washed with ice cold 0.17M Na-cacodylate to remove residual medium. Cells were then fixed in standard IM fixative (0.1% glutaraldehyde, 3.5% paraformaldehyde, 0.13M sodium cacodylate and 0.13mM calcium chloride, pH 7.4) for 2 minutes. Fixative was removed and cells were washed twice with 0.17M Na-cacodylate and then stored in 0.17M Na-cacodylate at 4°C until examined by IHC.

Before antibody labeling, fixed cells were incubated in permeabilization buffer (1x TBS, 2% BSA, 0.0001% Triton X-100) for 45 minutes at room temperature then washed 3 times for 5 minutes each in permeabilization buffer before addition of primary antibody diluted in blocking buffer (1x TBS, 2% BSA). Cells were incubated in primary antibody overnight at room temperature then washed 3 times for 5 minutes each in permeabilization buffer. Cells were incubated with secondary antibody (either Goat α-mouse IgG – AP1245, Chemicon or Goat α-rabbit IgG – AP1325, Chemicon) diluted in blocking buffer for 2-4 hours then washed 6 times for 5 minutes each in 1x TBS, once for 10 minutes in permeabilization buffer, with a final wash in 1x TBS for 5 minutes. Cells were counterstained with DAPI (Invitrogen cat#D3571) and kept hydrated in 1x TBS at 4°C until examined by confocal microscopy. Expression of proliferating cell nuclear antigen (PCNA, sc-7907, Santa Cruz Biotechnology), glial fibrillary acidic protein (GFAP, AB5804, Chemicon), microtubule associated protein (MAP2, cat#65783, ICN Biomedicals), Nestin (MAB353, Chemicon), Oct4 (AB3209, Chemicon), and Neurofilament M (NF-M, AB1981, Chemicon) were examined using this protocol.

Fluorescently labeled cells were visualized with a Zeiss Meta NLO2 photon laser scanning confocal microscope at the University of Missouri, Columbia Molecular Cytology Core Facility. Images were captured using Zeiss microscopy and image analysis software. Six fields of view or a total of 20 cells (whichever resulted in the higher number of cells) were analyzed for each condition in the experiment.

Isolation of Total Cellular RNA from Cultured Cells

Total cellular RNA was isolated from cultured cells or control tissue with the Qiagen RNeasy-mini kit. (QIAGEN cat# 74106) Cells were grown in standard T-25 flasks and trypsinized as in Chapter 2 then centrifuged to form a pellet. The pellet was washed once with ice cold 1x PBS and then resuspended in buffer RLT. The remainder of the procedure followed the manufacturer's instructions.

Neurogenic and Adipogenic Induction of Cells Analyzed by RT-PCR

MSCs were plated in T-25 flasks at a concentration of 2000 cells/cm^2 . RNA was purified from cells exposed to adipogenic and neurogenic differentiation protocols (see Chapter IV). For the adipogenic protocol, cells were collected and processed 24, 48, 120 and 240hrs after induction. For neurogenic induction, a total of ten plates were seeded for each protocol. At 2, 4, 6, 8, 12, 24, 48, 72, and 96 hours post-induction, medium was removed and RNA was isolated. In addition, three plates were seeded according to the BHA medium protocol, but at 24hrs after addition of induction medium, it was replaced by standard MSC growth medium. These cells were collected for RNA isolation at the 48, 72 and 96 hour time points (i.e. – 24, 48 and 72 hours after replacement of induction medium) to examine possible reversion.

Reverse Transcriptase – Polymerase Chain Reaction

Sequence specific forward and reverse primers for RT-PCR analysis of differentiated MSCs were designed with the aid of the Genetics Computer Group (GCG) software –PRIME function. Individual primers were selected based on compatible primer/template melting temperature (TM) and primer length. Selected primers were synthesized by Invitrogen's custome primer services.

Primer	Sequence	Accession#
CD34-f	794 5′- GCC AAT AGC ACA GAA CTT CC -3′ 813	NM133654
CD34-r	1428 5′- TCT TCC CAC CAC AAC TTG AC -3′ 1409	
CD44-f	441 5′- CCA ACA CCT CCC ACT ATG AC -3′ 460	M30655
CD44-r	1015 5′- CAG CTT TTT CTT CTG CCC AC -3′ 996	
CD73-f	2156 5′- TGG CAG GGA GGA GAG GAT GG -3′ 2175	NM011851
CD73-r	2782 5′- GAA GGA AGG AGA GAG GCA GGG -3′ 2762	
CD105-f	776 5′- TGC TAC CAT CCC TTA CCT CC -3′ 795	NM007932
CD105-r	1468 5′- TCA TGA CCT GAT TGC CAC AC -3′ 1449	
SCA1-f	27 5′- CCT TCT CTG AGG ATG GAC AC -3′ 46	NM010738
SCA1-r	563 5′- TTT CAC ACA CTA CTC CCA CC -3′ 544	
OCT4-f	538 5′- GGA GAA GTG GGT GGA GGA AG -3′ 557	X52437
OCT4-r	1192 5′- ATG ATG AGT GAC AGA CAG GC -3′ 1173	
NANO-f	573 5′- ACT CTC CTC CAT TCT GAA CC -3′ 592	AB093574
NANO-r	1144 5′- CTT TGC CCT GAC TTT AAG CC -3′ 1125	
TELO-f	1089 5′- AAC CTC CAG CCT AAC TTG AC -3′ 1108	NM009354
TELO-r	1748 5′- CTT GCT CCA CAC ACT CTT AC -3′ 1729	
NEST-f	3240 5′- GAA CAA GAG ACC CAG CAG CC -3′ 3259	NM016701
NEST-r	3831 5′- CTC CAT CCT CCA CCA CAT CC -3′ 3812	
AMYL-f	874 5′- TGA TGA TGA GGA TGT GGA GG -3′ 893	NM007471
AMYL-r	1570 5′- ATT GTA GAG CAG GGA CAG AG -3′ 1551	
GFAP-f	710 5′- GAG AGA GAT TCG CAC TCA ATA C-3′ 731	NM010277
GFAP-r	1273 5′- TCC TTA ATG ACC TCA CCA TCC -3′ 1253	
NEUD-f	311 5′- AGA AGA AGA GGA GGA GGA GG -3′ 330	NM010894
NEUD-r	1010 5′- AGG GTA GTG CAT GGT AAA GG -3′ 991	
NFLM-f	1278 5′- ACA GCC CTC AGT CAC AAT ATC -3′ 1298	NM008691
NFLM-r	1970 5′- TCC TCC TTT TTC TCC ACC TTC -3′ 1950	
SYNA-f	1405 5′- TGG ATG AAA TGG GTG GAG AG -3′ 1424	NM009305
SYNA-r	2089 5′- GAA AGG GTG GAG AAG GTA GG -3′ 2070	
BMP5-f	1673 5′- CGT GAG AGC AGC CAG CAA AC -3′ 1692	NM007555
BMP5-r	2348 5′- CCC ACC ACA CCC CAA CAA AAG -3′ 2328	
PRO2-f	1 5′- ATC ATC ACC ACC AAG AGC AG -3′ 20	NM008933
PRO2-r	538 5′- CAG ACA TCG ACA TGG AAT GG -3′ 519	
CERU-f	3159 5′- TGG TAT GTG ATG GGA ATG GGC -3′ 3179	BC062957
CERU-r	3691 5′- GGG GTG GGG AGG AGA AAG AG -3′ 3672	
LEPT-f	806 5′- ATA AGA GCC ATC CCA TCC CC -3′ 825	NM008493
LEPT-r	1384 5′- ACC CTC CCT CTA ACA CAT CC -3′ 1365	

Figure 3-1: Primers for RT-PCR screening of MSC transcripts. Primers were selected to produce products of 500-700bp in total length. Column 3 indicates the GenBank accession number of the cDNA sequence used to design the indicated primers.

(see Figure 3-1) All reactions were performed using the QIAGEN OneStep RT-PCR kit (QIAGEN Inc., Valencia, CA). Final concentration of template RNA was 50ng in a 50µl reaction. Primers were prepared according to the kit specifications at a final concentration of 0.6µM each and reactions were run on an Eppendorf Mastercycler Personal thermocycler (Eppendorf NA, Westbury, NY) with the following protocol:

Reverse transcription	50°C	30 minutes
PCR activation step	95°C	15 minutes
Denaturation	94°C	30 seconds
Annealing	58°C	30 seconds
Extension	72°C	2 minutes
(repeat Denaturation, Annealing and Extension cycles 30 times)		
Final Extension	72°C	2 minutes

RT-PCR products were separated on a 2% agarose gel and visualized by ethidium bromide fluorescence in a Bio-Rad Fluor-S Multi-imager (Bio-Rad Laboratories, Hercules, CA).

3. Results

FACScan Analysis of Surface Marker Expression

Numerous studies have examined the surface protein expression of MSCs in an effort to isolate a distinguishing marker or set of markers that will allow specific isolation of pure MSCs from bone marrow or peripheral blood. To date, no single marker or group of markers have been identified which allow for selection of a pure population of MSCs. However, it is possible through antibody labeling of a plastic adherent population to establish that cells expressing markers consistent with MSC identity are present and that cells expressing markers for other, potentially contaminating, populations are not. CD34 is known to be present on both HSCs and epithelial progenitor cells (EPCs) in BM and is not present on MSCs. CD44, CD73, CD105 and SCA1 are present on many isolates of murine MSCs. Therefore, we examined our cultured cells for expression of CD34, CD44, CD73, CD105 and SCA1 to demonstrate the presence of MSCs and determine the purity of our isolated population. Cells were counted as marker positive if their fluorescence level was at least .5 log units above that of unlabeled control cells.

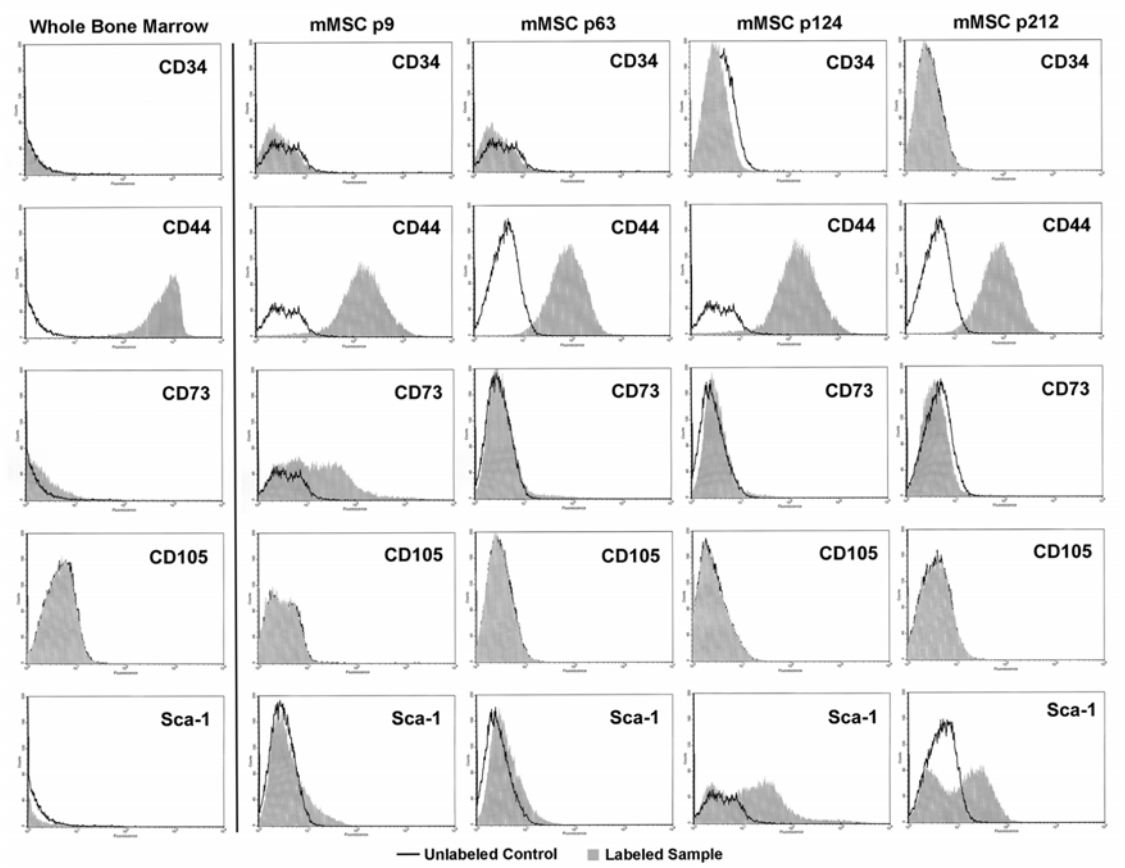

Figure 3-2: FACScan analysis of protein surface markers. Either cells from whole, fresh bone marrow or cultured murine MSCs of various passages were labeled with fluorescent antibodies and their fluorescence measured by FACScan analysis. Labeled cell samples (filled gray) are compared to unlabeled control samples (black line). Only labeled cells displaying a fluorescence value at least one log unit greater than the fluorescence measured at the population peak for unlabeled control cells were counted as positive for expression. Expression of these markers was also measured at passage 24, 77, 86, 192 and 272 (data not shown). The percentage of cells in each population counted as positive is displayed in Figure 3-3. X-axis = relative log fluorescence. Y-axis = % counts.

	Passage Number								
	9	**24**	**63**	**77**	**86**	**124**	**192**	**214**	**272**
CD34	4.2%	0.4%	0.4%	0.5%	0.5%	0%	0%	0%	0%
CD44	95.7%	91.1%	91.1%	92.5%	92.5%	98.1%	98.1%	95.8%	95.8%
CD73	40.9%	21.6%	15.2%	2.4%	1.1%	1.1%	3.7%	0.7%	0.7%
CD105	0%	0%	0%	0%	0%	0%	0%	0%	0%
Sca1	11.89%	19.1%	26.3%	24%	36.0%	49.6%	63.2%	70.3%	70.3%
Aldefluor	98.8%	98.8%	99.9%	99.9%	99.9%	99.0%	99.9%	99.9%	99.9%

Figure 3-3: Percentage of cells expressing surface antigens by time point. Expression of individual markers was tracked from the earliest passage where mMSC cultures appeared to become morphologically stable to a maximum of 272 passages. Cells were counted as positive for antigen expression if their fluorescence reading was at least 1 log unit higher than unstained control cells.

Figures 3-2 and 3-3 show expression levels for the indicated markers at several passage numbers. The data show that, at early time points, expression of CD34 was present on a small percentage (4.2%) of the cells examined, indicating that the MSC culture was contaminated with adherent EPCs or HSCs. However, at passage 24 and beyond, expression of CD34 is essentially zero, indicating that serial passage has eliminated these cells from the population. Expression of other MSC markers was mixed for this population of cells. CD44 is a cell-surface glycoprotein involved in cell-cell interactions, cell adhesion and cellular migration. It is a receptor for hyaluronic acid and collagen, both components of the extracellular matrix of the bone marrow. Our MSC cultures expressed CD44 at high levels at all time points we examined. Expression levels fluctuated between a minimum of 91.1% positive cells and a maximum of 98.13% positive cells. Given its roles in cell adhesion and cell-cell interaction it is not unsurprising that MSCs selected by plastic adherence and grown at high concentration express this marker consistently. Approximately 41% of passage 9 cells were positive for CD73 expression in our cultures, but expression of CD73 steadily declined until passage 64 where it plateaued at between 0.72 – 3.66% for all subsequent time points. Expression of SCA1 fluctuated between 10 – 20% during early passages in our cells but steadily increased after passage 84 until expression levels plateaued with ~70% of cells positive. At all time points examined, expression of CD105 was undetectable in our mMSCs.

Since our cells were derived from eGFP expressing donor mice, we were also able to visualize them on FACScan analysis by their green fluorescence. We observed that expression of eGFP was attenuated after 10-12 passages in culture and completely absent from all cultures after 20 passages. (data not shown) At 10-12 passages, two distinct populations of $eGFP^+$ and $eGFP^-$ cells could be observed in our cell populations with relatively little overlap between the two (i.e. cells tended to be bright or dark but not dim). Gene silencing is a common phenomenon in cells that have been transfected with a marker ex vivo, but it was unexpected for our cells, which are derived from mice which continue to express high levels of eGFP in all tissues throughout their lifetime. For transplantation experiments, cells young enough to retain high level expression of eGFP throughout the population were used.

FACScan Analysis of Aldehyde Dehydrogenase Expression

The Aldefluor reagent is a fluorescent marker system developed by StemCell Technologies Inc. Primitive haematopoietic cells are relatively resistant to alkylating agents such as the active derivatives of cyclophosphamide (e.g. 4-hydroxy peroxycyclophosphamide (4-HC) and mafosphamide). This resistance is due to the selective expression in primitive haematopoietic cells of the enzyme aldehyde dehydrogenase (ALDH). [91] Because mMSCs display these same resistances, we evaluated whether aldehyde dehydrogenase expression could be a useful marker for our cells.

We tested cells of different passage numbers, from passage 9 – 272, with the Aldefluor reagent. At all time points measured the vast majority of cells (between 98-100%) were not only positive for Aldefluor-specific fluorescence (i.e. – fluorescence was at least 0.5 log units higher than background) but highly positive (usually between 2-3 log units higher than background). Control reactions were performed with an inhibitor of ALDH function (diethylaminobenzaldehyde or DEAB) which blocks the accumulation of fluorescent substrate in HSCs by inhibiting aldehyde dehydrogenase activity. The cells in our control samples were also highly fluorescent. This result suggests that some or all of the fluorescence-inducing enzymatic activity observed in our isolated MSCs is coming from a source that is not aldehyde dehydrogenase. The manufacturer's technical literature notes that this is a possibility for some cell types. As a result, we concluded that the Aldefluor reagent is not an informative marker for our cells.

Fluorescence IHC Analysis of Undifferentiated and Neurodifferentiated mMSCs

Murine MSCs at passage 150 were plated and neurally differentiated using the Black/Woodbury BHA protocol as described in the Materials and Methods section of Chapter IV. In addition, 6-well plates of undifferentiated mMSCs at passage 8 and passage 150 were prepared and fixed as controls. The expression of GFAP, MAP2, Nestin, Neurofilament M (NF-M), Oct4 and PCNA were evaluated by fluorescence IHC. (see Figures 3-4 and 3-5) Proteins were labeled by fluorescently tagged antibodies (displayed in green) and cell nuclei were counterstained with DAPI. Co-staining with Cy5 and DAPI is displayed in yellow. Labeling revealed no differences

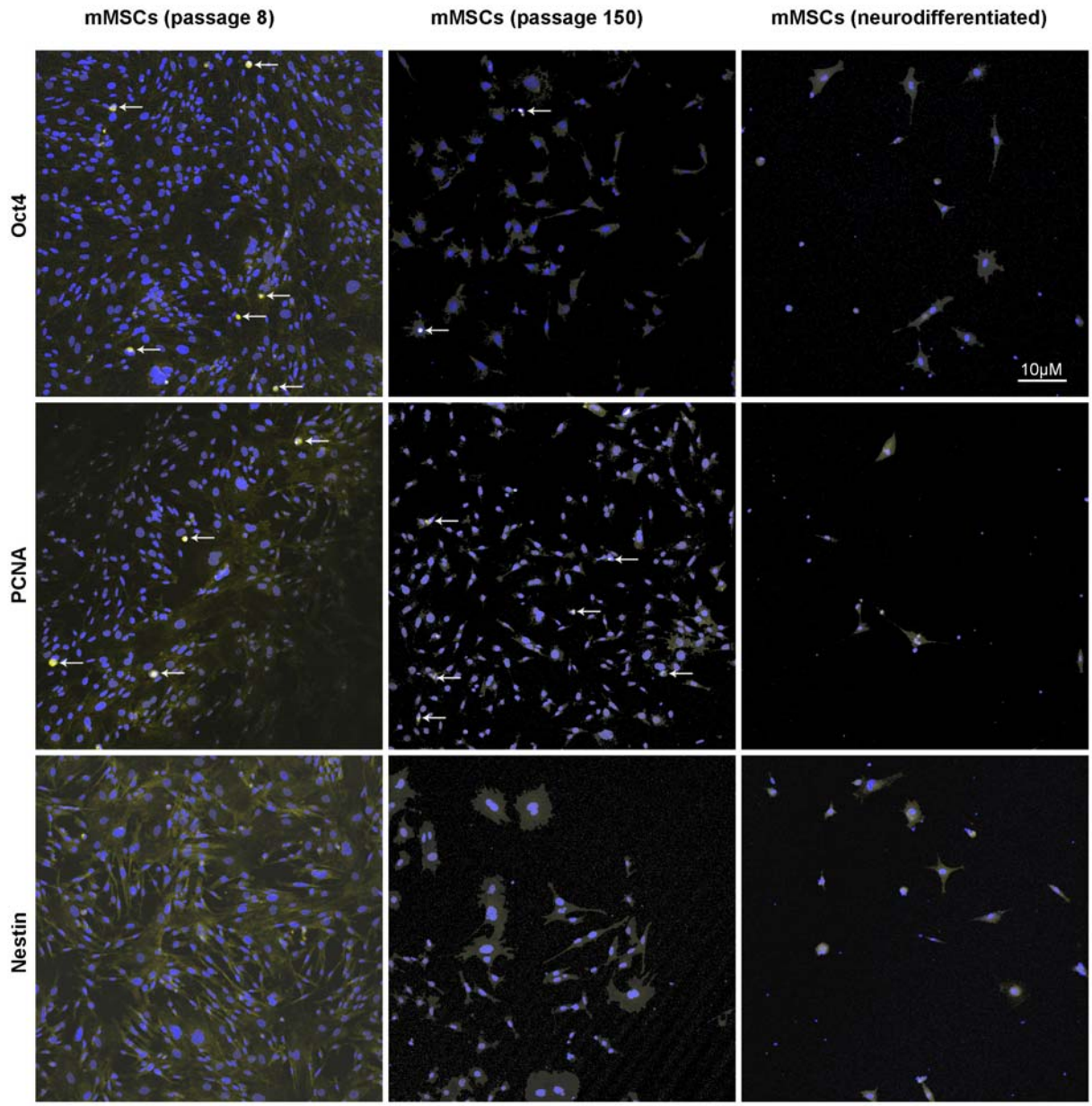

Figure 3-4: Murine MSCs at passage 8 (first column), passage 150 (second column) and after neurodifferentiation (third column). Cells were labeled with antibodies for Oct4 (top row), proliferating cell nuclear antigen (PCNA, middle row) and Nestin (bottom row). Secondary antibodies conjugated to the Cy5 fluorophore were used to detect the respective antigens (green). MSCs were counterstained with DAPI nuclear stain (blue). White arrows indicate nuclei co-stained with DAPI and Cy5 (white). Passage 150 MSCs were used in the neurodifferentiation experiment.

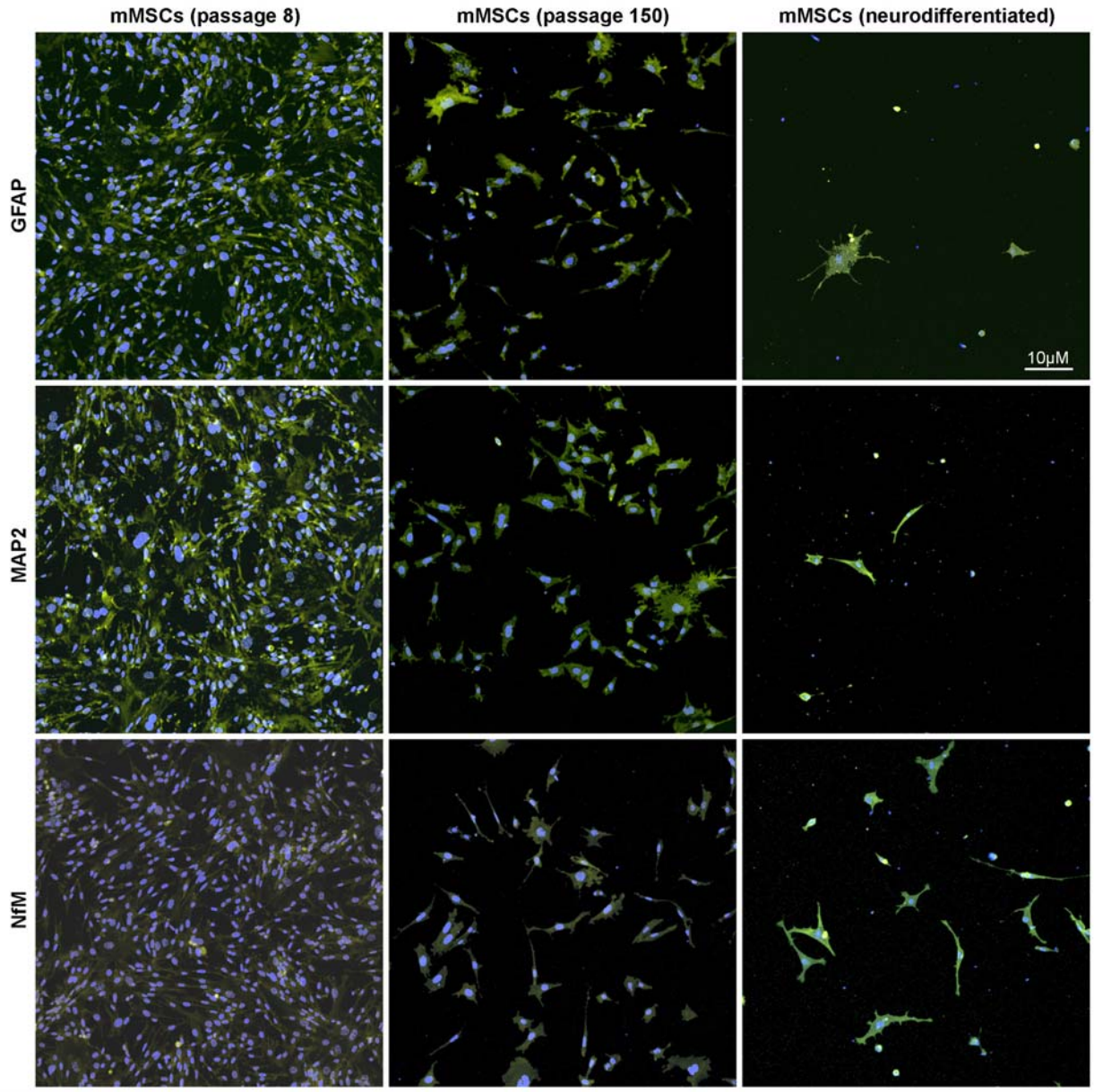

Figure 3-5: Murine MSCs at passage 8 (first column), passage 150 (second column) and after neurodifferentiation (third column). Cells were labeled with antibodies for glial fibrillary acidic protein (GFAP, top row), microtubule associated protein 2 (MAP2, middle row) and Neurofilament M (NfM, bottom row). Secondary antibodies conjugated to the Cy5 fluorophore were used to detect the respective antigens (green). MSCs were counterstained with DAPI nuclear stain (blue). Passage 150 MSCs were used in the neurodifferentiation experiment.

between low and high passage number undifferentiated mMSCs, but did indicate that neurally differentiated mMSCs stop proliferating and express different proteins. Undifferentiated mMSCs at passage 8 and 150 expressed detectable levels of GFAP and MAP2. They displayed low level expression of Nestin and a small number of individual cells in both cultures labeled positive for Oct4 and PCNA. No expression of neurofilament M was detectable in either group. Expression of these proteins is consistent with the results some other groups have reported for MSCs. [92][39][33] Neurodifferentiated mMSCs had a similar level of GFAP and MAP2 expression to their undifferentiated counterparts. However, the differentiation protocol eliminated expression of Nestin, Oct4 and PCNA and induced expression of NF-M. The strong expression of NF-M in a large number of cells (predominantly in cells which extended branching processes) coupled with the loss of PCNA expression indicates that the cells may have been responding to the differentiation protocol by up regulating neural-specific gene expression and discontinuing proliferation.

RT-PCR Analysis of Undifferentiated mMSC Gene Expression

We isolated total RNA from undifferentiated mMSCs at passages 14, 92 and 220. We examined these samples for the presence of 17 transcripts by semi-quantitative RT-PCR. Several of the transcripts were specific for cellular types that MSCs have shown the potential to be differentiated into after *in vivo* transplantation. Since it has been reported that MSCs express several neural specific genes before any differentiation, we also used a comprehensive panel of neural markers to examine the cells. In addition, we included several markers for MSCs and other primitive, undifferentiated stem cells. (see Figure 3-6)

CD34 is a marker of haematopoietic stem cells which is not found on MSCs. FACScan analysis revealed undetectable amounts of protein expression for CD34 in our mMSC population after passage 24. Initial detection of CD34 in our cultures is suspected to be a result of contamination by EPCs or HSCs adhered to other stromal cells capable of binding to plastic (HSCs adhere tightly to bone marrow osteoblasts as part of their interaction with the haematopoietic niche). Our RT-PCR results show that CD34 was undetectable in our MSC cultures at passage 14 and

beyond. Although this seems to disagree with the FACScan data, which detected low levels of CD34 at passage 14, our detection of CD34 protein at this time point was well within the margin of error for FACScan analysis, so the results are not incompatible. As a control for this experiment, we used RNA from whole BM which showed no detectable transcript for CD34. These results agree with the FACScan data we observed for whole BM, which did not label with α-CD34 antibody.

CD44 is a cell-surface glycoprotein involved in cell-cell interactions, cell adhesion and cellular migration. It is a receptor for hyaluronic acid and collagen, both components of the bone marrow stroma extracellular matrix. FACScan analysis revealed that our mMSC cultures expressed CD44 at a constant level at all time points examined. It is likely that CD44 plays a role in the ability of MSCs to adhere to plastic, so the constant levels of expression at all time points is unsurprising, since any non-adherent cells are excluded from analysis. Due to this dependable level of expression, we used CD44 signal as our loading control for the RT-PCR experiment (except in cases where we were not using adherent cells as a source of RNA). As a result, all cultured samples show a similar level of CD44 expression.

CD73 is a 5'-nucleotidase enzyme which is known to catalyze the phosphorylation and dephosphorylation of certain unknown protein substrates. It has been suggested that CD73 plays a role in T and B cell maturation due to its up regulation during immune cell development. Recent research into the nature of the MSC niche within BM indicates that MSCs may be responsible for guiding the proliferation and fate of HSCs and other immune cell precursors. [90] In FACScan analysis of CD73 protein expression levels, we found that CD73 expression decreased with time in culture. Our RT-PCR results do not mirror these data. We found detectable levels of transcript at passages 14, 92 and 220 for our MSCs. Whole BM control shows very high expression levels for CD73. Since CD73 is also highly expressed on all blood cells (erythrocytes, leukocytes, granulocytes, macrophages, etc.) these results are not unexpected.

CD105 (endoglin) is a type I integral membrane protein of the transforming growth factor β receptor (TGF-βR) family. It is expressed on stromal cells, lymphoid precursors, endothelial cells

and activated monocytes and tissue macrophages. Although the exact function of CD105 remains unknown, it has been suggested that it is involved in cytoskeletal organization affecting cell morphology and migration. It is known to be involved in cardiovascular development and vascular remodeling. Our FACScan analysis showed no detectable protein expression of CD105 for our cells. However, RT-PCR revealed detectable transcript at all passage numbers. Whole bone marrow control was negative for CD105 transcript.

SCA1 (Ly-6A/E) is a glycosylphosphatidylinositol-anchored membrane protein known for its role in T cell activation. It is transiently up regulated during cell-cycle withdrawal and blocking of SCA1 function with mAb promotes proliferation. [93] Studies of cell-cycle status in rapidly growing MSC cultures have revealed that only a very small percentage of the cells (~10%) are actively dividing at one time and that the vast majority are in cell cycle arrest in G_0/G_1 phase. These cells are not differentiated but quiescent and generally re-enter the cell cycle as growth continues after a lag phase of several hours. In HSCs (another population of stem cells which express the SCA1 antigen) it has been noted that the most primitive, quiescent stem cells express high levels of SCA1 and remain in cycle arrest at G_0/G_1, whereas the less primitive transit amplifying cells do not experience a lag time during cell division and express lower levels of SCA1. [94][95][96] At all time points examined, our mMSCs expressed SCA1 transcript. Whole BM control did not express detectable levels of SCA1.

Oct4 is a homeodomain transcription factor of the POU family. This protein is critically involved with self-renewal and maintenance of pluripotency in undifferentiated embryonic stem cells. Oct4 is also known to regulate differentiation in other somatic stem cells such as neural stem cells of the periventricular niche. Its presence in undifferentiated MSCs is controversial and we tested our cells to determine whether this important regulator was participating in maintenance of their multipotential phenotype. Our results showed detectable levels of Oct4 transcript in undifferentiated cells at all time points, which agrees with our IHC experiment findings. However, we also observed very high levels of Oct4 expression in whole BM, a result we did not expect based on previous data concerning the expression of Oct4 in somatic cells.

Nanog is another transcription factor involved in maintenance of self-renewal and pluripotency in ESCs. It is regulated by Sox, Oct4 and itself and acts, among other functions, to block BMP-induced differentiation signals. Nanog is highly expressed in undifferentiated cells and down-regulated during loss of pluripotency and terminal differentiation. Nanog expression in our mMSC line was high at all time points observed and undetectable in our whole BM control. The presence of Nanog is consistent with our other results indicating that our MSCs have remained undifferentiated during their time in culture.

Telomerase is a reverse transcriptase enzyme that catalyzes the addition of DNA sequences at the ends of chromosomes by copying an associated RNA ribozyme unit. This is a necessary function in self-renewing cells undergoing division, because each DNA replication reduces the size of the telomeres that cap the ends of chromosomes. Progressive decreases in telomere length during cell division appear to be responsible for the limited ability of differentiated cells such as fibroblasts to replicate in culture. If telomeres are lost completely, continued DNA replication results in loss of important genetic material and apoptotic cell death in most cases. Telomerase is expressed in dividing embryonic stem cells and in a subset of tissue-derived stem cells. We found that passage 14 and 92 cells did not express detectable levels of telomerase transcript, but contained detectable levels of transcript by passage 220. Whole BM samples did not express detectable levels of telomerase transcript.

Protamine 2 is one of two small, arginine-rich, nuclear proteins that replace histones late in the haploid phase of spermatogenesis and are believed essential for sperm head condensation and DNA stabilization in mice and humans. Previous research by Ira Black et al. indicated that rodent MSCs expressed protamine 2 transcripts and argued that this evidence supported the idea that MSCs are capable of transdifferentiation to cells of other germ layers, including germ line cells. [97] Since our MSC isolation procedures and neural differentiation protocol mimic some of the work done by this laboratory we also tested for the presence of protamine 2 in our cells. We found that our mMSCs expressed protamine 2 transcript and that our whole BM control sample

also contained detectable levels. All MSC isolates and our whole BM control were derived from male mice.

Ceruloplasmin (also known as ferroxidase or iron (II) oxygen reductase) is an enzyme synthesized in the liver. It catalyzes the oxidation of ferrous iron (Fe2+) to ferric iron (Fe3+), therefore assisting in its transport in the plasma in association with transferrin, which can only carry iron in the ferric state. MSCs have been shown to differentiate both in vitro and in vivo into functional hepatic cells, which have high levels of ceruloplasmin expression. We observed high levels of ceruloplasmin transcript in our undifferentiated mMSC cultures and no detectable transcript in whole BM samples. These results agree with previous experiments on rodent MSCs. [97]

Leptin is a protein hormone that plays a key role in regulating energy intake and energy expenditure, including the regulation of appetite and metabolism. It is produced by adipose cells and binds to the ventral medial nucleus of the hypothalamus, which controls the sensation of satiety. Circulating leptin levels also give the brain information on the amount of energy stored in adipose tissue throughout the body. In normal bone marrow, MSCs often give rise to adipose tissue which fills in space not occupied by

the haematopoietic stem cell niche. We found leptin transcript in our undifferentiated mMSC cultures and in our whole BM control sample. Bone marrow often contains adipose cells, especially in the “yellow marrow” found in the medial sections of long bones like the femur. Since many adipose cells would have been isolated along with the stromal and haematopoietic cells in our whole BM sample, it is not unexpected that leptin transcript is present in our control.

Bone morphogenetic protein 5 (BMP5) is a polypeptide member of the TGFβ superfamily of proteins. Bone morphogenetic proteins are known for their ability to induce bone and cartilage development. BMP5 is known to be expressed in MSCs before and during osteogenesis and chondrogenesis and promotes dendritic growth in cultured neurons. [98] BMP5 transcript was detected in our MSCs at all three passages examined, but was absent in whole BM control.

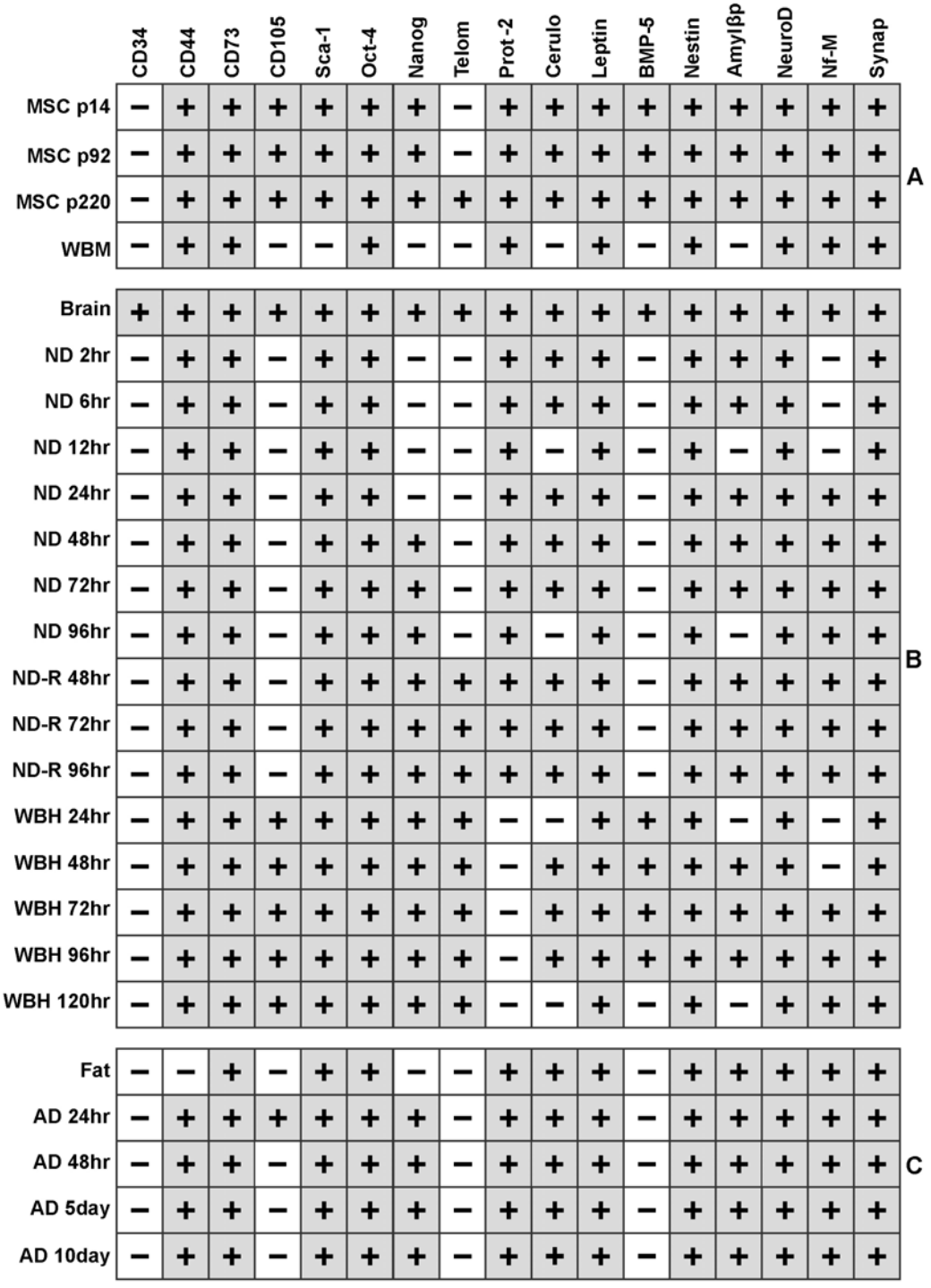

Figure 3-6: RT-PCR results for 17 genes (Telom= telomerase, Prot-2 = protamine 2, Cerulo = ceruloplasmin, Amylβp = Amyloid precursor protein β, Nf-M = neurofilament M, Synap = synaptophysin). (A) Undifferentiated murine MSCs of various passage numbers and whole bone marrow control (WBM). (B) Brain tissue control, neurodifferentiated MSCs (ND), neurodifferentiated with reversal (ND-R) and MSCs differentiated in whole brain homogenate medium (WBH) at various time points. (C) Fat tissue control and MSCs induced for adipogenic differentiation (AD) at various time points. For each reaction, total RNA template was the same. Plus signs indicate bands that were detectable when loading control (CD44) was held constant.

Nestin is a type IV intermediate filament that is expressed in cells during growth and development, but is usually suppressed in terminally differentiated cells. It is best known for its expression in neural precursor cells of the subventricular zone prior to terminal differentiation into neurons or glia. Nestin mRNA was expressed at all time points in our undifferentiated MSCs. We also detected high levels of expression in whole BM samples, which was not expected.

Amyloid precursor protein (APP) is an integral membrane protein expressed in many tissues and concentrated in the synapses of neurons. Its primary function is not known, though it has been implicated as a regulator of synapse formation and neural plasticity. APP is best known as the precursor molecule whose proteolysis generates amyloid beta, a 39-42 amino acid peptide whose amyloid fibrillar form is the primary component of amyloid plaques found in the brains of Alzheimer's disease patients. We included analysis of APP due to its up regulation during the process of neural differentiation. We observed no detectable APP transcript in whole BM control samples and moderate levels of transcript in our undifferentiated mMSC cultures which remained constant at all time points examined.

NeuroD is a basic helix-loop-helix (bHLH) transcription factor that initiates neurogenesis in ectodermal cells of the developing embryo. It is expressed in neuronal cells at the time of their terminal differentiation. It has also been shown that NeuroD regulates the production of insulin in conjunction with another HLH protein, E47. We found that our mMSCs expressed detectable levels of NeuroD transcript which were constant at all time points examined and were almost identical to the transcript levels we found in whole BM samples. Detection of NeuroD transcript in whole BM control was not expected.

Neurofilament-M (NF-M) is a type IV intermediate filament found in high concentrations along the axons of vertebrate neurons. It is a commonly used marker for neuronal differentiation in vitro and in vivo. We detected NF-M transcript in our undifferentiated mMSCs at all time points. Transcript was also present in whole BM samples. These data conflict with our results from IHC experiments showing that both low and high passage cells were negative for NF-M protein.

Synaptophysin is a synaptic vesicle glycoprotein present in endocrine cells, the brain, the spinal cord, and adrenal glands. It acts as a marker for neuroendocrine cells. It is generally accepted as a reliable marker of synapse formation within neural tissue. We observed moderate expression of synaptophysin transcript in our undifferentiated mMSCs which remained constant at all time points. Our whole BM control samples also exhibited detectable levels of synaptophysin transcript. The presence of synaptophysin signal in our undifferentiated mMSCs and BM control cells was unexpected.

RT-PCR Analysis of Neurodifferentiated mMSC Gene Expression

We used two different protocols (BHA-based and whole brain homogenate-based) to test the ability of our MSCs to undergo neurodifferentiation. We prepared total cellular RNA from them at several time points during the differentiation process. Cells subject to the BHA neurodifferentiation protocol had RNA extracted at 2, 6, 12, 24, 48, 72 and 96 hours after addition of induction medium. In addition, mMSCs which were induced in BHA for 24 hours and then returned to normal MSC growth medium for 24, 48 or 72 hours before RNA was isolated. This was done to determine whether the changes seen for short-term induction were permanent or reversible. Expression profiles for induced cells were compared to samples from undifferentiated mMSCs, whole BM and brain tissue for all 17 of the transcripts discussed in the above section.

Of the 17 transcripts examined, there was no discernible change in the expression of CD34, CD44, CD73, Oct4, SCA1, Protamine 2, Ceruloplasmin, Leptin, Nestin, Amyloid precursor protein, NeuroD, Neurofilament M, or Synaptophysin. CD44 continued to be expressed at a stable level by adherent cells and was, again, used as a loading control. CD105 transcript was lost in induced cells and was not regained during the induction reversal period. Nanog transcript was lost during the first 4 time points but appeared in samples taken after 48 hours of induction and in the reversal samples. Expression of telomerase was lost in induced samples but regained after induction was reversed. BMP5 transcript was not detected in induced or induction reversed samples.

Cells subject to whole brain homogenate (WBH) neurodiffferentiation had total cellular RNA extracted at 24, 48, 72, 96 and 120 hours post-induction. Of the 17 transcripts examined, expression levels for CD34, CD44, CD73, CD105, Oct4, Nanog, Telomerase, Ceruloplasmin, Leptin, Nestin, APP, NeuroD, Neurofilament-M and Synaptophysin did not change significantly from that seen for undifferentiated mMSCs. Expression of Protamine 2 was lost immediately upon induction with this protocol. BMP5 expression remained strong until the final time point, when it became undetectable. Ceruloplasmin and APP transcripts were also not observed at the 120 hour time point. However, these transcripts were barely above the threshold for detection at other time points and were not detected at the first time point in this experiment. As a result, it is difficult to determine whether their absence at 120 hours represents a true loss of transcript due to differentiation.

RT-PCR Analysis of mMSC Gene Expression After Adipogenic Differentiation

We induced mMSCs in adipogenic medium and isolated total cellular RNA 24, 48, 120 and 240 hours after induction. We used total cellular RNA from adipose tissue of an adult C57 mouse and undifferentiated mMSCs as a control. Evaluation of 17 transcripts revealed that expression levels for CD34, CD44, CD73, SCA1, Oct4, Nanog, Protamine 2, Ceruloplasmin, Leptin, Nestin, Amyloid precursor protein, NeuroD, Neurofilament-M and Synaptophysin were all virtually identical to undifferentiated MSCs at all time points examined. CD105, Telomerase and BMP5 expression were all lost by 48 hours after induction. In all three cases, the change in transcript matched the expression profile for tissue-derived adipose cells. Of those transcripts still present in induced MSCs, CD44 and Nanog were not found in adipose tissue.

4. Discussion

FACScan Analysis

We examined expression of five cell surface marker proteins (CD34, CD44, CD73, CD105 and SCA1) on our isolated population of MSCs. As expected, we found them to be negative for the HSC-specific marker CD34 after several passages in culture. They were also highly positive for the MSC marker CD44 at all time points examined. CD73, CD105 and SCA1 are all surface

proteins which have been associated with MSC isolates in previous research. [99][44][100] We did not find high levels of expression for any of these markers on the MSCs we examined. CD73 was moderately expressed on some cells at early passages. SCA1 was moderately expressed on a portion of the cells observed at higher passages.

These results indicate that we have a phenotypically heterogeneous population of cells. It also calls into question whether the cells we have isolated are actually MSCs. We believe that the majority of the cells in our culture after ~10 passages are MSCs for several reasons. First, the cells are derived from bone marrow and are self-renewing up to 300 passages. In bone marrow, there are only two populations of cells (HSCs and MSCs) which are known to be able to grow continuously in this manner. Our cells are plastic adherent and do not label with antibody directed against CD34, both strong indicators that they are not of haematopoietic origin. Second, as we demonstrate in the next chapter, our cells readily differentiate into osteocytes and adipocytes, a major feature of MSCs. Third, the cells we isolate are highly positive for CD44, a typical MSC marker. Although other cell types are known to express CD44 in the bone marrow stroma, the only other cell population in the bone marrow compartment capable of long term proliferation in culture (HSCs) are universally negative for this marker. Finally, other laboratories have reported MSC isolates which fail to express CD73, CD105 and SCA1 but which meet other, more definitive, criteria for identification as MSCs such as the ability to differentiate into bone, cartilage, fat and muscle. [29]

Although surface markers are a useful tool for identifying MSCs isolated directly from bone marrow, variances in experimental conditions can cause modification of surface protein expression during culture. [101] Since we examine our cells only after many days in plastic adherent culture, it is possible that they lose expression of some typical markers associated with MSCs. The changes we observed in CD73 and SCA1 expression over time would seem to argue in favor of this hypothesis. Although the surface marker labeling data are not sufficient, by themself, to demonstrate that our cells are MSCs, it does indicate that there is no significant

contamination by cells of haematopoietic origin and that the markers that are expressed are consistent with other MSC isolates.

As an initial characterization, these findings are sufficient for our purposes. However, we would like to establish a more comprehensive picture of the proteins expressed on the surface of our cells to aid in further experiments. Future labeling experiments will determine the expression profile of other markers mentioned in Chapter I such as CD29, CD45, CD90, CD106, CD117, CD133, Stro1, SSEA4 and *frizzled* in order to compare our MSC isolates with cells derived by other researchers. We expect to explore the use of surface markers to isolate our cells directly from whole bone marrow, either in place of or in conjunction with plastic adherence. Future experiments may also look at expression of cell surface receptors such as CXCR4 and CX3CR1 which may modulate the cell's ability to home to areas of inflammation and degeneration.

IHC Analysis

We examined expression of six proteins (Oct4, PCNA, Nestin, GFAP, MAP2 and NF-M) in undifferentiated MSCs at passage 8 and 150 and MSCs neurodifferentiated by the Black/Woodbury BHA protocol. We found that Oct4 and PCNA were expressed in a small number of undifferentiated cells at both passages examined. Low levels of Nestin were expressed in the majority of undifferentiated MSCs of both passages. Of the neural-associated proteins, GFAP and MAP2 were highly expressed in undifferentiated cells and NF-M was not present. These results agree with data reported by other groups. [23][20][92][102][103]

It has been observed before that, in proliferating MSC cultures, only a small number of cells (~10%) are actively dividing at any given time. The majority of MSCs are stationery at the G0/G1 phase of the cell cycle. Moreover, the G0/G1 population of MSCs includes a minor and variable subset of resting quiescent cells. [104] However, these resting cells are capable of continued proliferation and will eventually leave the G0/G1 phase and undergo mitosis again. This observation agrees with our results for expression of PCNA and Oct4. PCNA is found in the nuclei of proliferating cells and would not be present in most cells which have arrested at the G0/G1 phase. Oct4 is a transcriptional activator which controls genes involved in the

maintenance of self-renewal and pluripotency. It was also observed to be present in only a small number of nuclei in our undifferentiated cells. In other experiments, results have indicated that a very small subset of isolated stem cells in culture represent "true" stem cells. The majority of the culture is thought to be composed of progenitor or transit amplifying cells which continue to divide but have a limited self-renewal potential. [85] This mimics the function of the stem cell niche *in vivo* where a single stem cell, which divides very slowly, in an asymmetric manner, and gives rise to rapidly dividing cells that produce numerous terminally differentiated progeny. These slowly dividing or "quiescent" stem cells represent the most primitive, least committed cells in the niche. Expression of Oct4 would conform to the expected phenotype of such cells and its expression in a small portion of our cultured MSCs may be indicative of the presence of these foundational stem cells. In future experiments, we will perform double-labeling with PCNA and Oct4 to determine whether these proteins are co-expressed in our MSC population. This should indicate whether Oct4 positive cells are quiescent or actively dividing.

Nestin, GFAP, MAP2 and NF-M are all proteins involved with the cytoskeleton of neural cells. Although, they are most often associated with neural cells, they are known to be expressed in cells outside the nervous system as well, such as stromal cells. [92][20] Nestin and GFAP are also found in undifferentiated neural stem cells. In fully differentiated neural cells, Nestin is not usually expressed, while GFAP is found primarily in glia. MAP2 and NF-M are found primarily in mature neurons. The presence of these proteins in our undifferentiated cells could have several explanations. First, it has been established that certain culture conditions and stresses can induce changes in the cytoskeletal structure of cells. [105][103] It is possible that these proteins are activated due to cytoskeletal rearrangements caused by adherent culture having nothing to do with their expression in neural cells. Second, MSCs, which are potentially derived from cells of neural crest origin during embryogenesis, may express these proteins naturally. The function of Nestin and GFAP in adult neural stem cells is not known. It is possible that the function they serve in those adult stem cells is also important in MSCs. Finally, the presence of these proteins may indicate that MSCs express proteins appropriate to the terminally differentiated cells they have the ability to give rise to as part of their multipotent nature. It has been suggested that

MSCs possess a “multi-fate phenotype” in which they take on some characteristics of many terminally differentiated cells while still retaining multiple potential fates. [97] Thus, expression of neural proteins may indicate that our MSCs are prepared for but have not yet fully committed to differentiation toward a neural fate. The absence of NF-M indicates that, despite the presence of other neural proteins, our MSCs have not yet fully committed to a neuronal phenotype.

We observed several specific changes in expression of the proteins examined when MSCs were exposed to neurodifferentiation medium. No detectable expression of the proliferative marker PCNA was observed in the nuclei of cells after neuroinduction. This change indicates that cells exited from the mitotic cycle. This interpretation is supported by our observation that control cells, plated at the same density, continued to grow and became confluent by the end of the experiment, while induced cells did not visibly proliferate and remained at approximately the same density at which they were plated. Induced cells no longer stained positive for Oct4 and Nestin, proteins which are associated with a primitive stem cell phenotype in neural stem cells. This transition may be an indicator of terminal differentiation. We also observed that some induced cells gained expression of NF-M. The upregulation of this marker of mature neuronal cells, while not definitive, is another indicator that our induced MSCs are undergoing neural differentiation as predicted. In further experiments we hope to look at additional markers of stem cell identity and pluripotency such as the transcription factor Nanog and further indicators of neural differentiation. In addition, we will be transferring our examination of differentiated cells from an *in vitro* model to an *in vivo* model such as intraocular or intraventricular injections.

RT-PCR Analysis

Our results for RT-PCR analysis of 17 transcripts indicate that our undifferentiated MSCs express a large number of adult stem cell and tissue specific genes. While these results agree with RT-PCR results from other labs [97] they also raise questions regarding the efficacy of RT-PCR as an indicator of cellular phenotype. While some of our results may have provided insights to the biochemical workings of our cultured cells, others seem confusing in light of our other results.

One result that seems significant is the transition from telomerase negative to telomerase positive expression between passages 92 and 220. This is the only transcript which was observed to change in our experiment between undifferentiated MSCs of different passages. As observed for our IHC results, some researchers have suggested that MSCs and other adult stem cells in culture give rise to a mixed population of "true" stem cells and a much larger proportion of transit amplifying cells which divide rapidly but have a limited self-renewal capacity. In addition, it is known that many adult stem cells do not need to actively express telomerase under normal physiological circumstances due to their quiescent nature and their ability to undergo asymmetric cell division. [106] Telomerase replaces the ends of chromosomes (referred to as telomeres) which are not able to be copied by DNA polymerase during mitotic DNA replication. However, only the newly synthesized copy of the DNA undergoes this shortening. The original strand remains intact. Asymmetric cell division refers to the ability of a stem cell to retain its original DNA after every cell division, passing on the newly synthesized strand to its transit amplifying progeny. Since the retained strand isn't shortened by replication, the stem cell does not require telomerase activity to maintain the length of its chromosomal telomeres.

We hypothesize that our early passage cultures of MSCs contain very few "ultra-primitive" quiescent cells and are mostly composed of rapidly dividing transit amplifying progeny. These progeny still retain the ability to divide many times before undergoing senescence and are multipotent, but lack the ability to divide indefinitely. As culture continues, many of these MSC progenitors reach their division limit and drop out of the culture population. At the same time, quiescent stem cells that have been dividing very slowly become more active and replace not only the lost progenitor cells, but also undergo symmetric cell division to give rise to additional stem cells. In order to produce identical sister cells without shortened telomere regions, these cells require the activity of telomerase. As the proportion of these telomerase positive cells increases in the culture population, we begin to detect telomerase transcript in our RT-PCR experiments. Since telomerase is known to be expressed in tumorigenic cells, it is also possible that the emergence of telomerase expression indicates our cells have undergone transformation in culture to a tumorgenic phenotype. This explanation is not supported, however, by results from

our transplant and differentiation experiments. Transplanted cells were not observed to form tumors (see Chapter 6) and high passage number cells which were cultured in differentiation inducing media stopped dividing, lost expression of proliferative markers and underwent terminal differentiation.

Other results from our RT-PCR experiments are more difficult to interpret. For example, FACScan analysis and IHC data (both direct measurements of protein expression) indicate that our MSCs express almost no CD73 protein as early as passage 63, but we continue to see positive transcript signal to passage 220. We couldn't detect any CD105 protein at any time during culture, but show that the cells are positive for CD105 transcript at all times measured by RT-PCR. IHC indicates that undifferentiated cells express no NF-M protein, but transcript is present at all passages examined by RT-PCR. This disagreement between protein and RNA data could have several explanations. It is possible that we are getting false positives because of contamination in our RNA samples or due to poor primer design. However, we believe our experimental methods and controls were adequate to render this an unlikely possibility. No signal was detected for any transcript in control reactions using mouse genomic DNA as a template or in reactions lacking RT activity, eliminating the possibility that we were amplifying DNA rather than RNA signals. We also saw no reaction for any of the transcripts examined when using whole RNA from plants as a template (data not shown).

One alternative explanation is that RT-PCR may simply be more sensitive than antibody labeling. Very small amounts of transcript (which could still be significant to cellular function) may be detectable by RT-PCR but the resulting protein may not be above the threshold of detection for our other assay systems. Although our RT-PCR assays were semi-quantitative, we feel that the number of variables that can affect signal strength for a specific transcript and the unavailability of stringent internal controls for amplification efficiency renders any quantitative analysis of the data untrustworthy, so we cannot comment on whether the amount of transcript signal obtained for these three genes agrees with the hypothesis that low level expression causes their protein counterparts to go undetected.

Another potential explanation is that RT-PCR measures signal strength at the population level while protein labeling measures signal strength at the level of individual cells. With FACScan, for example, 1 cell out of 10,000 labeling highly positive for CD105 protein would yield a 0% result in our analysis, agreeing with our observations. However, with RT-PCR, 1 cell out of 10,000 which is highly positive for CD105 transcript might provide enough template to give a positive result in our analysis. Since RT-PCR does not allow us to measure how much of the signal is coming from individual cells, a positive signal cannot be used to extrapolate expression for the entire population of cells. This may also explain why we see expression of so many tissue-specific transcripts in our results. It was highly unexpected for us to find expression of synaptophysin, for example, in our undifferentiated MSC cultures. However, if synaptophysin transcript wasn't universally present, but was present only in a few cells whose signal was greatly amplifyed by the sensitivity of our RT-PCR assay, the data agree more closely with what other researchers have reported.

Perhaps an even more likely explanation is that expression of transcripts and proteins is not always synonymous for many genes. Cells use many mechanisms for regulation of their proteome other than activation or repression of genes at their promoters. Cellular mRNA is often regulated post-transcriptionally by alternative splicing and microRNAs. Conservative estimates of the number of regulatory microRNAs in the human genome put the number at somewhere around 800, indicating this method of regulation may be used extensively in human cells. [107] Protein expression is regulated by the abundance of tRNAs, the presence or absence of chaperone proteins, post-translational modification, compartmental targeting and protein degradation mechanisms. Promoters are also known to be "leaky" allowing occasional transcription through a gene even in the presence of strong transcriptional inhibitors. [108] While "leaky" promoters may allow transcripts for certain genes to exist at some detectable level in the cell, this doesn't mean that such transcripts give rise to proteins which actively contribute to the biochemical function of the cell. The abundance of regulatory options that function after the synthesis of mRNA suggests that a positive signal for RT-PCR should not necessarily be interpreted as an indicator of protein

expression or protein function within a certain cell population. As a result, we believe the results of our RT-PCR analysis must be interpreted with care.

Even though we must be careful about the conclusions we draw from our findings, we do believe that our RT-PCR analysis can give us some insights into the functional characterization of our isolated MSCs. In addition to examining the transcript profiles of undifferentiated MSCs, we also looked at RNA samples from MSCs exposed to two different neuroinduction protocols and MSCs cultured in adipogenic differentiation medium. For the first neuroinduction protocol (the Woodbury BHA protocol) we also explored the effect of induction reversal on transcript expression. We found that cells subjected to neuroinduction conditions lost expression of transcripts for CD105, telomerase and BMP5. Because our undifferentiated MSCs were already positive for transcripts for all of the neural-associated genes we examined, we could not detect induction of neuronal phenotype with this assay. However, loss of BMP5, which is associated with bone precursor cells, and CD105 which is associated with stromal and epithelial precursors, suggests the MSCs were losing their ability to differentiate toward mesodermal fates and may have been undergoing terminal differentiation. Loss of telomerase also suggests that the induction protocol was inducing terminal differentiation. Reversal of the BHA protocol after 24 hours revived expression of telomerase transcript but did not cause renewed BMP5 or CD105 expression. The cells retained transcripts for SCA1, Nanog and Oct4 throughout the induction. In addition to the explanations offered above, this could also be explained by a small population of primitive stem cells which continue to express these markers despite induction signals.

Neuroinduction with whole brain homogenate yielded different results from the BHA induction protocol. The only transcript which was drastically affected by this induction protocol was protamine 2, which was lost at the 24 hour time point. All other transcripts observed showed expression similar to that of undifferentiated cells until the last time point. At 120 hours post-induction no expression of transcripts for ceruloplasmin, BMP5 or amyloid β precursor (APP) were detected. Signal for both ceruloplasmin and APP was barely above the threshold for detection throughout the experiment (both showed no expression at the first time point either) so

it is difficult to attach much significance to their loss at 120 hours. However, BMP5 had a strong signal through the first 4 time points which was similar to that seen for undifferentiated cells and then completely disappeared at 120 hours. Since these findings agree with the phenotype seen in the other neuroinduction protocol, it is possible that loss of BMP5 transcript might be a reliable indicator of differentiation for our MSCs. Again, retention of SCA1, Oct4 and Nanog transcript expression is difficult to explain. Loss of protamine 2 transcript, which has been used in other research as an indicator of germline potential in MSCs, may be a further indication of terminal differentiation. [97]

MSCs were also subjected to adipogenic induction and examined for changes in their transcript profile. We observed loss of transcripts for CD105, telomerase and BMP5 in these cells (the same changes seen in the BHA neuroinduction experiment). These changes altered the expression profile of the induced MSCs to match the profile we observed for adipose tissue for all transcripts except two. While our induced cells remained positive for CD44 and Nanog transcripts, we did not see any evidence of these genes being expressed in murine adipose tissue. We were surprised to detect transcripts for Oct4, protamine 2, ceruloplasmin and neural-associated genes such as nestin, APP, NeuroD, NF-M and Synaptophysin in adipose tissue. Again, there are several possible explanations for the presence of these transcripts and the results should be interpreted with care. As expected, adipogenic induction of MSCs resulted in cells that expressed leptin transcript. However, since it was also present in uninduced MSCs this cannot be used as a definitive marker of differentiation into adipocytes.

Conclusions

In this chapter we have begun to characterize the molecular profile of our isolated MSCs. We have established that our cell population is free of contaminating HSCs after several passages and is homogeneous for expression of one marker of MSC identity (CD44). Our isolate is heterogeneous for two other MSC markers (CD73 and SCA1) and the proportion of cells positive for these markers changes over time. Another putative marker of MSCs, CD105, was not found by FACScan analysis, but transcript was detected by RT-PCR. Our MSCs are also positive for

protein markers of proliferation (PCNA), pluripotency (Oct4) and primitive neural cells (Nestin) which are lost upon exposure to neurodifferentiation medium. The same differentiation protocol also induces expression of NF-M protein, a marker of mature neurons. Finally, inconsistencies between our RT-PCR and IHC/FACScan analysis results are difficult to interpret, but it appears that neurogenic or adipogenic induction causes loss of stromal specific transcripts such as CD105 and BMP5 as well as telomerase, an indicator of self-renewal potential. These results further support the identity of our isolate as MSCs and provide some evidence that they are capable of differentiating into multiple tissue types.

Chapter IV

Differentiation of Murine Mesenchymal Stem Cells Toward Adipogenic, Osteogenic and Neurogenic Fates

1. Introduction

As we discussed in Chapter I, MSCs are adult stem cells which seem to possess the ability to differentiate into an astounding array of terminally differentiated cell types. In their stromal niche, MSCs regularly give rise to osteocytes (which produce bone) and adipocytes (which comprise the majority of cells in the yellow marrow), in addition to numerous other stromal cell types. Some evidence also suggests that MSCs are able to leave the stromal niche and contribute to wound healing and tissue regeneration in other parts of the body. MSCs have been observed to differentiate into multiple cell types *in vitro* or after transplant into living donors, including cells which have their origin in all three germ layers.

One of the reasons for our interest in using MSCs for treatment of neurodegenerative diseases is their reported ability to differentiate into neural cells. While cellular replacement isn't the goal of our proposed MSC therapy, the ability of transplanted cells to integrate into host tissues without disrupting normal function is important. Transplanted cells which do not undergo terminal differentiation or which differentiate into cells that are incompatible with surrounding tissue are not attractive as therapy options, especially for neural tissues because of the potential for interfering with synaptic connections. A cell transplanted into neural tissue for the purpose of providing neurotrophic factors or soluble enzymes may provide a safer and more effective therapy if it is able to assume an identity compatible with the tissue surrounding it.

As noted in Chapter II, the most common definition of an adult stem cell is one which is clonogenic, self-renewing and able to terminally differentiate into one or more tissue-specific cell types. In Chapter II, we presented evidence that our isolated MSCs are self-renewing. We have also addressed the issue of clonogenicity, which we feel may be an inappropriate standard for

adult stem cells, especially those which are cultivated for transplant therapies. In this chapter we address the ability of our isolated MSCs to exhibit the third defining property of adult stem cells, the ability to differentiate. We show that our MSC isolate is capable of osteogenic and adipogenic differentiation even after many passages in culture. We further show that, in addition to developing some molecular characteristics of neurons and glia as reported in Chapter III, our MSCs assume the morphological features of neuronal and glial cells upon neurodifferentiation *in vitro*.

2. Materials and Methods

Adipogenic Differentiation

For adipogenic differentiation MSCs at passage 8, 24 or 250 were plated in either T-25 flasks or 6-well plates at a concentration of 5000 cells/cm^2 and cultured in Adipocyte Maintenance Media (Zen-Bio Inc. cat# AM-1, Research Triangle Park, North Carolina) consisting of DMEM/Hams F-12 (1:1 v/v mix) at pH 7.4 supplemented with 3% FBS, 1mM Dexamethasone, 100nM human insulin, 33mM D-biotin, 17mM Na-pantothenate, 15mM HEPES, 1% Penicillin, 1% Streptomycin and 1% Amphotericin B in a 5% CO_2 and 100% humidity atmosphere at 37°C. Media was changed every 3 days and cells were examined for differentiation at either 7 or 14 days. [109]

Oil Red O Staining

Cells plated in 6-well plates were washed once with 1x PBS to remove residual media then stained with Oil Red O and counterstained with hematoxylin using the American Mastertech Scientific Oil Red O stain kit according to the manufacturer's instructions. (AMS cat# KTORO, Lodi, CA) After staining cells were fixed in standard EM fixative and photographed at 20x magnification using standard light microscopy on an inverted microscope.

Osteogenic differentiation

For osteogenic differentiation MSCs at passage 8, 24 and 250 were plated in either T-25 flasks or 6-well plates at a concentration of 5000 cells/cm^2 and cultured in Osteocytic Differentiation Media (DMEM plus 10mM ß-glycerophosphate, 0.1mM dexamethasone, 0.2mM ascorbic acid) in a 5%

CO_2 and 100% humidity atmosphere at 37°C. Media was changed every 3 days and cells were examined for differentiation at either 7 or 14 days. [109]

Von Kossa Staining

To demonstrate differentiation into osteocytes, calcium deposits were detected by Von Kossa staining. [109] Culture media was removed from the 6-well plate and cells were washed with ice cold 0.17M Na-cacodylate to remove residual media. Cells were then fixed in standard EM fixative for 2 minutes. Fixative was removed and cells were washed once in 0.17M Na-cacodylate and once in ddH_2O. 1% aqueous silver nitrate was added and the plate was exposed to UV light for 30 minutes. The plate was then rinsed 3 times with ddH_2O before addition of 5% sodium thiosulfate for 5 minutes to remove unreacted silver. Cells were then washed again with 3 changes of ddH_2O before counterstaining with Nuclear Fast Red for 5 minutes. After a final wash with 3 changes of ddH_2O cells were kept hydrated in the plate in 0.17M Na-cacodylate. Cells were then photographed at 20x magnification using standard light microscopy on an inverted microscope.

Neurogenic Differentiation

For neurogenic differentiation MSCs at passage 8, 24 and 250 were plated in either T-25 flasks or 6-well plates at a concentration of 2000 cells/cm^2. Cells were allowed to adhere in standard MSC growth medium for 2 hours. At this time, plating medium was removed and one of two induction protocols were employed. For one set of cells, pre-induction medium consisting of standard MSC growth medium plus 0.1% ß-mercaptoethanol was added. Cells were maintained in pre-induction medium for 24 hours before the addition of neurogenic induction medium consisting of DMEM plus 0.2mM butylated hydroxyanisole (BHA), 2% DMSO and 0.5% ITS+ culture supplement (cat# 354342, BDbiosciences, Franklin Lakes, NJ) . Medium was changed every 2 days. [110]

For the second set of cells, neurogenic induction medium consisting of Gibco ά-MEM + 2% FBS, 2mM L-Glutamine, 1% Penicillin/Streptomycin solution, whole mouse brain homogenate (10ug of brain wet weight/ml of medium), 1nM dexamethasone and 0.2mM ascorbic acid was added.

Whole brain homogenate (WBH) was prepared from 6-8 week old C57BL6J mice by removing the whole brain, which was homogenized by both mechanical disruption and ultrasound in 5ml of 1x PBS + 0.1% Tween-20. The homogenate was then centrifuged in a small benchtop centrifuge at 6,000rpm for 2 minutes to remove the insoluble fraction and the supernatant filtered through a .22 micron filter before being added to the base medium. Medium was changed every 3 days. [111][112][113]

Morphological Documentation of Neurodifferentiated Cells

MSCs were plated in 6-well plates as described above and examined for morphological characteristics. Three plates for each induction protocol were used for this experiment and photographs were taken at 20x magnification using phase-contrast microscopy on an inverted microscope at 0, 2, 4, 6, 8, 12, 24, 48, 72 and 96 hours after addition of differentiation medium for BHA protocols and 24, 48, 72, 96, 120 and 168 hours after addition of differentiation medium for whole brain homogenate protocols. In addition, three plates were seeded and induced using the BHA medium protocol, but, at 24 hours after addition of the induction medium, it was replaced by standard MSC growth medium for the remainder of the experiment to determine whether cells could undergo induction and subsequent reversion.

3. Results

Adipogenic Differentiation of Murine MSCs

Murine MSCs at passage 8, 24 and 250 were analyzed for their ability to differentiate into adipocytes. Adipose tissue is an integral constituent of the marrow stromal environment and adipocytes may help regulate the space devoted to the haematopoietic stem cell niche in the yellow marrow. [27] After 7-14 days in adipogenic differentiation medium, all mMSC samples tested demonstrated the ability to readily differentiate into adipocytes. Cultures stained with Oil Red O revealed that over 95% of MSCs had arrested their growth and developed large fat deposits in their cytosol. The ability to undergo adipogenic differentiation did not vary with passage number. Representative cells shown in Figure 4-1(A) were subject to adipogenic differentiation at passage 250.

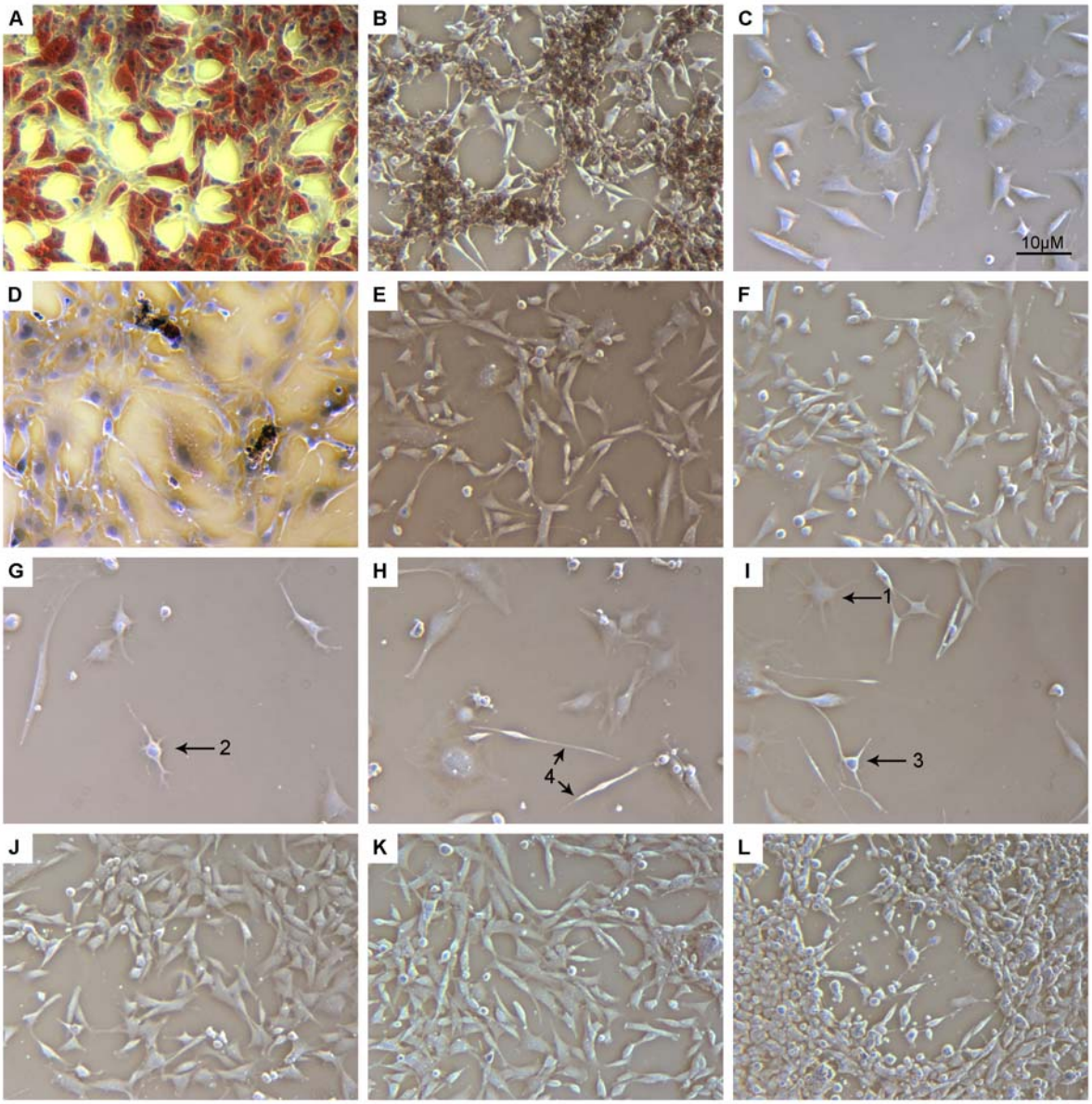

Figure 4-1: Murine MSC differentiation experiments. MSCs were subjected to adipogenic, osteogenic or neurogenic differentiation protocols. Both adipocyte-induced (A) and uninduced controls (D) were stained with Oil Red O. Only adipocyte-induced cells accumulated large numbers of cytosolic lipid droplets. Both osteocyte-induced (B) and uninduced controls (E) were stained by the Von Kossa method. Only osteocyte-induced cells contained dark-staining calcium deposits. MSCs were subjected to neurogenic induction (C, G, H, I) or cultured at the same concentration in normal MSC medium as controls (F, J, K, L) for 24 (C&F), 48 (G&J), 72 (H&K) or 96 (I&L) hours and then examined for morphological changes consistent with neurodifferentiation. Cells in neurogenic medium stopped proliferating and assumed morphologies similar to astrocytes (1), oligodendrocytes (2), pyramid cells (3) and other neurons (4). Control cells continued to proliferate and maintained a predominantly fibroblast-like morphology during the same period of time.

Osteogenic Differentiation of Murine MSCs

Murine MSCs at passage 8, 24 and 250 were analyzed for their ability to differentiate into osteoblasts. MSCs are the source of bone and cartilage forming cells in adult vertebrates. [29] Bone is formed by osteoblasts, which originate from osteoprogenitor cells within the periosteum and the marrow stroma. Osteoblasts secrete extracellular matrix elements and mineralize the extracellular matrix surrounding them through the secretion of calcium deposits. [29] After 7-14 days in osteogenic differentiation medium, all mMSC samples tested showed the ability to arrest their growth and form large colonies of cells similar to osteoblasts in morphology (small and round, with colonies growing closely packed and above the surface of the plate). These colonies formed a scaffold of calcified extracellular matrix called a nodule. These nodules were shown to be positive for calcium deposits by von Kossa staining. The ability to undergo osteogenic differentiation did not vary with passage number. Cells shown in Figure 4-1(B) were subject to adipogenic differentiation at passage 250.

Neurogenic Differentiation of Murine MSCs – Whole Brain Homogenate Protocol

It has been widely demonstrated that MSCs cultured with neural cells or neural cell conditioned medium *in vitro* or transplanted into neural tissue *in vivo* have the ability to differentiate along neural cell lineages. [114] To demonstrate the ability of our cultured mMSCs to mirror the plasticity of similar cells, we incubated them in medium containing the soluble fraction of homogenized whole mouse brain. After 120 hours in induction medium, mMSCs arrested their growth and began to display morphologies characteristic of neurons, astrocytes and oligodendrocytes. Response to the induction protocol did not vary with passage number. No difference in morphology was observed between the WBH protocol and the BHA protocol. After one week (168 hours) of exposure to induction medium, cells began to lose their ability to adhere to the plastic culture flasks and the majority of cells that remained adhered to the flask stained positive with trypan blue, indicating that the culture was undergoing widespread cell death (data not shown).

Neurogenic Differentiation of Murine MSCs – Chemical Protocol

Another neuro-induction protocol widely used by researchers studying MSC differentiation employs the chemical butylhydroxyanisole (BHA) as an inducer of neurodifferentiation. Several researchers have shown that cells treated with BHA, DMSO and β-mercaptoethanol rapidly assume neural morphologies and express neural differentiation markers. [114][110] In order to show that our cultured mMSCs are able to replicate the results of these other experiments, we exposed them to a similar BHA-based neurodifferentiation protocol. We observed that our cells behaved similarly to the results described for other rodent MSCs exposed to this treatment. As with the WBH medium, cells assumed morphologies characteristic of neurons, astrocytes and oligodendrocytes over a period of several days (see Figure 4-1). The morphological changes we observed did not happen as quickly as some other researchers have reported. Other experiments have documented morphological changes within the first 2-6 hours of induction, whereas we did not observe noticeable changes in our experiment until at least 24 hours after the addition of BHA-containing medium. It is possible that the small differences in media composition and cell density in our experiment account for these differences in the time of onset for morphological changes. Response to the induction protocol did not vary with passage number. No difference was observed between morphologies induced by the whole brain homogenate protocol and the BHA protocol. Cells shown in Figure 4-1 were subjected to the BHA protocol at passage 250.

Cells subject to reversal of induction 24 hours after addition of BHA differentiation medium were observed 24, 48 and 72 hours after returning to standard MSC culture medium. During this time we did not observe renewed proliferation. We also did not observe significant morphological changes in our induction-reversed samples after they were returned to normal MSC medium. However, most of the morphological transformation we observed in our induced cells occurred after the 24 hour time point, so further exposure to induction medium prior to reversal might have yielded different results. The failure of cells subject to reversal to resume proliferation indicates that the induction protocol, while not sufficient to change their morphological features, did cause permanent changes in the exposed cells. Trypan Blue staining of the cultures at the end of the

observation period showed that the majority of cells were able to exclude the dye, indicating that cell death did not account for the lack of proliferation.

4. Discussion

Stem Cell Identity

One of the primary goals of this research is to establish that we are able to successfully isolate MSCs from bone marrow. We have already established that we are able to cultivate cells from bone marrow and that our isolate meets one of three criteria for classification as adult stem cells (i.e. self-renewal). The results in this chapter also show that our cells meet a second criterion, the ability to differentiate into at least one tissue-specific cell type. We demonstrate that our cultured MSCs are able to arrest their proliferation and differentiate into both adipocytes and osteocytes when exposed to specific induction medium. We draw two conclusions from these results. First, that our isolated cells sufficiently conform to the required criteria to allow for their classification as MSCs. Second, that these MSCs have not undergone tumorigenic transformation even after 250 passages in culture. As a result, we feel comfortable in moving forward with transplantation studies in animal models of NCL.

Neural Differentiation

We chose to test two different protocols for induction of neurodifferentiation in our MSCs. Although, depending on the protocol used, the metamorphoses we observed took place at different rates, both protocols resulted in treated MSCs assuming morphologies consistent with cultured neural cells. These protocols have been standard induction protocols in the field of MSC research for several years. [114][110] However, recent evidence has called into question the efficacy of BHA-based induction. [114][115]

In 2006, Chen et al. conducted a comparative review of studies which included the BHA protocol developed by Woodbury and Black (and used in our research) and several other induction protocols. These comparisons cast some doubt on the efficacy of using simple chemical induction to produce true neural differentiation. One remarkable feature of the BHA protocol is

the rapid onset of morphological and molecular changes reported by Woodbury. Transformation of the cellular morphology occurred in a matter of hours, whereas differentiation of MSCs along adipogenic or osteogenic lines usually occurs over a matter of days to weeks. Results from additional characterization of BHA-induced cells indicated that changes in cell morphology that resemble neuronal differentiation could, in fact, be due to cell shrinkage and loss of focal contacts resulting from chemical disruption of the actin cytoskeleton. [116] Treatment with low pH, high salt and other cellular stressors (e.g. EDTA, cytocalasin D, detergents) produced similar morphological changes to those observed for BHA treatment. In addition, treatment of fully differentiated cells, such as fibroblasts, with BHA, low pH, high salt and cellular stressors also produced morphological changes similar to that seen for MSCs. [117] Morphological changes were further challenged by the finding that the development of cellular processes did not co-occur with clear observations of neurite growth cones and could not be blocked by inhibition of protein synthesis with cycloheximide. [117]

Molecular changes, such as increases in NeuN and NF-M expression were observed to occur under BHA induction, but Lu et al. observed that much of the protein was aberrantly localized in the cell and that some of the other markers reported by Woodbury, such as GFAP and βIII-tubulin, were already expressed at high levels in untreated MSCs. [117] In a more in-depth probe of changes in the transcriptome, Bertani et al. showed by a 21,000 gene microarray analysis of MSCs 6 and 48 hours after induction that the BHA protocol has little effect on the overall transcription profile of the population. [115]

Although evidence from other laboratories calls into question the usefulness of results from our own experiments using BHA induced neurogenesis *in vitro*,, there are several differences in both our protocol and our results which bear examining. In the studies where BHA induction was found to cause drastic cytoskeletal changes without specific neural induction, culture medium contained no serum and no other growth supporting factors. Lack of serum alone has been shown to induce neurogenic phenotypes in rodent MSCs, up regulating the expression of Nestin, which is thought to be a necessary precursor for further neural differentiation. [92] However,

MSCs transferred to medium without serum or other growth factors also undergo massive cell death, indicating that all cells in the culture are likely to be undergoing significant cellular stresses. In order to avoid this, we supplemented our BHA neuroinduction medium with ITS+ culture supplement, containing insulin, transferrin and selenous acid. This culture supplement has been shown to reduce the cell death associated with serum-deprivation. [39] Thus, our induction medium presented a less stringent environment than other BHA induction media examined. We also observed a significant delay in the onset of morphological changes with our induction protocol compared to previously reported results. Whereas the Woodbury BHA protocol induced morphological changes as early as 2 hours after addition of differentiation medium, we observed no significant morphological transformation in our experiments until after the 24 hour time point. This may indicate a reduced effect of cell stress and a greater role for true cellular differentiation in our experiments

Because of potential problems associated with the BHA induction protocol, we also subjected our MSCs to neural induction using whole brain extracts as the induction signal. Both protocols produced similar morphological changes in the treated cells. The brain extract induction medium contained low levels of serum (2% FBS) in addition to other supplements. It did not contain harsh cell stressors like those shown to induce stress-related cytoskeletal rearrangements by Lu et al. and Neuhuber et al. We chose this method of induction because previous research has shown that co-culture with astrocytes, astrocyte conditioned medium and organotypic brain slices has been effective in inducing neural differentiation in stem cells. [113][118][111] Although the exact mechanism of induction with these protocols isn't fully known, it is unlikely that morphological changes observed in these induction protocols were due solely to rearrangement of the actin cytoskeletal structure as suspected for BHA.

Finally, we did not observe complete reversion to MSC phenotype after replacing our BHA induction medium with normal MSC culture medium. This indicates that the BHA medium induced some form of terminal differentiation in exposed MSCs. Hung et al. noticed in similar experiments that the morphological and proliferative changes observed after BHA exposure and

serum deprivation were transient, reverting back to normal MSC phenotype after 5 hours. [119] This lack of reversion does not prove that such differentiation was along neural lines, but stress-induced cytoskeletal arrangement alone is insufficient to explain the widespread inhibition of proliferation we observed even 72 hours after returning induced cells to normal MSC culture medium. These facts set our methods and results apart from the other instances of BHA-induced neurogenesis in the literature.

Recent reports suggest that there are more trustworthy and efficient methods of inducing neural differentiation for MSCs. Better understanding of the biochemical pathways necessary for MSC neurodifferentiation have led to protocols that employ specific growth factors and culture conditions which more closely mimic the conditions known to induce neurodifferentiation *in vivo*. One chemical based protocol developed by Kohyama et al. used the DNA demethylating agent 5-azacytidine along with a cocktail of neurotrophic factors including nerve growth factor (NGF), neurotrophin-3 (NT3) and brain-derived neurotrophic factor (BDNF) induced morphologies resembling neurons and glia after 9 days. After 28 days, some cells with neuronal morphology exhibited a resting potential, rectifying K^+ current and response to certain neurotransmitters. [120] Sanchez-Ramos et al. produced similar results using either epidermal growth factor (EGF) or a combination of retinoic acid and BDNF. [111] Locatelli et al. and Hermann et al. both observed the formation of neurosphere-like cell aggregates that were Nestin positive after MSCs were induced for 5-7 days in culture medium containing basic fibroblast growth factor (bFGF) and EGF. [121][122] In the latter study, neurosphere-forming cells were further differentiated *in vitro* into mature glia and neurons which had outward and inward rectifying currents and released dopamine. In addition, manipulation of oxygen-tension, culture surface modification and specific signaling pathways have been employed to induce MSCs toward specific neuronal fates. [123][124][21] In any future experiments we conduct on the *in vitro* neurodifferentiation of MSCs, the use of these alternative methods of induction will be carefully considered.

Chapter V

Genetic Manipulation of Murine Mesenchymal Stem Cells By Small Fragment Homologous Replacement

1. Introduction

The therapeutic use of autologous mesenchymal stem cells without genetic modification is possible for diseases which do not involve inborn genetic defects. Unmodified MSCs have been successfully used to treat such ailments as myocardial infarction and renal failure, where the injured or degenerating tissue is not the result of a genetic defect inherent to all of the patient's cells. [125][53] Use of autologous MSCs for treatment of genetic disorders such as the NCLs, however, is more complex. In order for autologous transplants to avoid degeneration themselves, let alone provide aid to cells surrounding them through enzymatic diffusion, the genetic defect present in the donor/patient MSCs must be corrected prior to transplant.

Several methods exist which are capable of introducing genetic modifications to MSCs. Adenovirus, Adeno-associated virus, Lentivirus and Retrovirus-based vectors are all capable of infecting MSCs and promoting the non-sequence-specific incorporation of imported transgenes into the host genome. [126][127][128] Other methods of introducing transgenes such as nucleofection and electroporation have also been successful. [129][130] These methods have many advantages, but also suffer from the same limitation, which is reliance on the expression of a randomly inserted transgene, usually under the control of a non-native promoter. Some of the disadvantages associated with this technique were already discussed in chapter I. While these methods may be useful in the process of studying autologous stem cell transplant in a laboratory setting, we felt that, ultimately, transfer of treatment techniques to human NCL patients in the clinic would benefit from genetic modifications that repaired existing genes rather than inserting new ones. As a result we chose to examine the potential of small fragment homologous replacement (SFHR) as a means of modifying autologous MSCs.

SFHR uses cellular recombination and mismatch repair machinery to introduce nucleotide changes in the genomic DNA of targeted cells. Utilizing this process, we could repair existing genes in autologous cells rather than introducing new ones. Such genes would remain under the control of their native regulatory elements, allowing them to be expressed in a tissue-specific fashion when appropriate and at normal physiological levels. This process is limited to modifications of just a few nucleotides due to the fact that high levels of homology (near 100%) must be maintained between the target sequence and the modifying vector, so large deletions or insertions are not amenable to SFHR repair. However, many of the genetic mutations associated with NCLs consist of single-base alterations and would be treatable with SFHR. [131][132][133]

Since SFHR is not compatible with the simultaneous introduction of a selectable marker to identify modified cells and many of the genes responsible for the NCLs do not provide a phenotype that readily lends itself to post-modification screening, a high efficiency of correction (at least 1%) is necessary to make SFHR a viable option for autologous MSC correction. Treated cells would need to be genetically screened for successful correction before re-implantation into the donor. The object of the work in this chapter was to develop techniques for SFHR mediated modification of MSCs which would yield correction efficiencies at a level which would allow for rapid and economical identification of altered cells by genetic screening. As a result, we chose to develop an assay system that would allow us to monitor recombination efficiency with a selectable marker. We chose the herpes simplex virus thymidine kinase gene (*HSVtk*) as the target for SFHR modification because of its properties as a suicide gene responsive to the substrate gancyclovir. We created an MSC line expressing *HSVtk* which was able to convert gancyclovir to its cytotoxic form after addition to the culture medium and subsequently undergo cell death. We then exposed this cell line to SFHR treatment with a targeting vector designed to disrupt production of the *HSVtk* protein by modification of several nucleotides in a coding region of the gene and measured the recombination efficiency by monitoring the number of treated cells that became resistant to gancyclovir cytotoxicity. We observed low, but measurable, recombination efficiency in our treated MSCs. Further refinement

of our SFHR technique will be undertaken with this assay system to increase recombination efficiency before transferring the technique to modification of NCL-specific genes.

2. Materials and Methods

MSC Transformation With a *neo*^{r}*/HSVtk* Cassette

A line of MSCs expressing the Herpes Simplex Virus thymidine kinase (HSV-tk) gene was engineered by electrotransformation of cells with a construct containing the HSV-tk gene and a selectable neomycin resistance marker. We used the pPNT vector kindly provided by Dr. Richard Mulligan through the University of Michigan Transgenic Animal Core facility in Ann Arbor, MI (see Appendices). The vector was digested with *AseI* and *HindIII* restriction enzymes to release a 4838bp fragment containing the *neo*^{r}/HSV-tk construct, which was separated on a 1% agarose gel and purified using a QIAEX-II gel extraction kit (QIAGEN Inc. Valencia, CA). The DNA was resuspended at 200ng/ul in sterile ddH_2O and electrotransformed into MSCs using an ECM 830 Electro-square Porator (Genetronics San Diego, CA). Cells were prepared for electroporation by trypsinization (as described in Chapter II) followed by washing once in room temperature 1x PBS and resuspension in PBS at 1x10^7 cells/ml. A 500µl aliquot of cells was then mixed with 50µl of DNA in an electroporation cuvette and pulsed with the instrument on the following settings:

Mode: Low Voltage
Voltage: 250V
Pulse Length: 1ms
Number of Pulses: 5
Desired Field Strength: 625V/cm

After treatment, cells were incubated at room temperature for 10 minutes, then transferred to a flask containing standard MSC growth medium. Cells were incubated for 24 hours before G418 (Invitrogen Life Technologies Carlsbad, CA) was added at a final concentration of 1mg/ml. An aliquot of cells grown in the presence of G418 was taken at two weeks and examined for presence of the HSV-tk gene by PCR from genomic DNA with primers HSVtk-BamHI-F1 and HSVtk-HindIII-R2 (see Figure 5-1). Additional confirmation of the uniform presence of the HSV-tk gene throughout the culture was obtained by exposing an aliquot of cells to a cytotoxic dose of

A

Primer	Sequence
HSVtk-BamHI-F1	423 5′-CTGCCGGATCCCGCTTAACAGCGTCAACAG-3′ 452
HSVtk-HindIII-R2	1749 5′-CCGCAAGCTTGAACAAACGACCCAACACCC-3′ 1720
HSVtk-MUT-F2	1258 5′-GGTATCTGCAGGGCGGCGGGTAGTGACGGG-3′ 1290
HSVtk-MUT-R1	1290 5′-CCCGTCACTACCCGCCGCCCTGCAGATACC-3′ 1258

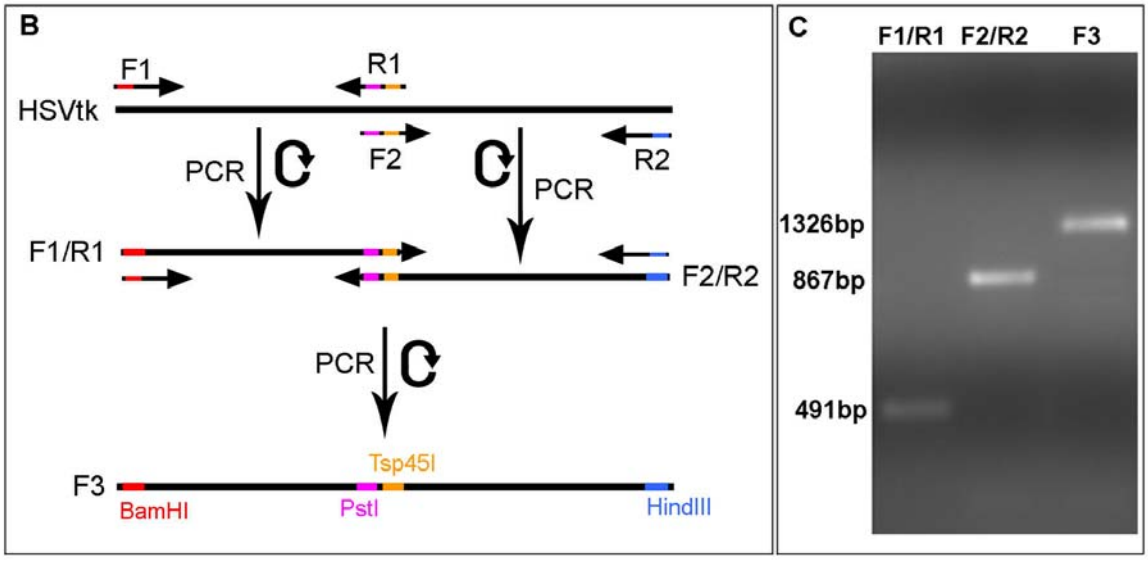

Figure 5-1: (A) Primers used to create the pTKmut vector. Restriction enzyme recognition sites are depicted in bolded red (BamHI), blue (HindIII), purple (PstI) and orange (Tsp45I). Underlined bases represent the two sites of mutagenesis incorporated into pTKmut by primers MUT-F2 and MUT-R1. (B) Using HSV thymidine kinase as template for PCR, primer pairs F1/R1 and F2/R2 amplified overlapping portions of the thymidine kinase gene, introducing two base changes in the overlap region. A second PCR, incorporating fragments F1/R1 and F2/R2 as template for primers F1 and R2 created a single, continuous DNA molecule containing the modified bases and capped by BamHI and HindIII restriction sites. In this reaction, fragments F1/R1 and F2/R2 primed themselves at the internal overlap point, creating full length F3. The presence of the F1 and R2 primers allowed amplification of this full length molecule in the reaction. The F3 fragment was digested with BamHI and HindIII and ligated into complementary restriction sites in pUC19 to form pTKmut. (C) PCR products for F1/R1, F2/R2 and F3 all ran at the appropriate molecular weight.

gancyclovir (0.02mg/ml) and ensuring that all neomycin resistant cells were also gancyclovir sensitive.

Creation of the pTKmut Targeting Vector

A vector containing a mutagenized version of the *HSVtk* gene was created by PCR amplifying the gene from the pPNT plasmid with mutagenic primers (see Figure 5-1A). Overlapping 5' (bp 423-1290 of the pPNT plasmid) and 3' (bp1258-1749 of the pPNT plasmid) ends of the *HSVtk* gene were amplified separately using forward (primer HSVtk-mut-F2) and reverse (primer HSVtk-mut-R1) primers corresponding to internal sequences in the gene (bp1258-1290 of the pPNT plasmid) along with matching forward (primer HSVtk-BamHI-F1) and reverse (primer HSVtk-HindIII-R2) primers specific to the 5' and 3' ends of the gene. The internal primers were complementary copies of each other that incorporated two nucleotide changes (C1281→A and G1285→A) which transform S209 and W210 of the HSVtk protein (accession# AAA45817) into an amber (UAG) and umber (UGA) stop codon, respectively. The G1285→A mutation also generates a unique Tsp45I restriction site which can be used to confirm presence of the mutation in a PCR or RT-PCR product. The amplified products were purified and then 5ng of each was used in a second PCR reaction with primers HSVtk-BamHI-F1 and HSVtk-HindIII-R2 only. The overlapping internal sequence of each PCR product allowed them to act as primers for each other, generating a full length product, while the peripheral primers allowed amplification of the full length template (see Figure 5-1B&C). The resulting PCR fragment was gel purified and ligated into pUC19 using the BamHI and HindIII restriction sites engineered into the F1 and R2 primers to create the HSVtk targeting vector, pTKmut. The pTKmut vector was tested for presence of the newly generated nucleotide polymorphisms by restriction digestion with Tsp45I to confirm the presence of the newly created unique restriction site and sequencing of the *HSVtk* gene to confirm the rest of the sequence was as expected.

Nucleotide Sequencing of pTKmut

The pTKmut vector was transformed into E. coli DH5ά competent cells and selected on LB agar plates containing ampicillin (100μg/ml). Plasmid was purified from bacterial cultures using the

QIAprep Spin Miniprep Kit (Qiagen Inc. Valencia, CA cat. #27104), concentrated by ethanol precipitation and resuspended in ddH2O prior to sequencing. Nucleotide sequencing was performed at Davis Sequencing (Davis, CA 95616) using Applied Biosystems Big Dye Terminator V3.0 sequencing chemistry on ABI 3730 DNA sequencers with primers specific to sequences lying outside the BamHI and HindIII sites in the pUC19 multiple cloning site.

Gancyclovir Cytotoxicity Assays

To determine the optimum level of gancyclovir to use for toxicity assays, a series of 6-well plates were seeded with *neo*^{r}/HSV-tk$^+$ cells and normal MSCs as controls at a concentration of 5x10^4 cells/well. After incubation in standard MSC growth medium for 2 hours to allow for adherence, cells were exposed to varying levels of gancyclovir (0, 6.25, 12.5, 18.75, 31.25 and 50µg/ml) for 48 hours. At the time of examination, non-adherent cells were washed away with 1x PBS and cells were stained with Trypan Blue (Invitrogen Carlsbad, CA cat#15250-061) to reveal dead or dying cells. Live cells were counted in four fields of view by light microscopy for each sample group.

To test the efficiency of SFHR treatment, cells were seeded in 6-well plates at a concentration of 5x10^4 cells/well. Three plates were created for each of four groups: SFHR treated HSVtk+ (gancyclovir sensitive) cells, untreated HSVtk+ cells, SFHR treated control (gancyclovir resistant) cells and untreated control cells. Cells were tested against gancyclovir at a concentration of 6.25µg/ml in four of six wells. One well of each plate contained no gancyclovir (positive survival control) and one contained a high dose of gancyclovir (100µg/ml) which should be 100% cytotoxic to sensitive cells (see Figure 5-2). Plates were incubated under normal conditions for 2 days, then surviving cells for each group were determined by the process described above.

Electrotransformation of the pTKmut Targeting Fragment

Cells to be treated with the pTKmut vector were prepared by trypsinization and washing in 1 x PBS as described above. In an electrotransformation cuvette, 500µl of cells at a concentration of 1x10^7 cells/ml was combined with 50µl of pTKmut targeting fragment. Targeting fragment was prepared by digesting the pTKmut plasmid with BamHI and HindIII to release the *HSVtk*

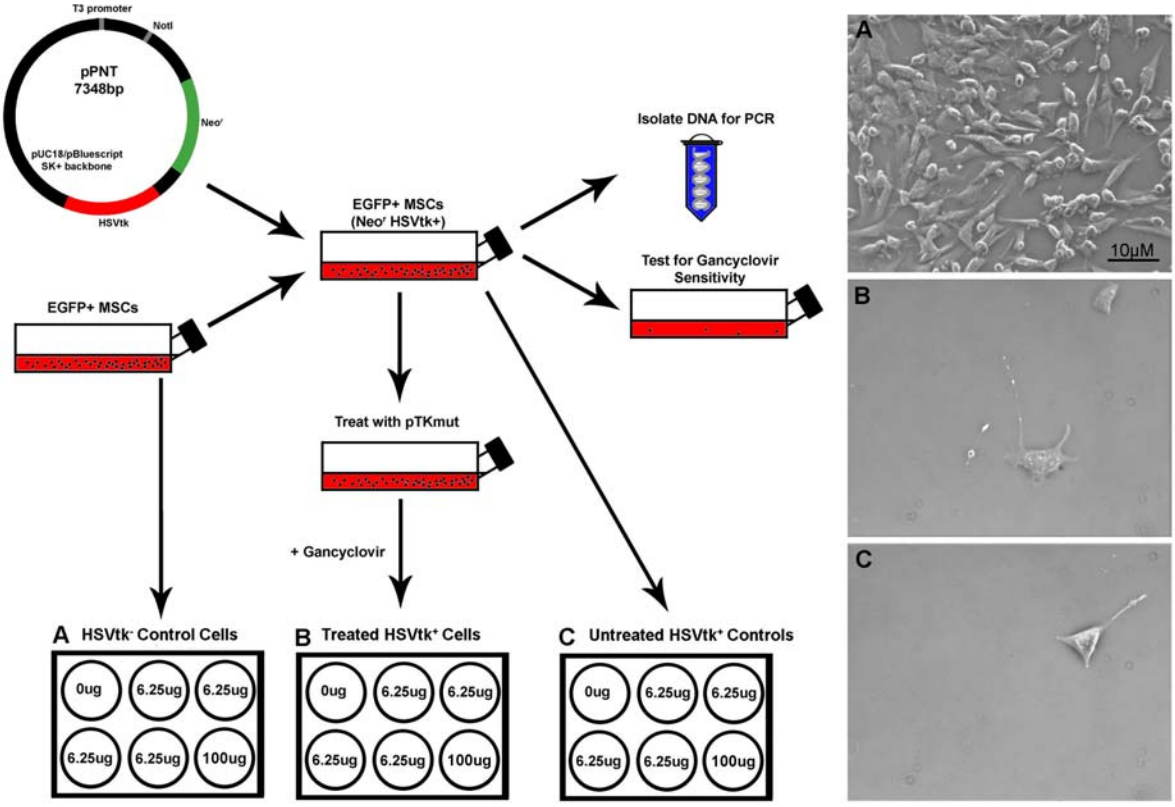

Figure 5-2: MSCs were transformed with linearized pPNT and selected with G418 for neomycin resistance. Cells that were neo^r positive were then tested for the presence of the HSVtk gene by PCR of genomic DNA with HSVtk-specific primers and susceptibility to gancyclovir cytotoxicity. HSVtk$^+$ MSCs were treated by SFHR with pTKmut (B) and their survival in a gancyclovir cytotoxicity assay was compared to HSVtk$^-$ (A) and HSVtk$^+$ (C) controls which had not undergone SFHR. Cytotoxicity was documented by staining cells with trypan blue dye and counting live (unstained) cells by microscopy.

homologous segment; which was then gel purified with a QIAEX-II gel extraction kit and resuspended at a concentration of 50ng/µl. Cells were pulsed as described above and grown to confluency before replating for gancyclovir cytotoxicity testing.

3. Results

Creation of a Herpes Simplex Virus Thymidine Kinase Positive mMSC Cell Line

In order to examine the efficiency of SFHR in our mMSC line we chose to use resistance to gancyclovir cytotoxicity as a phenotypic marker of gene conversion. In order to do so we first established an mMSC cell line which carried the *HSVtk* gene. The construct contained both the *HSVtk* gene and a neomycin resistance element. After electroporation with the vector, cells were selected for resistance to G418. For three separate electroporation treatments, survival rates in the presence of G418 averaged 28.3 ± 3.2% (versus unselected controls) one week after selection. (data not shown) Genomic DNA was purified from G418 resistant cells and tested for the presence of the *HSVtk* gene by PCR (see Figure 5-3). G418 resistant cultures treated with a cytotoxic dose (20µg/ml) of gancyclovir displayed a survival rate (based on staining with Trypan Blue) of approximately 0.5% compared to untreated cells. These data were deemed sufficient evidence that the G418 resistance cells were also HSVtk positive and this cell line was used for all subsequent SFHR experiments.

Creation of an HSVtk Targeting Vector

An HSVtk targeting vector (referred to hereafter as pTKmut) was created as described in the Materials and Methods section. The final vector was subjected to restriction fragment length polymorphism (RFLP) analysis at the Tsp45I site and nucleotide sequencing to confirm the correct introduction of the necessary DNA modifications. RFLP analysis showed that when compared to a Tsp45I digest of the normal HSVtk construct, the pTKmut vector contained two new bands of 362bp and 292bp and lacked the 654bp band present in the normal HSVtk digest. Nucleotide sequencing in both the forward and reverse direction agreed that the nucleotide changes C1281→A and G1285→A were incorporated as expected.

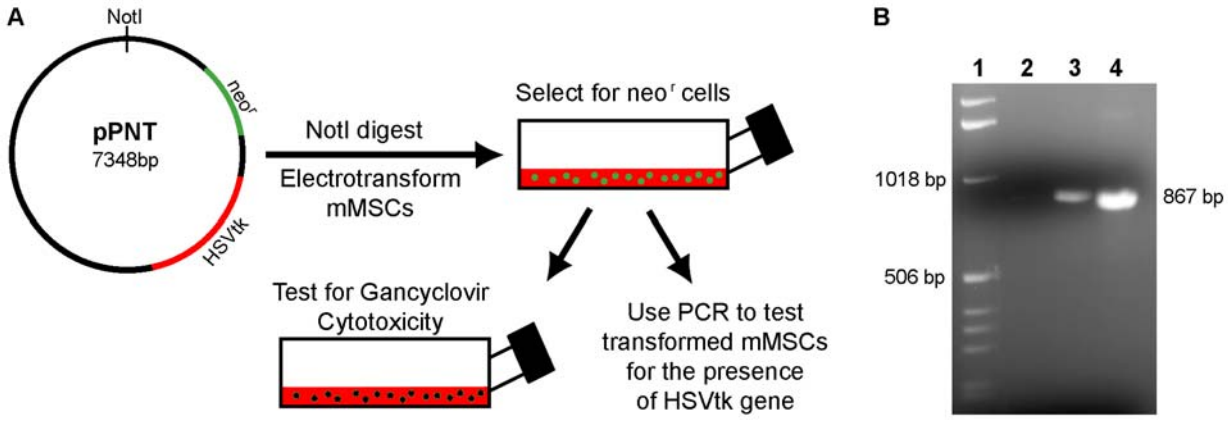

Figure 5-3: (A) Creation of an HSVtk+ mMSC cell line. Vector pPNT was linearized by restriction digestion with NotI and electrotransformed into normal mMSCs. Cells were selected for neomycin resistance, subject to nucleotide sequencing with HSVtk-specific primers and screened for sensitivity to gancyclovir to confirm successful incorporation of the plasmid into the genome. (B) Primers HSVtk-mut-F2 and HSVtk-HindIII-R2 were used to amplify the F2 fragment of HSVtk. When transformed MSC genomic DNA was used as template, it produced a PCR product which was identical to that produced using the pPNT plasmid as template. Genomic DNA from untransformed MSCs did not produce a detectable product. Gancyclovir cytotoxicity testing indicated that greater than 99.5% of the neo^r cells in our culture were HSVtk positive.

Cytotoxicity-based Measure of Small Fragment Homologous Replacement Efficiency

Although normal mMSCs have not been reported to express measurable levels of thymidine kinase activity, our normal HSVtk negative cells did display some cytotoxicity when treated with gancyclovir. We tested $HSVtk^+$ and control cells at various concentrations of gancyclovir to determine which concentration gave us the highest level of control cell survival compared to $HSVtk^+$ cell killing. Of the concentrations tested (0µg/ml, 6.25µg/ml, 12.5µg/ml, 18.75µg/ml, 31.25µg/ml, and 50µg/ml) 6.25µg/ml showed the best survival for $HSVtk^-$ cells and an acceptable degree of variance in survival between the control and test samples (88% survival for $HSVtk^-$ cells vs. 4% for $HSVtk^+$ cells) (see Figure 5-4A), so this concentration was used in all subsequent cytotoxicity experiments as our test condition.

We treated our $HSVtk^+$ mMSC line with pTKmut as described in the Materials and Methods section and examined the resulting cells for gancyclovir cytotoxicity resistance. A total of 90 fields of view were examined for live cells. The percent survival for treated cells was computed by comparing to $HSVtk^-$ cells plated at the same concentration and with the same amount of gancyclovir. We compared the average percent survival of our treated cells to the average percent survival of untreated $HSVtk^+$ mMSCs under the same conditions. We found a small but significant (p = 0.001) difference in % survival between the treated and untreated groups (see Figure 5-4B). This indicates that our SFHR treatment is successful in initiating small fragment homologous replacement at a low efficiency (0.307% of treated cells) in our mMSC line. Further experiments will be necessary to determine whether the efficiency of this treatment can be increased to the minimum 1% efficiency required for productive use as a treatment tool. We also plan to culture surviving cells and sequence the *HSVtk* gene to show that survival is a product of SFHR induced genetic changes to the target gene once we have established culture conditions which allow for clonal growth of our MSC line.

4. Discussion

In order to make effective use of autologous MSCs for treatment of NCLs, it is necessary to develop methods for repairing the genetic defect in the host-derived cells responsible for the

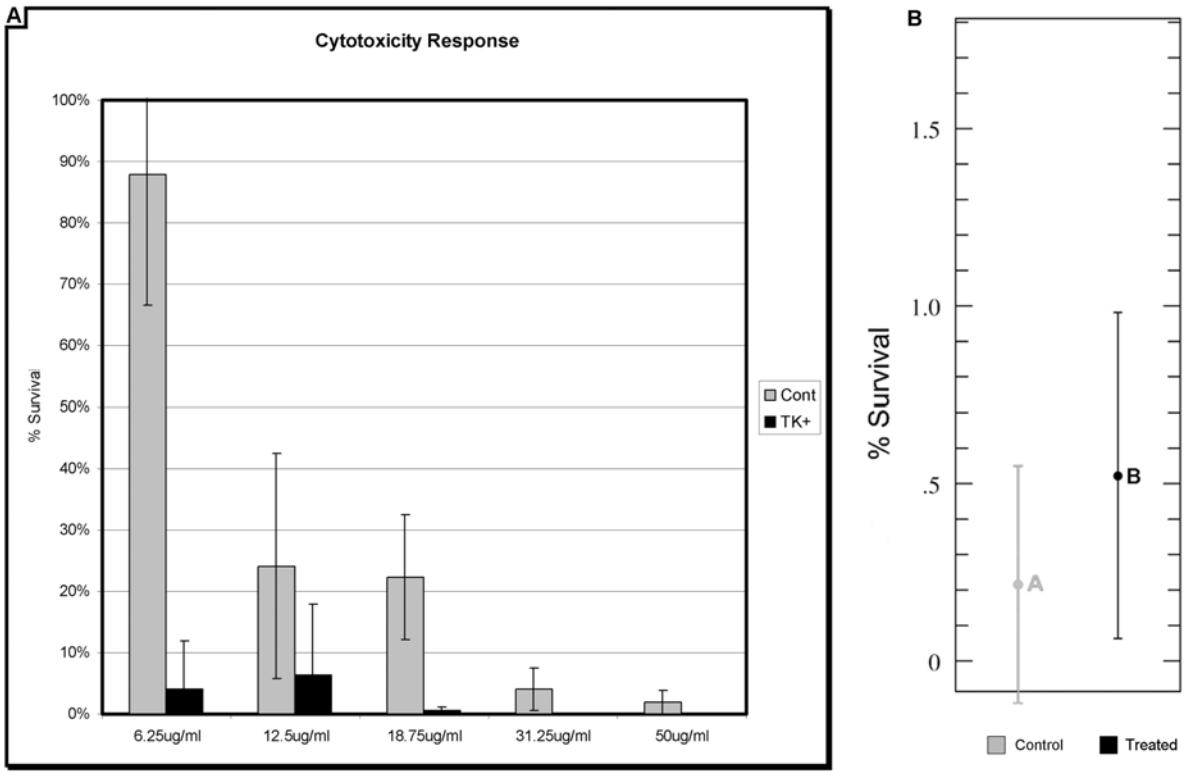

Figure 5-4: (A) Comparative analysis of gancyclovir sensitivity. Murine MSCs transformed with the pPNT vector and thymidine kinase negative controls were exposed to gancyclovir at the indicated concentrations to determine the optimum concentration to use for cytotoxicity assays. TK^- cells showed some sensitivity to gancyclovir at higher concentrations, but were only mildly affected at the lowest concentration, whereas all concentrations were nearly 100% cytotoxic to TK^+ cells. Since it produced the largest variance in % survival, we selected 6.25µg/ml as our standard concentration for subsequent assays. (B) Survival of pTKmut treated cells. SFHR treatment with linearized pTKmut vector increased survival of $HSVtk^+$ mMSCs from 0.22% (control) to 0.527% (treated), an increase of 0.307% (p=0.001). Percent survival was calculated as the number of cells surviving compared to a control well plated at the same concentration which did not receive any exposure to gancyclovir. Error bars are equal to 1.96 x SEM, which corresponds to the 95% confidence interval.

disease phenotype. In this chapter we describe the development of a cytotoxicity-based assay system for measuring the gene repair efficiency of SFHR and demonstrate a low, but significant rate of homologous replacement in treated MSCs. The goal of future experiments will be to increase the efficiency of recombination by altering the parameters of our SFHR protocol. Our current method uses a linearized, double-stranded (ds) targeting vector of 1326bp containing two nucleotide alterations in the approximate center. The molecule is heat-denatured prior to electrotransformation into target cells. While such methods have been used successfully in the past to generate recombination efficiencies as high as 4%, more recent findings indicate that altering this protocol may generate better results. [75] The DNA concentration we used (50ng/µl) is lower than other studies which have reported higher recombination efficiencies. [134] These studies also showed greatly increased efficiencies of gene repair (up to 20% *in vitro*) by performing repeated SFHR treatments on the same cells.

In 2005, Tsuchiya et al. reported a 12-fold increase in targeting efficiency over a standard dsPCR fragment of similar size when a 606nt single-stranded (ss) DNA fragment, prepared by restriction enzyme digestion of a ss-phagemid DNA molecule corresponding to the sense DNA strand of the target gene, was employed as the targeting vector. [76][135] Controls using the anti-sense strand of the target gene resulted in greatly reduced recombination efficiency, suggesting that the mechanisms responsible for SFHR may be related to active transcription of the target sequence. They also tested the effects of certain features of the DNA molecule on recombination efficiency, finding that the presence of methylated adenine (a by-product of phagemid growth in *E. coli* bacteria) was necessary for this dramatic increase in recombination and that the optimal targeting vector length was between 500 and 1200 nucleotides. A 12-fold increase in recombination rate from our current 0.307% would give us a targeting efficiency of approximately 3.6%, which is well within the range that would be useful as a therapeutic tool. We will evaluate the effectiveness of these methods with our cytotoxicity assay system in future experiments.

Chapter VI

Transplantation Experiments with Murine Mesenchymal Stem Cells

1. Introduction

Our proposed treatment of NCLs through autologous transplant depends upon two properties inherent to MSCs. The first is their ability to migrate to areas of degeneration and integrate into affected tissue. The long-term survival and integration of MSCs in host tissues after transplantation has already been documented in previous chapters. The experiments in this chapter are aimed at demonstrating that our cells display the same ability to become long-term residents in the tissue of their transplant host.

The second property of MSCs essential to our proposed therapeutic treatment is their ability to release soluble lysosomal enzymes into the extracellular milieu which can be transferred to other cells by means of mannose-6-phosphate receptor mediated uptake. This process, called cross-correction when it leads to amelioration of some disease phenotype, has proven to be an effective means of treatment in several models of lysosomal storage disease. [136][137][138] At least two forms of NCL (the infantile and late infantile forms caused by mutations in the *CLN1* gene and *CLN2* gene respectively) are know to involve soluble lysosomal enzymes and are theoretically capable of being treated by enzymatic cross-correction. [3]

A third property of MSCs, which is not essential to their usefulness in our therapeutic model, but which may add to their efficacy as a treatment for NCLs, is a generalized trophic effect mediated through their secretion of growth factors and anti-inflammatory cytokines. MSCs have been shown to produce numerous trophic factors such as angiopoetin-1, brain-derived neurotrophic factor (BDNF), connective tissue growth factor (CTGF), fibroblast growth factors (FGF) 2 & 7, granulocyte-colony stimulating factor (G-CSF), hepatocyte growth factor (HGF), interleukins (IL) 1, 6, 10, 11 & 13, leukemia inhibitory factor (LIF), macrophage-colony stimulating factor (M-CSF),

placental growth factor (PGF), platelet-derived growth factor (PDGF), transforming growth factor (TGF) -β, tumor necrosis factor (TNF) -α, and vascular endothelial growth factors (VEGF) A & B. [139][140][141][142][143] These secreted factors are capable of promoting repair and survival of injured tissue by suppressing local inflammatory responses, inhibiting fibrosis and apoptosis, enhancing angiogenesis and stimulating mitosis of other local stem/progenitor cells. [141] In many experiments where MSCs have contributed to tissue repair without significant cellular replacement, as has been reported for some myocardial infarction and nerve constriction models, the majority of the therapeutic benefit from transplanted MSCs has been attributed to secretion of paracrine factors such as those listed above. [60][143][83][62]

We have chosen to use a mouse knockout model of the CLN1 (infantile or INCL) form of the disease (CLN1-KO model mice), bearing an insertion mutation in the murine protein palmitoyl thioesterase-1 (*PPT-1*) gene as our experimental model for MSC-based therapy for human NCL. Although the human form of INCL often results from a single nucleotide mutation in the affected gene, and would be amenable to SFHR treatment of autologous cells, the mutation in the mouse model is far too large for us to correct with this method. As a result, we have chosen to use allogeneic MSCs rather than autologous MSCs for our initial transplant experiments. While the eventual goal is to make use of autologous MSCs to avoid issues of immune rejection, we do not believe the use of allogeneic MSCs in these experiments renders the results uninformative. Transplanted MSCs have been shown to interact in unique ways with the host immune system to avoid activation of immune responses. In addition to lacking MHC-II molecule expression, which allows them to avoid recognition by the T cells responsible for allograft rejection, MSCs also display various factors which have cognate ligands on T-cells such as CD90, vascular cell adhesion molecule (VCAM), intracellular adhesion molecule (ICAM-1) and activated leukocyte cell adhesion molecule (ALCAM), which would seem to indicate that MSCs interact with T-cells in some capacity. The presence of MSCs inhibits T-cell proliferation *in vitro* by inducing a state of division arrest anergy without inducing apoptosis. This anergy is mediated by an inhibition of cyclin D2 and upregulation of $P27^{kip-1}$. [144] Antibodies to hepatocyte growth factor (HGF) and TGFß have been shown to block this anti-proliferative effect. [145] In addition, MSCs have been

observed to upregulate production of indoleamine 2,3,-dioxygenase (IDO), an enzyme which exerts major immunosuppressive effects on T-cell responses to auto-antigens and fetal allo-antigens *in vivo*, as a result of exposure to pro-inflammatory cytokines released during T-cell activation. [146] Thus, it seems that MSCs possess an immuno-privileged phenotype which ameliorates some of the disadvantages of using allogeneic rather than autologous cells. While this is beneficial for our current studies, we still believe that MSC therapy in human NCLs would benefit from the use of autologous cells. When the conditions of our experimental models permit, we will begin development of protocols for autologous treatments.

In this chapter we describe experiments which measure the ability of our MSCs to demonstrate the first and second properties mentioned above. We examine the ability of our cells to integrate and survive in host tissue by transplantation into the medullary cavity of the femur and the intra-vitreal space of the eye in CLN1-KO model mice. We also test their ability to affect, through an *in vitro* model of enzymatic diffusion, the build-up of autofluorescent storage material in organotypic brain slices derived from CLN1-KO model mice. Initial results indicate that our cells are able to survive after transplant and disburse PPT-1 enzyme to surrounding cells at a level which drastically reduces the amount of autofluorescent lysosomal storage material present in the cytosol.

2. Materials and Methods

CLN1 Knockout Model Mice

CLN1 knockout model mice were generated by Sandra Hofmann's lab on a mixed background of C57BL/6J x 129S6/SvEvTac by deletion of the portion of the PPT-1 gene between exons 5 and 9 with concurrent insertion of a neomycin resistance cassette. [147] Correct recombination of the targeting construct was confirmed by neomycin resistance, thymidine kinase resistance and Southern blot analysis. Knockout mice develop characteristic autofluorescent lysosomal storage material in neural and other tissues which was determined to have the characteristic granular osmophilic deposits (GROD) structure normally associated with human INCL. At approximately 7

weeks of age, homozygous PPT-$1^{-/-}$ mice developed abnormal behaviors, seizures and displayed pronounced neurodegeneration similar to human INCL.[147]

The mice generated by Sandra Hofmann were subsequently backcrossed to C57BL/6J animals for over 10 generations in the laboratory of Mark Sands at Washington University. Animals with the mutation on the C57BL/6J background were kindly provided by Dr. Sands. To confirm that the backcrosses had replaced most of the parent strain genome with the C57BL/6J genome, genomic DNA from the breeders used to generate mice for our work was genotyped at 110 polymorphic marker loci spanning the genome at approximately 15 centiMorgan intervals. Genotyping was performed at Charles River Laboratories using their MaxBax service. Mice that were homozygous for the C57BL/6J alleles at all 110 loci were used to breed the animals that have been used in these experiments.

Our laboratory has established several more phenotypic parameters of the disease phenotype in these mice which can be used as a measure of therapeutic success. These include declines in electroretinogram (ERG) signal, retarded pupillary light response (PLR), retinal photoreceptor cell loss, accumulation of autofluorescent lysosomal storage granules in retinal tissues and behavioral changes. [148][149]

Brain Slice Cultures

CLN1-KO model mice between 6 and 8 weeks old were anesthetized by Isoflurane inhalation before decapitation and medial dissection of the skull. The entire brain was removed intact with sterile instruments and immediately placed in ice-cold, sterile, High Serum (HS) medium consisting of α-MEM + 25% horse serum, 25% Hank's solution (Invitrogen cat#14025-092), 6.5mg/ml Glucose, 10µl/ml Pen/Strep, 10µl/ml Fungizone (Invitrogen cat#15290-018). The cerebellum and a small portion of the forebrain were removed and the brain was divided in half medially. Each half of the cortex was placed in room temperature, liquid 4% agarose. When the gel had solidified, 400µm slices were cut on a Vibratome Series 1000 (Vibratome St. Louis, MO) and immediately placed into HS medium. Slices were microscopically examined to identify intact slices that contained regions of hippocampus which were then transferred to a Millicell

organotypic tissue culture plate transwell insert (Sigma-Aldrich Z354996). Slices were cultured on membranes suspended above 5ml of HS medium in a humidified 5% CO_2 atmosphere at 37°C. Only the bottom portion of the brain slices actually touched the culture medium. On each of the first five days of culture, 1ml of the existing media was replaced with Serum Free (SF) medium consisting of DMEM F-12 + 2% B27 serum-free medium supplement (Invitrogen cat#17504-044), 1% N2 supplement (Invitrogen cat#17502-030), 1% Pen/Strep and 1% Fungizone. SF medium was completely replaced once per week thereafter. [118]

mMSC Transplantation onto Organotypic Brain Slices

Murine MSCs expressing eGFP and cultured for no more than 12 passages were prepared for transplant by trypsinization as described in Chapter II – Materials and Methods. Cells were washed once in 1x PBS and resuspended in SF medium at a concentration of 5,000-50,000 cells/µl. A total of 0.2µl of cells were deposited onto each brain slice. At several time points after transplant, treated brain slices were fixed and examined with either fluorescence microscopy or electron microscopy to examine migration, integration, morphology and protein expression profiles of transplanted cells.

Fluorescent Microscopic Examination of Tissue

For fluorescent microscopy, tissues and cells were fixed in standard immunohistochemistry compatible fixative (IM) composed of 0.1% glutaraldehyde, 3.5% paraformaldehyde, 0.13M sodium cacodylate and 0.13mM calcium chloride, pH 7.4 for 45 minutes, washed twice with 0.17M sodium cacodylate buffer and stored in 0.17M sodium cacodylate buffer at 4°C until used. Tissues were embedded in Tissue-Tek OCT compound (Electron Microscopy Sciences Hatfield, PA cat#62550-01), frozen on dry ice and sections were cut at a thickness of 5 µm with a crysostat. Sections were mounted on uncoated, Superfrost/plus glass microscope slides (Fisher Scientific). Sections were examined on a Zeiss Axiophot fluorescence microscope.

For eye samples to be examined in cross-section, the cornea, iris and lens were removed immediately after enucleation. Posterior portions of the eye were incubated in fixative and embedded as described above. Cryostat sections for eye and brain slice samples were cut at a

thickness of 5 μm. Fluorescence microscopy was used to determine the extent of eGFP-expressing donor cell incorporation into host retinas and femurs and the amount of autofluorescent lysosomal storage granules in brain slices. Immunohistochemistry with fluorescent antibodies (as described in Chapter III) was used to detect markers of cellular proliferation (PCNA) and neurodifferentiation (βIII-tubulin) in retinal transplant samples. Fixed, undifferentiated mMSCs and mESCs were used as labeling controls for retinal IHC.

Femur Medullary Cavity Transplantation of mMSCs into Adult CLN1-KO Model Mice

Allogeneic mMSCs expressing eGFP and cultured for no more than 12 passages were prepared for transplant into the medullary cavity of the right femur of congenic adult mice who were either PPT-$1^{+/+}$ (C57BL6J mice) or PPT-$1^{-/-}$ CLN1-KO model mice. Mice were anesthetized before transplant with a subcutaneous injection (at the base of the neck) of 150-200μl of mouse cocktail (7.5mg/ml xylazine, 43.5mg/ml ketamine). Anesthetized mice were kept warm on heating pads warmed to 35°C until they were fully unconscious. Mice were then transferred, one at a time, to a sterile surgical area. All procedures were conducted with the mice on another heating pad covered by sterile labmat. The abdomen and hind legs of the mice were washed with 70% ethanol and the entire right, hind leg was shaved with clippers then swabbed with betadine surgical scrub.

Cells were prepared as described for the brain slice procedure and resuspended in sterile-filtered 1x PBS at a concentration of $1x10^6$ cells/ml. 50μl of the cell suspension was drawn up into a 1cc insulin syringe with a 28½ gauge needle (Becton Dickinson cat#329420) and stored on ice until injected. In order to prevent the transplant needle from clogging, a slightly larger 28 gauge needle was used to make a hole in the distal end of the femur before injection. With the mouse's knee bent at a 90° angle, the needle was inserted from the lateral side of the leg, underneath the patella into the space between the lateral and medial condyle (see Figure 6-1). Using a twisting motion, a hole was bored through the end of the bone until the needle could be felt to enter the medullary channel. While holding the leg steady, the boring needle was withdrawn and the injection needle was inserted to its fullest extent. Cells were injected in 10μl intervals while slowly

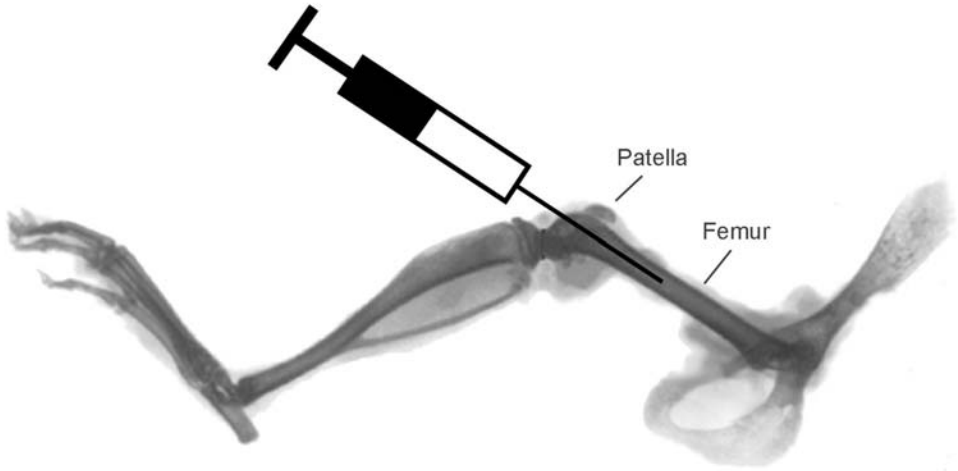

Figure 6-1: To perform injections of MSCs into the femoral medullary cavity of life, anesthetized mice, we positioned the leg such that the patella was displaced upward and allowed access to the *facies patellaris* of the femur. The needle was inserted through the *facies patellaris*, using the ridges of the *condylus laterallis* and *condylus medialis* as guides to find the correct area. By keeping the needle at the correct angle we were able to penetrate the end of the bone and insert it into the trabecular canal. The needle was inserted to the midpoint of the femur and the cells were injected as the needle was withdrawn to allow maximum room for the injected liquid (~40µl). Mice recovered well from this treatment with no infections or other complications for any treated mice. Usually, the mice were mobile within 24 hours of the procedure and showed normal use of the injected leg.

drawing the needle out of the bone to improve distribution throughout the marrow cavity. After transplant, the injected leg was swabbed once again with betadine surgical scrub and a subcutaneous injection of 100µl of 10µg/ml Bupernorphine analgesic was administered. Mice were placed in a clean cage warmed to 35°C to recover from anesthesia and were observed daily for signs of post-operative infection.

Decalcification and Cryosectioning of Injected Femurs for Fluorescence Microscopy

Femurs were dissected from mice 0, 2 and 4 weeks after transplant. Mice at the 0 week time point were examined immediately after injection of eGFP positive cells. Femurs were removed as described in Chapter II. Both ends of the bone were removed and then the long portion was split down the middle. All four pieces were incubated in IM fixative with rotation at room temperature for at least 2 hours then washed several times with 1.7M Na-cacodylate (pH 7.4) buffer. Before embedding in OCT compound, the bone was subjected to a decalcification procedure consisting of incubation in 0.17M Na-cacodylate buffer (pH 7.4) +10% EDTA for 7 days. [150][151] Embedding and cryosectioning of decalcified femur fragments was carried out as described above for brain and eye tissue.

Intraocular Transplantation of mMSCs into Adult CLN1-KO Model Mice

Allogeneic mMSCs expressing eGFP and cultured for no more than 12 passages were prepared for transplant into the intra-vitreal space of 4-8 week old CLN1-KO model mice by trypsinization (as described in Chapter II) and resuspension in 1 x PBS (pH 7.4) at a concentration of ~40,000 cells/µl in a total volume of 1.5µl. Mice were anesthetized as described above for femoral transplants. Cells were injected into the intra-vitreal space with a 10µl Hamilton syringe using a 31 gauge needle. [152] Mice were allowed to survive after implantation for 1, 2 or 5 weeks before being euthanized and the eyes prepared for fluorescence microscopy.

Polyacrylamide Gel Electrophoresis and Western Blotting of PPT1 Protein

Brain cortex and cerebellum samples from control $PPT1^{+/+}$ (C57BL6J) mice and CLN1-KO model mice were mechanically homogenized in a buffer of 20mM HEPES, 50mM NaCl, 50mM Sucrose and 1% protease inhibitor (Pierce cat#78410) at a concentration of 0.2g of tissue/ml.

Homogenates were spun at high speed in a benchtop microfuge to pellet insoluble material. Tissue homogenate was diluted in 2 volumes of Laemmli sample buffer (Bio-Rad cat#161-0737) and mechanically disrupted by sonication before heat denaturation in boiling water for 5 minutes. Samples were then centrifuged at high speed again immediately before loading onto Criterion Pre-cast Tris-HCl polyacrylamide gels of appropriate density (Bio-Rad Laboratories Hercules, CA) with molecular weight markers. Separation was carried out in a Criterion Cell tank (Bio-Rad cat#165-6001) at 200V (constant voltage) in 1x Tris/Glycine/SDS running buffer (Bio-Rad cat#161-0732) until the dye marker reached the bottom of the gel (approximately 50 minutes).

After electrophoresis, gels were removed from the Criterion Cell apparatus and equilibrated in cold Transfer Buffer (90% 1x running buffer, 10% methanol) for 20 minutes. At the same time, a sheet of Trans-Blot nitrocellulose transfer medium (Bio-Rad cat#162-0116) cut to a size slightly larger than the gel was equilibrated in cold Transfer Buffer as well. Transfer of the gel contents to the nitrocellulose was performed in a Criterion Blotter (Bio-Rad cat#170-4070) according to the manufacturer's instructions. After blotting, the nitrocellulose membrane was first washed in 1x TBS (Tris-buffered saline 2mM Tris-HCl, 50mM NaCl, pH 7.4) briefly then incubated in 1x TBS + 2% bovine serum albumin (BSA) + 1% goat serum either at room temperature for 2 hours or at 4°C overnight. After blocking, the blot was incubated with primary antibody diluted in blocking buffer at room temperature with gentle agitation for at least 4 hours. To improve signal detection, some blots were incubated an additional 12 hours at 4°C. Blots were developed with rabbit α-human PPT-1 primary antibody (Proteintech Group Inc. Chicago, IL cat#PTG10887-1-AP). Blots were then washed with 1x TBS three times for 5 minutes each before application of alkaline phosphatase conjugated goat α-rabbit IgG secondary antibody (Chemicon cat# AP307A) at a dilution of 1:1000. Blots were incubated in secondary antibody at room temperature with gentle agitation for 30-45 minutes then subject to four washes consisting of 1x TBS for 5 minutes, 1x TBS + 0.1% Tween-20 (Bio-Rad cat#161-0781) for 5 minutes (twice) and 1x TBS for 5 minutes. Blots were developed with the alkaline phosphatase sensitive chromogenic substrate BCIP/TNBT (Chemicon cat# ES007).

3. Results

Cross-correction by mMSCs Transplanted onto Organotypic Brain Slices of PPT1$^{-/-}$ Mice

Prior to transplantation experiments, we were interested in determining whether transplanted cells would actually be able to cross correct for NCL defects related to deficiencies in soluble lysosomal enzymes. It has been shown with other models that soluble lysosomal enzymes (such as the PPT1 protein) are released by cells into the extracellular milieu where they can be taken up by neighboring cells in a mannose-6-phosphate dependent manner. [153][154] To test whether our mMSCs could perform a similar function in neural tissue, we cultured organotypic brain slices obtained from PPT1$^{-/-}$ mice and transplanted EGFP-expressing mMSCs (which are obtained from congenic PPT1$^{+/+}$ mice) onto them as described in the Materials and Methods section. We suspected that the vast majority of the cells might remain on the surface of the brain slices after transplant, with only a few migrating into the tissue. This was not the case. In cross sections of the tissue, we observed that donor cells, which were transplanted on the upper surface of the brain slices, migrated into the tissue rapidly. In fact, very few EGFP positive transplanted cells were observed at the surface of the cultured brain slices. The vast majority were observed deep within the tissue after only a few days. We did not quantitatively track cell survival or location within the tissue slices, but we were able to observe many cells spread throughout the tissue 7-10 days after transplant, indicating that a good portion survived and actively migrated into the tissue.

In addition, we observed that, in areas where EGFP positive transplanted cells were located, the storage material content of the tissue was very low, while in areas with no transplanted cells present, autofluorescent storage material was abundant. (see Figure 6-2) Control brain slices which were not exposed to transplanted cells showed similarly high levels of storage material throughout the tissue. Although levels of storage material were variable, no areas of low autofluorescence like those observed around transplanted cells were seen in control tissue. Quantitative analysis of autofluorescent material in control and treated samples will be necessary to firmly establish the link between transplanted cells and a reduction in storage body levels.

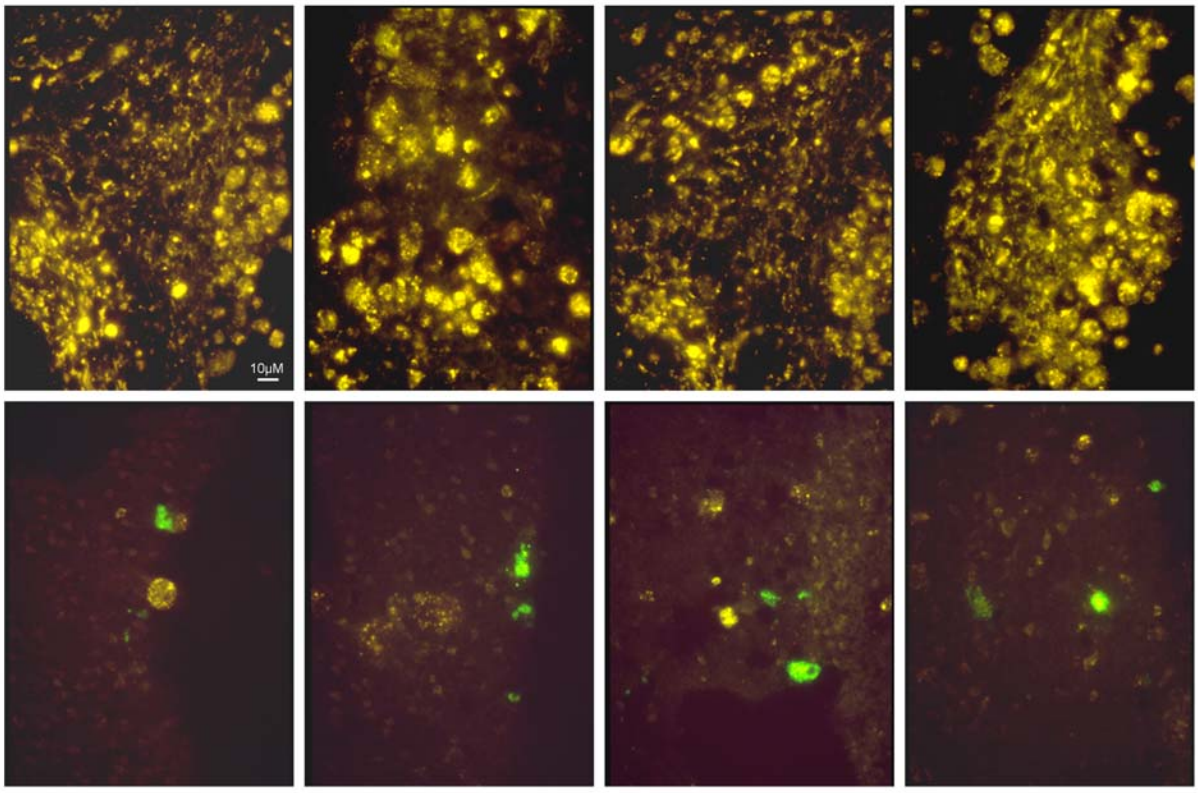

Figure 6-2: The effect of mMSC transplantation onto organotypic brain slice cultures derived from CLN1 knockout model mice. Areas of the cultured brain slices which were free of transplanted cells (upper row) displayed high levels of the golden autofluorescence typical of NCL storage material. Areas seeded with eGFP expressing mMSCs from CLN1 $^{+/+}$ mice displayed a drastic reduction in the amount of storage material present 10 days after treatment. We hypothesize that this reduction in autofluorescence is the result of enzymatic cross-correction, mediated by release of the *CLN1* gene product palmitoyl protein thioesterase 1 (PPT1) from transplanted cells and its endocytosis by host cells through the mannose-6-phosphate receptor pathway. The presence of functional PPT1 in lysosomes of affected cells leads to restored lysosomal function and digestion of accumulated storage material.

Intramedullary Bone Marrow Transplant of mMSCs

Previous research suggests that the method used for delivering MSCs to the host plays a significant role in their long-term survival and eventual localization within the host. The two most common methods in the past have been direct injection into a specific tissue site and intra-ventricular systemic infusion. Direct injection into a tissue such as the ventricles of the brain, the intra-vitreal or sub-retinal space of the eye, osteochondral defects of the cartilage and the myocardial layer of the heart usually leads to significant levels of engraftment in the surrounding tissue. [64][127][67][58][83][55] Systemic injection of MSCs has yielded much more variable results, usually with significantly lower levels of engraftment. [155][156][157][158] In addition, neither transplant methodology encourages injected MSCs to return to the MSC niche in the bone marrow stroma and take up long-term residence there as stem cells. Instead, most transplant methods lead to rapid differentiation of donor MSCs. Recently, intra-bone marrow transplant (IBMT) has been suggested as an alternate method for MSC transplant. [159][160] This method has proven 100 times more efficient at producing long term engraftment of donor MSCs than intra-ventricular infusion. [161] The mechanism for this improvement may be the elimination of the need for circulating MSCs to home to the BM niche prior to engraftment. In addition, it may be more likely to produce a population of undifferentiated donor stem cells that persist after treatment by immediately localizing transplanted cells to native stem cell niches in the bone marrow. This could prove beneficial for diseases, such as the NCLs, where degeneration takes place in a wide range of tissues over lengthy periods of time.

We have performed preliminary experiments to assess the feasibility of intra-marrow transplant. We implanted eGFP expressing, allogeneic mMSCs into the medullary cavity of femurs in CLN1-KO model mice and looked for eGFP positive cells in fixed sections 0, 2 and 4 weeks after transplant. In all samples, we were able to detect only a very small number of transplanted cells in the marrow cavity. We believe that the low engraftment ratio is due to difficulties with the transplant procedure itself and are not indicative of low survival or significant cell death on the part of the transplanted MSCs. This hypothesis is supported by results from our 0 week time point mice, which were euthanized immediately after the transplant procedure and also contained

very small numbers of transplanted cells. In these samples, eGFP positive cells would not have had time to undergo apoptosis, migration away from the marrow cavity or silencing of their eGFP gene. When the eGFP-expressing MSCs were mixed with mouse bone marrow extracts and examined immediately, the green fluorescing cells were present in the expected proportion to non-fluorescent cells from the bone marrow. This indicates that if the donor MSCs are present, we are able to detect them.

We found it very difficult to perform the injections depicted in Figure 6-1 due to the small size of the medullary cavity in a mouse femur and the awkward angle of insertion through the knee joint. It is likely that many of the injections penetrated the bone after insertion into the bone marrow cavity and injected cells were transplanted into the hind leg muscles rather than within the bone marrow. Unfortunately, it is not possible to visualize the location of the injection needle without doing much more invasive surgery. In addition, the injection of liquid into the confined space of the femoral bone marrow compartment may have caused an increase in pressure that caused the implanted cells to exit the medullary cavity through the injection site as soon as the needle was removed. This would have resulted in the transplanted MSCs being localized to the knee joint and surrounding connective tissue rather than inside the femoral bone marrow cavity. Options are being considered for improving our intra-marrow transplant techniques, including, extraction of a portion of the bone marrow in injected mice and moving to a larger animal model of NCL for the experiments (such as our canine models).

Intraocular Transplant of mMSCs

Allogeneic mMSCs expressing eGFP were transplanted into the intra-vitreal space of the eye in CLN1-KO model mice to examine their potential for survival and engraftment in neural tissue undergoing degeneration as a result of NCL. Treated mice were euthanized 1,2 or 5 weeks after cells were injected. Fluorescence microscopy was used to detect the presence of eGFP expressing donor cells. Fluorescently labeled antibodies were used to examine the expression of markers for cellular proliferation and neural differentiation.

In our samples, we found many eGFP expressing donor cells in the eyes of transplant hosts at 1, 2 and 5 weeks after implantation (see Figure 6-3). At the 2 week time point, donor cells were more closely associated with the retinal tissue than at 1 week post-transplant, but we did not see any integration of donor cells into the host tissue. By 5 weeks many of the donor cells had moved into the inner retina (data not shown).

Immunohistochemistry results for our intraocular injections are difficult to interpret. As positive labeling controls for our antibodies, we chose mESCs for PCNA and retinal tissue for βIII-tubulin. Both should label highly positive for their respective proteins. However, we observed no detectable labeling for PCNA in our mESC samples and only low levels of PCNA labeling in undifferentiated mMSCs (which should also be highly positive for PCNA). We also observed only low levels of labeling for βIII-tubulin in neural retinal tissues, which should be highly positive for this protein. In addition, a high level of non-specific background fluorescence was present in our samples, which interfered with detection of fluorescence from the Cy5-labeled antigen-specific antibodies. As a consequence of our ambiguous controls and other technical difficulties, we cannot fully trust the results we observed for experimental samples. Further experiments are being conducted to eliminate technical problems and improve our ability to assess the behavior of our mMSCs after transplant. One conclusion that we can draw from these experiments is that our transplanted cells survived for at least 5 weeks and appeared to migrate into closer contact with the retina over time.

Polyacrylamide Gel Electrophoresis and Western Blotting of PPT1 Protein

After transplantation of mMSCs into CLN1-KO model mice, we want to track the activity of the cells in several ways. Most importantly, we would like to be able to determine how effective the cells are at supplying PPT1 protein to host cells surrounding them. Fluorescence IHC using an α-PPT1 antibody on sectioned tissue is one way of observing this phenomenon.

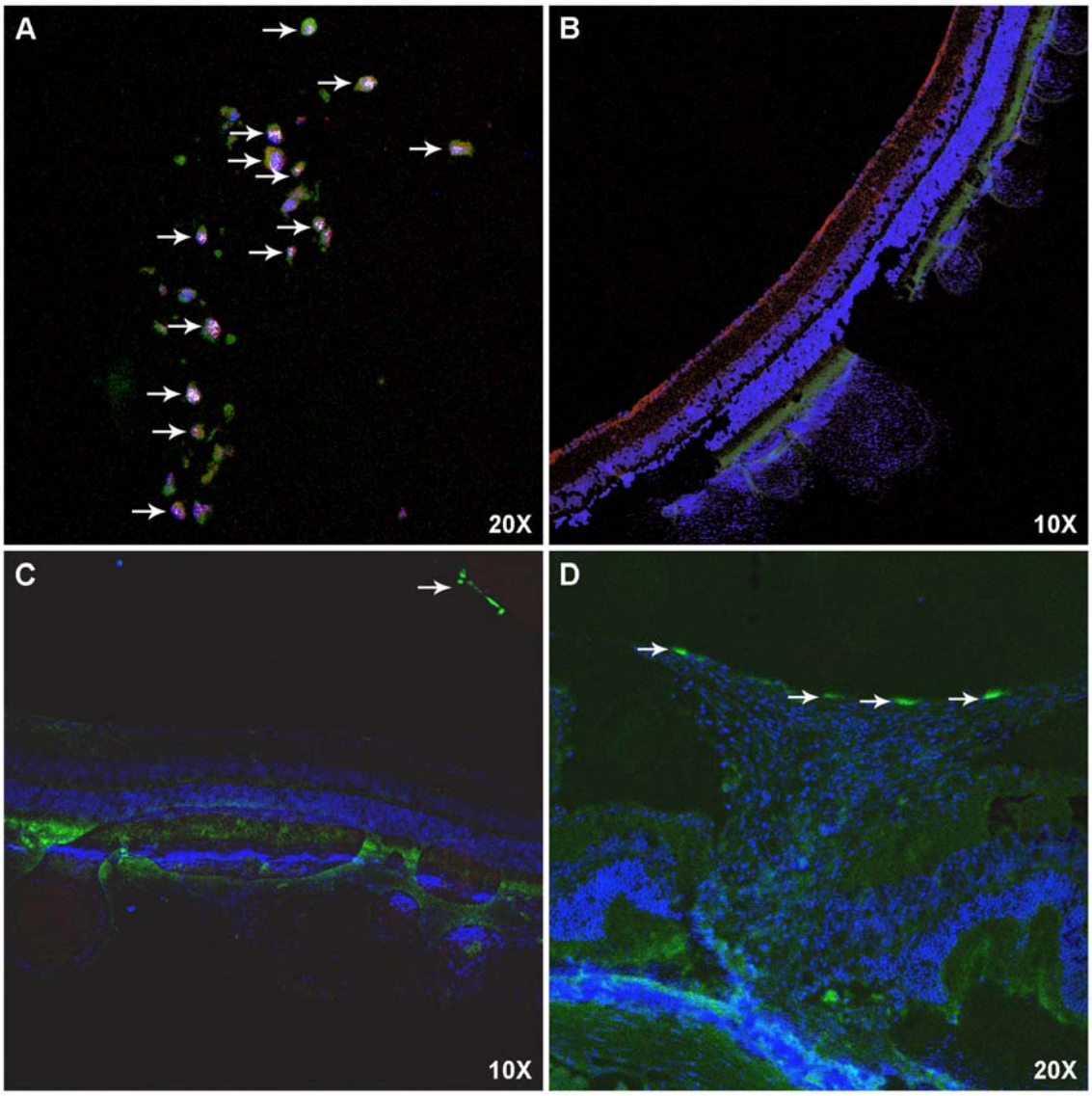

Figure 6-3: Immunohistochemical analysis of intraocular injections. Green indicates eGFP fluorescence, nuclei are counterstained with DAPI (blue), PCNA and βIII-tubulin are labeled with Cy5-conjugated antibody (red). Double labeling of DAPI and PCNA in the nucleus appears white. (A) Untransplanted mMSCs label positive for PCNA expression (PCNA positive nuclei indicated with white arrows). (B) Retina labeled with anti-βIII-tubulin antibody shows only low levels of staining. (C) Retina 1 week after transplant. Green fluorescent donor cells (white arrow) still remain in the vitreous and unassociated with retinal tissue. (D) Retina 2 weeks after transplant. Green fluorescent donor cells (white arrows) are closely associated with retinal tissue.

We tested our α-PPT1 antibody's ability to detect PPT1 on a Western blot (see Figure 6-4) in order to confirm that it could detect the correct protein accurately. Using an alkaline phosphatase conjugated secondary antibody we observed a single primary band at ~35kDa which stained strongly in cerebral cortex and weakly in cerebellum. At higher sample concentrations, a smaller band, running at about 23kDa appeared in cerebral cortex samples. We suspect this is a partially degraded or modified version of the PPT1 protein which is at a lower overall concentration in our samples than the full length protein. Examination of samples from $PPT1^{-/-}$ mice will indicate whether this hypothesis is correct. Our initial findings indicate that this antibody may be effective in labeling fixed tissue sections for fluorescence IHC.

4. Discussion

In this chapter we have established through *in vitro* experiments that our mMSC isolate appears to be reverse the build-up of autofluorescent storage material in neural tissue of NCL affected mice, presumably through diffusion of the PPT-1 enzyme from transplanted cells. An alternative explanation for our current results could be that transplanted mMSCs migrate into affected neural tissue and seek out areas where lysosomal storage material is already present at low levels. Results from untreated brain slices argue against this interpretation. While distribution of autofluorescent material is not uniform in control slices, the areas of low fluorescence still contain significant storage material, with levels far above that observed around transplanted cells in treated samples. A systematic and quantitative survey of tissue from both untreated and treated slices derived from the same animal will provide more conclusive information concerning the cross-correction effects of transplanted mMSCs.

We have also shown that transplanted allogeneic mMSCs survive for at least 5 weeks after intraocular transplant and slowly migrate through the vitreous and into the retina in CLN1-KO model mice. In addition, our results revealed that the protocol we are currently using for IBMT of MSCs is ineffective and needs to be revised. We hypothesize that the IBMT protocol suffers from

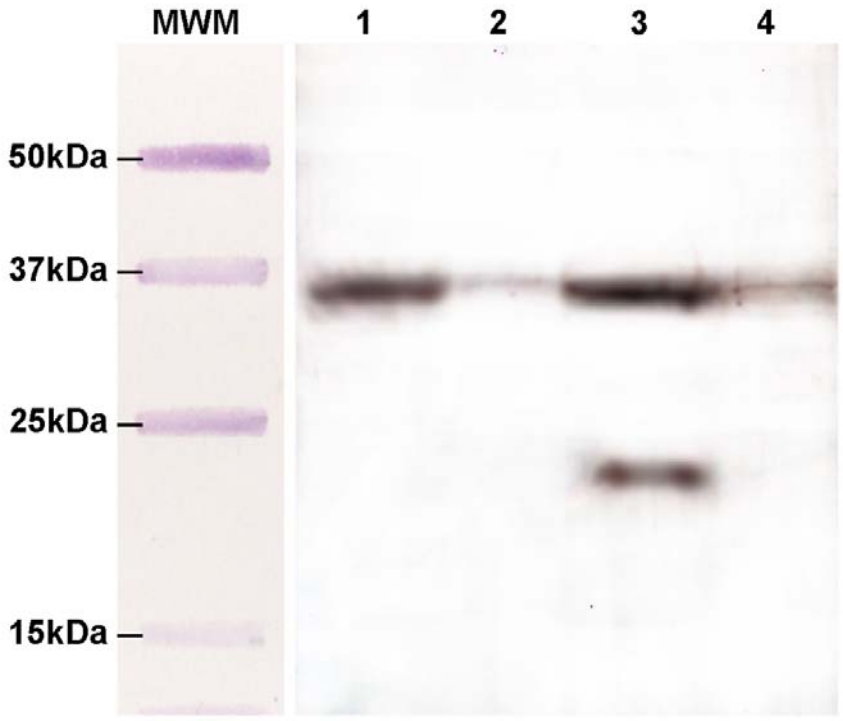

Figure 6-4: Western blot of cerebral cortex (lanes 1 & 3) and cerebellum (lanes 2 & 4) lysates demonstrating specific labeling of PPT1 protein (~36kDa) by an anti-PPT1 antibody. PPT1 appears to be less abundant in the cerebellum. At higher concentrations of sample (lanes 3 & 4), a lower molecular weight band is also detected in the cortex sample. This may represent a post-translationally modified or truncated form of the PPT1 protein.

two problems. First, because of the difficulty of inserting a needle into the medullary cavity, the cells are often not injected directly into the bone marrow. In order to prevent transplantation from being defined as a surgical procedure, we do not expose the bone during injection. This means we cannot always observe when the point of the needle penetrates the side of the femur and is, in fact, injecting cells into the thigh muscle rather than the marrow cavity. Second, even when cells are injected with the needle in the medullary cavity, the limited space inside a mouse femur and the rigid composition of the bone marrow stroma cause a buildup of pressure at the time of injection which presumably forces the cells (which are suspended in liquid) to leak out of the marrow compartment into the surrounding tissue through the injection site as soon as the needle is removed. Refinement of this protocol may call for additional steps which remove some of the marrow before donor MSCs are injected. This would create a space in the medullary cavity for injected liquid, eliminating any pressurization of the marrow compartment, and might also open up biochemical niches for new MSCs to replace host MSCs lost by removal of the existing stroma.

For now, we plan to focus on intraocular injections as a means of evaluating the behavior of our mMSCs after transplant into an NCL affected host. Intraocular injection has a number of advantages over IBMT for our current set of experiments. First, due to the nature of the mutation introduced into the CLN1-KO model mice, we must use allogeneic MSCs rather than autologous cells. Although MSCs possess the ability to avoid stimulation of an active immune response, it is not know whether their differentiated progeny reap the benefits of this immune-suppression. The blood-retinal barrier makes the eye an immune-privileged organ where transplanted cells are much less likely to undergo autoimmune rejection. [162] In other experiments performed with murine ESCs, we observed no inflammatory reaction up to 16 weeks after intraocular injection into allogeneic mice. [152] Thus, we can track survival of our cells in the absence of immune rejection even after they differentiate into tissue-specific cells, giving us a more accurate picture of survival and engraftment. Second, this barrier will also impede migration of the transplanted cells out of the eye, which will also make our assessment of cell survival more accurate. Finally, many parameters for disease phenotype related to the eye of this mouse model have been

defined. By transplanting mMSCs into the eye we can look for improvement in these disease phenotypes such as photoreceptor cell loss, storage material accumulation, ERG amplitude and pupillary light response. Changes in these phenotypes will act as a measure of the cells' therapeutic potential in the treatment of NCLs.

There are, however, reasons to pursue a transplant model system which provides for systemic dispersal of implanted MSCs. Although the primary effect of the NCLs is neurodegeneration, the disease does not affect only neural tissues. Storage material is present in a number of other tissues including the spleen, liver and kidney and appears to have some affect on function. Mitochondria derived from the liver of dogs affected with canine NCL show abnormal oxidative phosphorylation and respiration activity. [177] Some forms of the disease also cause abnormal proteins to accumulate in serum and urine of affected individuals. [178] While the neurodegenerative phenotype of the NCLs is the primary factor in their morbidity and mortality, the effects of the disease on these other organs might eventually lead to life-threatening complications if non-neural tissues are not addressed in the treatment methodology. Thus, it may be beneficial for treatment of NCLs in humans to find a transplant procedure which allows systemic dispersal of implanted MSCs. We believe, despite our current difficulties, that IBMT is a viable treatment technique. By implanting MSCs into the bone marrow stroma, we would allow some transplanted cells the opportunity to take up residence in their natural niche environment, hopefully leading to a long-term pool of donor-derived stem cells. IBMT also opens the possibility of implanting cells and then mobilizing them *in vivo* with drugs such as G-CSF, heparanase, dextran sulfate and AMD3100. [163] Treatment with mobilizing drugs causes phenotypic changes on the cell surface of MSCs present in the peripheral bloodstream which renders them more sensitive to signals from injured or degenerating tissue and activates pathways important for transmigration across blood/tissue barriers. [163] In addition, some mobilization treatments may cause circulating MSCs to become more susceptible to differentiation signals in tissues where they engraft. [35] A two-stage treatment of transplant and mobilization might lead to transplanted cells which are more effective at engrafting and repairing degenerating tissues than systemic transplant alone. IBMT is also less invasive than other proposed transplant methods

such as direct injection of MSCs into the ventricles of the brain or the cerebrospinal fluid (CSF). IBMT with whole bone marrow has previously been shown to improve retinal function in a murine model of lysosomal storage disease. [136] We believe using a similar technique, but with purified MSCs rather than whole bone marrow, will lead to even better therapeutic results.

Further experiments involving MSC transplantation into NCL model systems will be conducted on several fronts. We expect to perform additional intraocular transplants into CLN1-KO model mice with examination of longer time points post-transplantation. In addition to looking for changes in disease phenotype we plan to refine our IHC technique and determine whether transplanted cells are losing protein markers of MSC identity and proliferation and gaining markers of neural identity. Since it has been suggested that pre-treatment with mobilizing agents promotes integration and differentiation of MSCs, we also plan to explore the effect of such drugs on MSCs implanted in our intraocular system. Eventually, we plan to develop alternate NCL model systems in larger animals both as a means of improving the efficacy of IBMT and in order to examine the effectiveness of our methods on animal models which more closely recapitulate human forms of NCL. The next chapter describes experiments to characterize several dog models of NCL which we believe will be useful additions to our repertoire of model systems for examining the transplant of autologous MSCs as a treatment for human NCLs.

Chapter VII

Canine Models of Neuronal Ceroid Lipofuscinosis

1. Introduction

Animal models have been invaluable in the study of the biomolecular characteristics of the neuronal ceroid lipofuscinoses. While mice have been the most popular model for study by a wide margin, other animals have also proven helpful. As an experimental model, dogs have many characteristics which make them an excellent choice as models of human diseases. Since their domestication over 17,000 years ago, dogs have shared our environment, lifestyle and diet to a greater degree than any other animal. [164] Since the 17th century, dogs have been used as model animals for human physiology, metabolism and anatomy. Because of their similarity to humans in physiology, disease progression and clinical responses, dogs are often used as models for the study of aging, pharmacology, toxicology, neurology, cancer and genetics in humans. [165] The canine genome is organized in a way very similar to the human genome. Over 58% of dog diseases attributable to genetic mutations are true homologs of human diseases. [166] Recently, the canine genome has been sequenced, making direct comparisons between human and canine genomics possible. For many organs important to our work, such as the eye, brain and bone marrow, the size and physiology of canine tissues is much closer to humans than equivalent mouse models. [167] For all of these reasons, canine models represent an invaluable tool in the study of NCLs.

In this chapter we describe our work to characterize several canine populations which develop neurodegenerative diseases similar to NCLs. Tibetan Terriers develop a late-onset neurodegenerative disease which is accompanied by massive accumulation of autofluorescent storage material in neural tissues, loss of vision, seizures and other symptoms associated with several forms of NCL. [10][9] We describe our nucleotide sequencing analysis of the candidate gene tripeptidyl peptidase 1 (*TPP1*), the ortholog of which causes the late infantile form of NCL in humans, and its exclusion as the cause of Tibetan Terrier canine NCL (CNCL). [168] In addition,

we characterize the protein content of storage material found in neural tissue from affected Tibetan Terriers and report that glial fibrillary acidic protein (GFAP) constitutes the major protein component of Tibetan Terrier lysosomal storage granules.

We also report on the expression of the protein activating transcription factor 2 (ATF2) in a canine form of neurodegeneration with many similarities to NCLs. This is a previously undescribed, neonatal-onset disease recently characterized in poodles. (Katz, unpublished results) The disease, termed neonatal encephalopathy with seizures (NEWS), is caused by a methionine to arginine conversion at position 51 in the ATF2 protein. Western blots were carried out with ATF2 specific antibodies to determine whether the mutated protein is still present in affected animals.

Finally, we show that we are able to culture both canine MSCs and canine fibroblasts from normal dogs and dogs affected with a canine form of late infantile neuronal ceroid lipofuscinosis (LINCL), which we hope to use as an extension of our mouse studies. This disease, which was identified in Dachshunds, occurs as the result of a single nucleotide deletion in exon 4 of the canine *TPP1* gene and would be amenable to treatment by SFHR. [169] Initial characterization of affected dogs indicates that the disease progression and symptoms are very similar to that observed in human patients afflicted with LINCL.

2. Materials and Methods

Animals and Samples for *TPP1* Gene Sequencing

Blood or tissue samples were obtained from Tibetan Terrier and English Setter dogs that were either affected with NCL or were phenotypically normal. The disease status of animals in our study was rigorously determined. The English Setter samples were isolated from a colony of dogs that has been maintained for research for over 50 years. [170] English Setter NCL invariably results in death between 22 and 26 months of age. Affected dogs were identified by the appearance of characteristic behavioral symptoms at about 16 months of age, and the diagnoses were confirmed on all affected dogs by examining neural tissues postmortem for the presence of the disease-specific storage material (see Figure 7-1). Unaffected English Setter

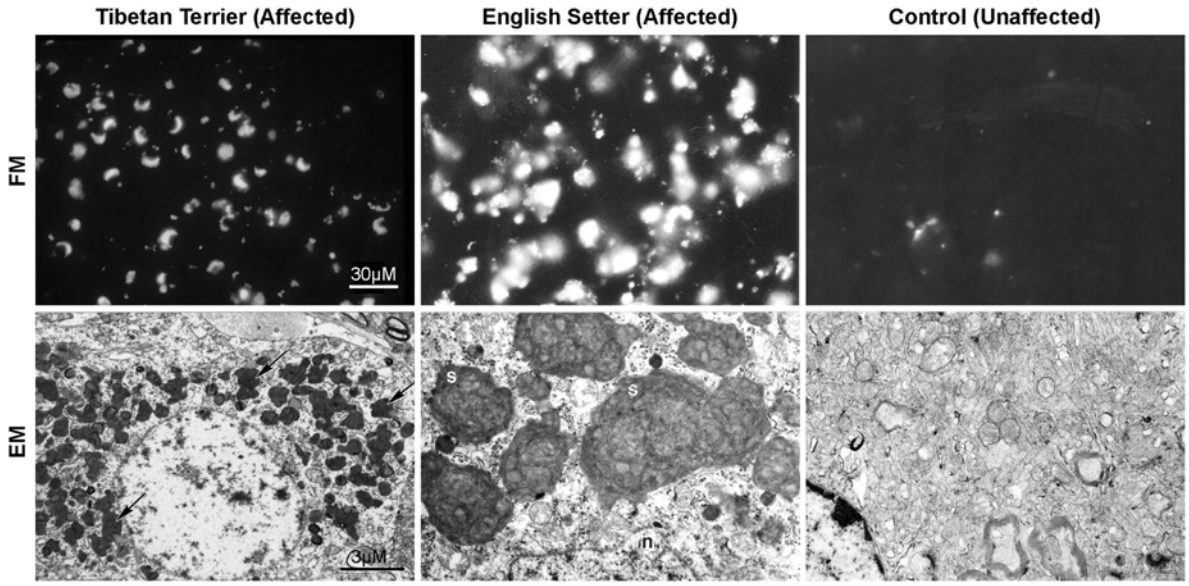

Figure 7-1: Fluorescence (FM) and electron (EM) micrograph images of canine storage bodies. With UV excitation, Tibetan Terrier and English Setter lysosomal storage material is autofluorescent and appears as yellow-gold deposits within the cytosol of affected cells. Unaffected tissue accumulates age pigment (a related material) but at a much lower level. Using transmission electron microscopy, canine storage material appears as electron dense granules. Granules display different morphological features depending on the exact mutation responsible for the disease. Calibration bars are for all FM (30 μm) and EM (3 μm) images respectively.

samples came from dogs outside of the colony who showed no signs of the disease and who were all at least 3 years old at the time of sampling. Unaffected English Setters included in the genetic analyses were euthanized and tissue samples were collected for morphologic analyses. Absence of disease in the normal Setters was confirmed by the absence of storage bodies in the cerebral cortex and cerebellum. Normal dogs came from pedigrees with no reported cases of NCL, so it is likely that they were homozygous for the normal allele of the disease gene. Frozen tissue samples from the dog colony and from the unrelated normal English Setters have been archived and were used as a source of DNA for these studies.

In Tibetan Terriers, the behavioral signs of NCL do not appear until 5 to 6 years of age and affected dogs can live to be 10 years old. [9] To identify affected dogs, we solicited responses to an exhaustive behavioral and health questionnaire from owners of hundreds of Tibetan Terriers (see Appendix). Respondents to the questionnaire provided us with blood samples from their dogs and pedigree information. Based on the questionnaire responses, we identified many dogs that were tentatively classified as affected. The owners of these dogs were asked to donate retinal and brain tissues for analysis when the dogs were euthanized. These tissues were examined with fluorescence and electron microscopy to determine whether disease-specific storage material was present. [9] Dogs were designated as affected with NCL only if they exhibited clinical and behavioral symptoms characteristic of the disease in this breed, and if there was accumulation of disease-specific storage material in the retina. cerebellum, and cerebral cortex upon examination by fluorescence and electron microscopy (see Figure 7-1). Animals who survived to at least 8 years of age without displaying any symptoms of the disease were diagnosed as unaffected. Animals which could not be definitively placed in either group were excluded from the study.

Fluorescent and Electron Microscopic Examination of Tissue

For fluorescent microscopy, tissues and cells were fixed in standard immunohistochemistry compatible fixative (IM) composed of 0.1% glutaraldehyde, 3.5% paraformaldehyde, 0.13M sodium cacodylate and 0.13mM calcium chloride, pH 7.4 for 45 minutes, washed twice with

0.17M sodium cacodylate buffer and stored in 0.17M sodium cacodylate buffer at 4°C until used. Tissues were embedded in Tissue-Tek OCT compound (Electron Microscopy Sciences Hatfield, PA cat#62550-01), frozen on dry ice and sections were cut at a thickness of 5 µm with a cryostat. Sections were mounted on uncoated, Superfrost/plus glass microscope slides (Fisher Scientific). Sections were examined on a Zeiss Axiophot fluorescence microscope.

For electron microscopy, tissues and cells were fixed and stored in standard electron microscopy compatible fixative (EM) composed of 2% glutaraldehyde, 1.12% paraformaldehyde, 0.13M sodium cacodylate, 0.13mM calcium chloride, pH 7.4. Tissues were embedded and sectioned using standard EM sample protocols (available from the UMC Electron Microscopy Core website at http://www.emc.missouri.edu/pandp.htm).

Nucleic acid isolation

Genomic DNA for cloning and sequencing was extracted from blood leukocytes of healthy and NCL affected animals. Briefly, erythrocytes were lysed in a solution of 1X Tris-EDTA (TE, Fisher cat. No. BP1338-1) and leukocytes were isolated by centrifugation. Leukocytes were then lysed for at least 48 hours in Nuclei Lysis Buffer (NLB, .4M NaCl, .01M Tris-HCl, 2mM EDTA, .2% SDS, .15% dithiothreitol and 1.4 mg/ml Proteinase K). After incubation, the sample was centrifuged at 13,000rpm in a benchtop centrifuge to remove undigested cells or tissue and extracted with phenol/chloroform/iso-amyl alcohol (Fisher Scientific cat#BP1753-100). Samples were centrifuged to separate the aqueous and organic layers and the aqueous supernatant transferred to a new test tube. The DNA was precipitated by ethanol and 3M sodium acetate and resuspended in ddH_2O. DNA concentration was determined by spectrophotometric absorbance at 260nm.

Genomic DNA was also extracted from tissues and cultured cells with the above method. For certain tissues, incubation times in Nuclei Lysis Buffer were lengthened to increase the quality and yield of genomic DNA. Otherwise, the procedure was as described above.

A

Primer	Primer Sequence
dc1p-f	5′ – atc g**aa gct t**gg tgt ggc ggt gga aca tag – 3′
dc1p-r	5′ – tag c**gc atg c**ag tgg atg act cca aag gct c – 3′
dc2p-f	5′ – atc g**aa gct t**at gtc ctc ctc cag tca gac tc – 3′
dc2p-r	5′ – tag c**gc atg c**ta gcg atg aaa ctc agc ccc ag – 3′
dc3p-f	5′ – atc g**aa gct t**tg atc tct gac ctc cag aca g – 3′
dc3p-r	5′ – tag c**gc atg c**tc acc tga ggc aaa gag cag – 3′
dc4p-f	5′ – atc g**aa gct t**ta cat cca gcg ggt caa cac tg – 3′
dc4p-r	5′ – tag c**gc atg c**ag cca ggc tga ttc tta ccg ag – 3′
dc5p-f	5′ – atc g**aa gct t**ta ctg ggt ggt cag taa cag cg – 3′
dc5p-r	5′ – tag c**gc atg c**gg aag acc tga gca tga tgg ag – 3′

B

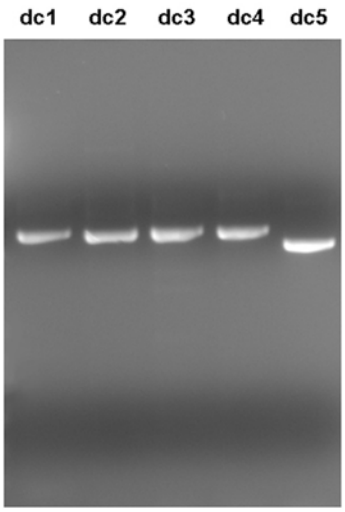

Figure 7-2: (A) Primers used for PCR cloning of canine tripeptidyl peptidase 1 (TPP1). All forward primers (designated "-f") contain a HindIII restriction site and all reverse primers (designated "-r") contain an SphI restriction site. These are bolded in the primer sequence. (B) Products of PCR amplification with TPP1 cloning primers. All products ran at their correct sizes (dc1=1184bp, dc2=1166bp, dc3=1174bp, dc4=1178bp, dc5=1048bp). These products were digested with HindIII and SphI, then ligated into complementary sites in pUC19 vector.

Cloning and Nucleotide Sequencing of the Tibetan Terrier *TPP1* Gene

The normal canine *TPP1* gene sequence was determined from GenBank record AAEX01017594.1 which contains the sequence from a Boxer used for the canine genome sequencing project. This sequence was used to design primer pairs for PCR amplification and cloning of the *TPP1* gene from an NCL affected Tibetan Terrier (see Figure 7-2). Amplified fragments overlapped at each juncture to allow full sequencing of the *TPP1* gene. PCR amplified fragments were cut with the appropriate restriction enzymes, gel purified and ligated into pUC19 vector. The resulting constructs were transformed into E. coli DH5ά and selected on ampicillin (100µg/ml). Plasmid was purified from bacterial cultures using the QIAprep Spin Miniprep Kit (Qiagen Inc. Valencia, CA cat. #27104), concentrated by ethanol precipitation and resuspended in ddH2O prior to sequencing. Nucleotide sequencing was performed at Davis Sequencing (Davis, CA 95616) using Applied Biosystems Big Dye Terminator V3.0 sequencing chemistry on ABI 3730 DNA sequencers and the resulting sequences were compared to English Setter (GenBank accession no. AF114167) and canine genome sequences to discover polymorphic sites. Each nucleotide in the gene was sequenced at least 4 times (twice in both directions) and individual polymorphisms were confirmed by an additional 2 sequencing reactions (once in both directions).

PCR amplification

All PCR amplifications were performed with Roche Diagnostics' *Expand* high fidelity PCR system (Roche Diagnostics Indianapolis, IN) according to the manufacturers instructions. Forward and reverse primers were used at a final concentration of 0.6µM each and the amount of template DNA used was either 50ng (genomic DNA) or 5ng (plasmid DNA) per reaction. PCR cycling was performed in an Eppendorf Mastercycler Personal thermocycler (Eppendorf NA, Westbury, NY) according to the protocol below. PCR products were separated on a 2% agarose gel and visualized by ethidium bromide fluorescence in a Bio-Rad Fluor-S Multi-imager (Bio-Rad Laboratories, Hercules, CA). PCR products for cloning or sequencing were purified using a QIAquick PCR Purification Kit (QIAGEN cat#28106) according to the manufacturer's instructions.

Initial denaturation	95°C	2 minutes
Denaturation	95°C	30 seconds
Annealing	58-62°C	30 seconds (depending on optimal primer annealing temperature)
Extension	68°C	2-4 minutes (depending on target sequence length)
(repeat Denaturation, Annealing and Extension cycles 30 times)		
Final Extension	68°C	2 minutes

Pyrosequencing of Tibetan Terrier Samples

After identifying a polymorphic site in the coding region of the *TPP1* gene from an NCL affected Tibetan Terrier, a pyrosequencing assay was developed to screen multiple Tibetan Terrier genomic DNA samples at this locus. Pyrosequencing of this polymorphism was performed with a PSQTM 96 Pyrosequencer as directed in the PSQTM Sample Preparation Guidelines for SNP Analysis Manual (Biotage). The primers used for pyrosequencing are listed in Figure 7-3.

Polyacrylamide Gel Electrophoresis and Western Blotting of Canine Tissue Samples

Canine tissue proteins were separated on Criterion Pre-cast Tris-HCl polyacrylamide gels of appropriate density (Bio-Rad Laboratories Hercules, CA) for Coomassie staining, western blotting or protein purification. Tissues or purified storage bodies were suspended in 2 volumes of Laemmli sample buffer (Bio-Rad cat#161-0737) and mechanically disrupted by homogenization and/or sonication before heat denaturation in boiling water for 5 minutes. Samples were loaded on the gel with appropriate molecular weight markers and separated in a Criterion Cell tank (Bio-Rad cat#165-6001) at 200V (constant voltage) in 1x Tris/Glycine/SDS running buffer (Bio-Rad cat#161-0732) until the dye marker reached the bottom of the gel (approximately 50 minutes).

Gels were Coomassie stained by first fixing them in fixing solution (50% methanol, 10% glacial acetic acid) for 2 hours with gentle agitation at room temperature. Gels were developed with staining solution consisting of fixing solution + 0.05% (w/v) Coomassie brilliant blue R-250 (Pierce Biotechnology Rockford, IL cat#20279) applied for 4 hours with gentle agitation at room temperature and then destained with destain solution (5% methanol, 7% glacial acetic acid) until

Primer	Sequence
CLN-11	5'-biotinyl-AAGCAGACCATACTCACTCAACA-3'
CLN-12	5'-TGGTAGGTGGGGACTGGAG-3'
CLN-13	5'-TGGAGCTCAGGAACTGG-3'

Figure 7-3: Primers used for pyrosequencing of canine TPP1 polymorphism PM4334T→C. CLN-11 and CLN-12 were used to amplify across the region of interest and CLN-13 primed the sequencing reaction.

protein bands became visible. Coomassie stained gels were visualized and recorded on a Bio-Rad Fluor-S Multi-imager (Bio-Rad).

For identification of the major protein component of isolated storage bodies in Tibetan Terrier samples, the prominent protein band at 49kDa in Coomassie stained gels was excised from the gel and sent to the University of Missouri – Columbia Proteomics Core facility for gel extraction and identification by mass spectrometry.

For Western blotting, gels were removed from the Criterion Cell apparatus and equilibrated in cold Transfer Buffer (90% 1x running buffer, 10% methanol) for 20 minutes. At the same time, a sheet of Trans-Blot nitrocellulose transfer medium (Bio-Rad cat#162-0116) cut to a size slightly larger than the gel was equilibrated in cold Transfer Buffer as well. Transfer of the gel contents to the nitrocellulose was performed in a Criterion Blotter (Bio-Rad cat#170-4070) according to the manufacturers instructions. After blotting, the nitrocellulose membrane was first washed in 1x TBS (Tris-buffered saline 2mM Tris-HCl, 50mM NaCl, pH 7.4) briefly then incubated in 1x TBS + 2% bovine serum albumin (BSA) either at room temperature for 2 hours or at 4°C overnight. After blocking, the blot was incubated with primary antibody at room temperature with gentle agitation for at least 4 hours. To improve signal detection, some blots were incubated an additional 12 hours at 4°C. Glial fibrillary acidic protein (GFAP) was detected with rabbit α-human GFAP antibody (Chemicon Temecula, CA cat#AB5804) at a 1:1000 dilution. Activating transcription factor 2 (ATF2) protein was detected with rabbit α-human ATF2 antibody (Santa Cruz Biotechnologies Santa Cruz, CA cat#sc-187) at a 1:200 dilution. Blots were then washed with 1x TBS three times for 5 minutes each before application of alkaline phosphatase conjugated goat α-rabbit IgG secondary antibody (Chemicon cat# AP307A) at a dilution of 1:1000. Blots were incubated in secondary antibody at room temperature with gentle agitation for 30-45 minutes then subject to four washes consisting of 1x TBS for 5 minutes, 1x TBS + 0.1% Tween-20 (Bio-Rad cat#161-0781) for 5 minutes (twice) and 1x TBS for 5 minutes. Blots were developed with the alkaline phosphatase sensitive chromogenic substrate BCIP/TNBT (Chemicon cat# ES007).

Isolation of Canine Fibroblasts

Canine skin fibroblasts were cultured from skin biopsies of NCL affected and unaffected control dogs. Biopsies were taken in accordance with procedures approved by the University of Missouri, Columbia Animal Care and Use Committee (ACUC) and placed immediately in Canine Fibroblast Growth Medium (CFGM) consisting of Dulbecco's Modified Eagle's Medium (DMEM, Invitrogen Carlsbad, CA cat#11965-092) + 20% heat inactivated Fetal Bovine Serum (FBS) + 1% Penicillin/Streptomycin solution (Invitrogen cat#15140-122). Biopsies were shipped and stored in CFGM at room temperature for up to 3 days before processing without loss of fibroblast yield.

To derive fibroblasts, skin samples were minced with a sharp razor blade or scalpel into fine pieces (about .5mm^3) in a petri plate. The samples were kept moist with growth medium during this process. The petri plate was then transferred to a sterile hood and each of these pieces was placed in an uncoated T-25 flask using Teflon coated forceps or a thin glass rod. Each piece of tissue was placed at least 2cm from any other piece. Tissues were allowed to dry in the flask for 15-30 minutes, until there was no visible liquid surrounding the tissue. This allowed the epidermal tissue to adhere to the plastic flask when media was gently added. Samples were maintained in CFGM at 37°C in complete humidity with 5% CO_2. Upon initial addition of medium, some sample pieces remained adhered to the flask while others floated off the surface. Floating pieces were allowed to remain in the culture until the first medium change 14 days after plating when they were drawn off along with the spent medium. Adhered pieces were maintained in culture after the initial two week incubation with medium changes ever 3-4 days until fibroblast cells were observed to migrate out from underneath by phase-contrast light microscopy. At this point, skin pieces were removed from the flask by gentle suction and fibroblast cells were maintained in culture until they became confluent, at which time they were either passaged or processed for cryogenic storage. Fresh medium was made every 14 days.

Passaging Canine Fibroblasts

Cells were passaged when they reached 90-100% confluency. Media was aspirated by vacuum and replaced with 2ml of Gibco brand 0.05% Trypsin-EDTA (Invitrogen cat#25300) which was

allowed to wash over the cells briefly before being aspirated. 1ml of Trypsin-EDTA was added back into the flask and cells were incubated at 37°C. After 3 minutes, flasks were struck vigorously against a solid surface 5 times to loosen cells and then placed back in the incubator for another 2 minutes. After incubation was complete, the Trypsin-EDTA was neutralized with 9ml of culture medium. Cells were pipetted up and down with a 10ml culture pipette 20 times to create a single cell suspension. The 10ml of cell suspension was then divided into two T-25 flasks (5ml in each), which were immediately placed back into the incubator to allow cells to adhere.

Cryopreserving Canine Fibroblasts

Frozen aliquots of cells were prepared for long term storage from flasks near 100% confluency. Cells were treated with Trypsin-EDTA as described above and neutralized with 9ml of culture medium. The resulting cell suspension was transferred to a 15ml conical tube and cells were pelleted by centrifugation in a clinical centrifuge at low speed and the supernatant decanted. The cell pellet was resuspended in 4ml of freezing medium consisting of culture medium + 10% dimethylsulfoxide (DMSO, Sigma-Aldrich St. Louis, MO cat#D-5879). The cell suspension was divided into 2ml aliquots which were slow-frozen in isopropyl alcohol freezing chambers at -70°C. After 3 days in the freezing chambers, frozen aliquots were transferred to storage boxes and kept at -70°C until used.

Thawing Canine Fibroblasts

Frozen aliquots of cryopreserved cells were quickly thawed by immersion in 37°C water. The 2ml of cell suspension was then pipetted into 10ml of growth medium in a 15ml conical tube. The tube was inverted several times and then cells were pelleted by centrifugation in a clinical centrifuge at low speed and the supernatant decanted. The pellet was resuspended in fresh growth medium and the whole aliquot was transferred to a T-25 flask. Cells were incubated as above and medium was changed after 24 hours.

DNA Isolation from Cultured Canine Fibroblasts

To test the efficacy of cultured canine fibroblasts as a renewable source of genomic DNA, cells were trypsinized as described above and washed several times in 1x PBS to remove culture media. They were then lysed for at least 48 hours in Nuclei Lysis Buffer (NLB, .4M NaCl, .01M Tris-HCl, 2mM EDTA, .2% SDS, .15% dithiothreitol and 1.4 mg/ml Proteinase K). After incubation, the sample was centrifuged at 13,000rpm in a benchtop centrifuge to remove undigested cells or tissue and extracted with phenol/chloroform/iso-amyl alcohol (Fisher Scientific cat#BP1753-100). Samples were centrifuged to separate the aqueous and organic layers and the aqueous supernatant transferred to a new test tube. The DNA was precipitated by ethanol and 3M sodium acetate and resuspended in ddH_2O. DNA concentration was determined by spectrophotometric absorbance at 260nm.

To determine whether frozen canine fibroblast samples could be used as a reliable source of DNA, we plated a frozen sample from a normal dog after 1 month at -70°C and isolated cells after 2 post-thaw passages. Cells were resuspended by trypsinization and the total weight of the isolated fibroblasts was determined by centrifuging the isolated cells and determining the weight of the cell pellet. Equal amounts of cultured fibroblasts, canine spleen and canine tongue were subject to DNA extraction and the DNA yield was compared by gel electrophoresis.

Isolation of Canine Bone Marrow-Derived Mesenchymal Stem Cells

Canine bone-marrow derived mesenchymal stem cells (cMSCs) were isolated from the rib and femur of NCL-affected Dachshunds, unaffected Dachshunds and unaffected control dogs of other breeds. After dissection, cells were flushed from the medullary cavity with MSC growth medium consisting of Gibco ά-MEM (Invitrogen cat# 12561) + 20% FBS, 2mM L-Glutamine, 1% Penicillin/Streptomycin solution. Extracted cells were pelleted by centrifugation in a clinical centrifuge at low speed and the supernatant decanted. The pellet was resuspended in 5ml of MSC culture medium and cells were transferred to a T-25 flask and allowed to adhere for 24 hours before growth medium was changed. MSCs were maintained at 50-100% confluency at all times in a 37°C incubator with complete humidity and a 5% CO_2 atmosphere. Medium was

changed every 2 days and fresh medium was made every 14 days. When necessary, cells were passaged, cryopreserved and thawed as described for murine MSCs in Chapter II.

3. Results

Nucleotide Sequencing of the Canine *TPP1* Gene in Normal and NCL-affected Dogs

A composite nucleotide sequence for 1885 bp of *TPP1* cDNA was obtained from overlapping RT/PCR and RACE amplicons from English Setter RNA (GenBank Accession number AF114167). No differences in *TPP1* cDNA sequences were detected between a normal English Setter and an English Setter with NCL. The cDNA sequence contains an open reading frame of 1689 bp that encode a predicted protein of 563 amino acids (see Figure 7-4). Within the open reading frame, the English Setter nucleotide sequence is 90% identical to that reported for the human cDNA. The amino acid sequence translated from the cDNA sequence is also 90% identical to the predicted human amino acid sequence and 88% identical to the predicted mouse sequence. Likewise, the English Setter and mouse predicted amino acid sequences are 88% identical, as are the mouse and human sequences.

The exon/intron organization of the canine *TPP1* gene was determined by comparing the cDNA sequence to that of the genomic sequence (GenBank accession number AF114167). The canine *TPP1* gene consists of 5483 nucleotides organized into 13 exons (see Figure 7-5). The twelve introns ranged in size from 82 to 1192 bp. [171] No polymorphisms between the affected and normal English Setter intron sequences were identified.

Sequencing of the *TPP1* gene of an NCL affected Tibetan Terrier and comparison of that sequence with the English Setter and Boxer canine genome sequences revealed a total of 38 polymorphisms (see Figure 7-6). Of these, three were found to lie within coding regions. The first, PM2890A→G is a silent mutation occurring in Exon 7. It modifies the third base of an alanine codon, but produces no change in the protein sequence. The second, PM3064T→C also appears in Exon 7 and occurs only in the Boxer breed. It produces another silent mutation, affecting the third base of a proline codon, but producing no amino acid change. The third,

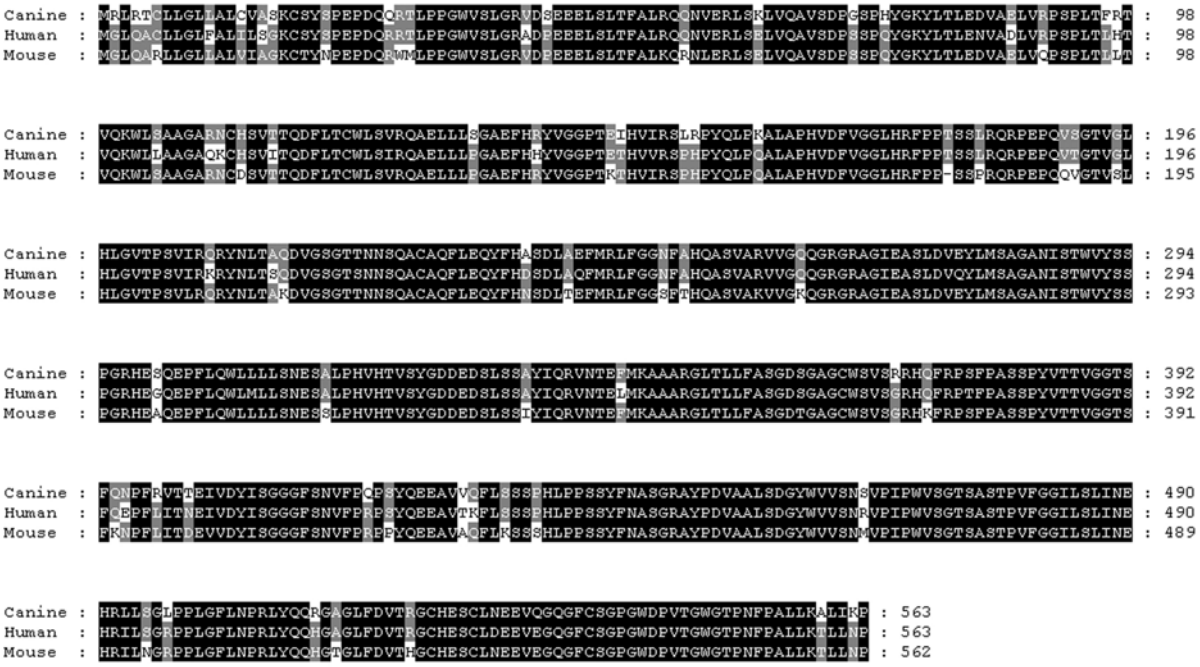

Figure 7-4: Multisequence alignment of predicted canine (Acc#001013869), human (Acc#AAC98480) and mouse (Acc#NP034036) tripeptidyl peptidase 1 (TPP1) proteins. Mismatches are indicated by either a white (no other amino acid in the column matches) or grey (one other amino acid match in the column) background. The canine TPP1 protein is 90% identical to the human and mouse sequences.

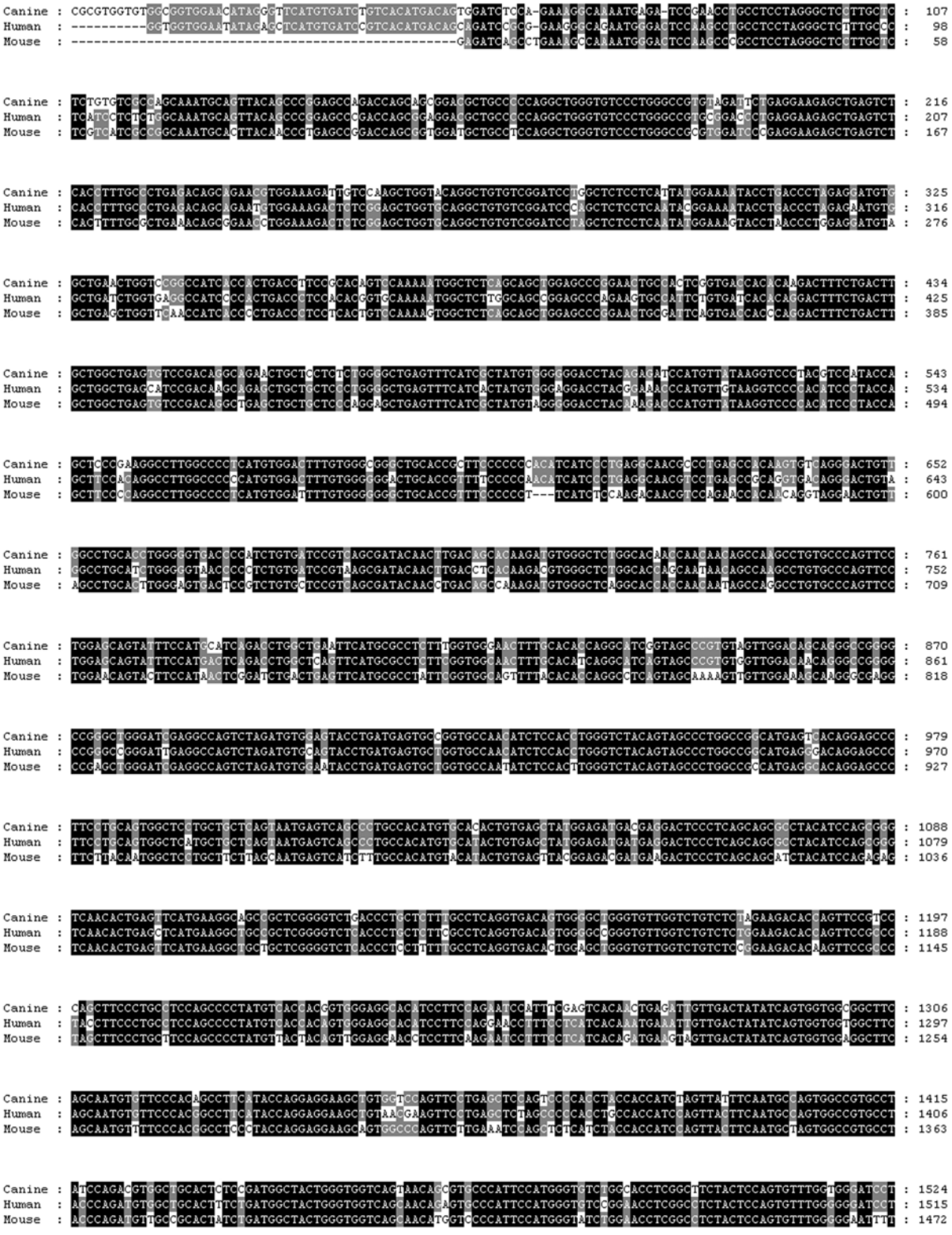

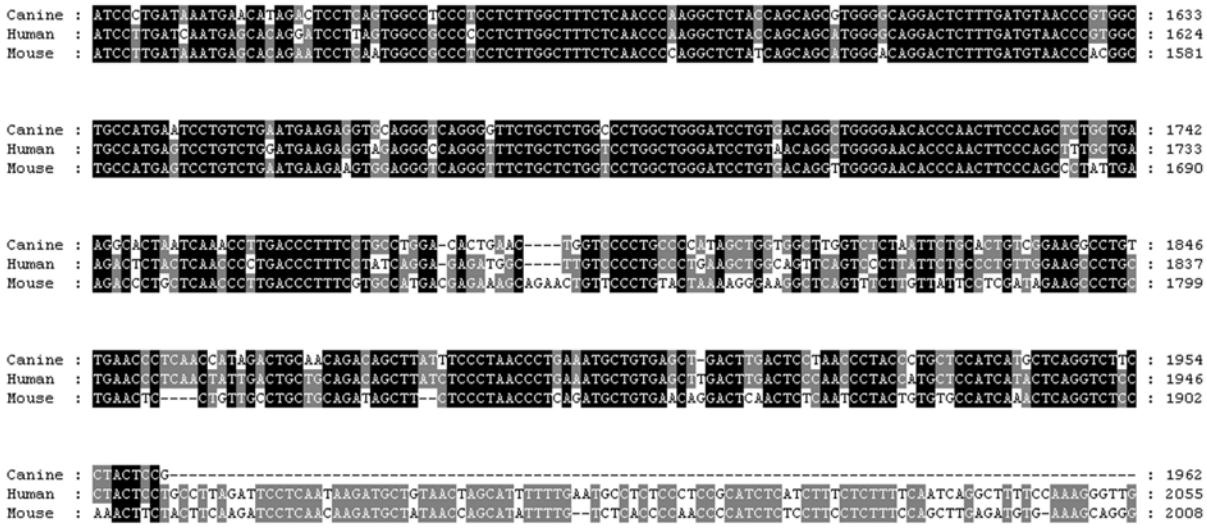

Figure 7-5: Multisequence alignment of canine (Acc#AF114167), human (Acc#NM000391) and mouse (Acc#NM009906) TPP1 cDNA. Mismatches are indicated by either a white background (no other nucleotide matches in the column) or a grey background (one other nucleotide match in the column). The canine sequence is 90% identical to both the human and mouse sequences.

Locus Name	Polymorphism Type	English Setter	Boxer	Tibetan Terrier
PM19	deletion	A	A	-
PM284-287	deletion	CTGC	-	-
PM303	mismatch	G	T	T
PM503	mismatch	C	C	T
PM703	mismatch	A	G	G
PM895	mismatch	C	T	T
PM1351	mismatch	C	T	T
PM1398	mismatch	A	A	G
PM1417	mismatch	A	A	G
PM1470	mismatch	G	C	G
PM1771	mismatch	A	C	C
PM2084	mismatch	A	G	G
PM2110	mismatch	T	G	G
PM2145	mismatch	C	T	C
PM2153	mismatch	C	C	G
PM2711	mismatch	A	A	G
PM2890	mismatch	A	A	G
PM3064	mismatch	T	C	T
PM3119	mismatch	C	C	T
PM3543	mismatch	T	T	C
PM3566	mismatch	C	A	A
PM3841	mismatch	A	G	G
PM3972	mismatch	C	C	T
PM4334	mismatch	T	C	C
PM4601	mismatch	C	T	C
PM4610/4611	insertion	-	C	C
PM4615	mismatch	T	C	T
PM4696	mismatch	T	C	T
PM4718/4719	insertion	-	TG	-
PM4754	mismatch	T	C	T
PM4826	mismatch	T	C	T
PM4829	mismatch	C	T	C
PM5057	mismatch	T	T	C
PM5081	deletion	T	-	-
PM5300	mismatch	C	G	G
PM5302	mismatch	C	G	G
PM5380	mismatch	C	T	C
PM5429/5430	insertion	-	T	T

Figure 7-6: TPP1 polymorphisms in the canine genome. Sequencing of the TPP1 gene of the English Setter (Acc#AF114167), Boxer (Acc#AAEX01017594) and an NCL affected Tibetan Terrier (Acc#DQ100344) revealed 38 polymorphic sites. Positions are numbered according to GenBank accession no. AF114167. Highlighted rows indicate polymorphisms which occur within exons.

Dog #	Phenotype	Genotype
TT-1	Affected	C/T
TT-2	Affected	C/T
TT-3	Affected	C/T
TT-4	Affected	C/C
TT-5	Affected	T/T
TT-6	Affected	T/T
TT-7	Affected	T/T
TT-8	Affected	T/T
TT-9	Affected	T/T
TT-10	Affected	T/T
TT-11	Unaffected	T/T
TT-12	Unaffected	T/T
TT-13	Unaffected	C/T
TT-14	Unaffected	T/T
TT-15	Unaffected	C/T
TT-16	Unaffected	T/T
TT-17	Unaffected	T/T
TT-18	Unaffected	T/T
TT-19	Unaffected	T/T

Figure 7-7: Genotype/Phenotype correlations in Tibetan Terriers. Pyrosequencing established the genotype at polymorphic position 4334 for 19 Tibetan Terriers (10 NCL-affected and 9 unaffected controls). No genotype co-segregated with the disease phenotype.

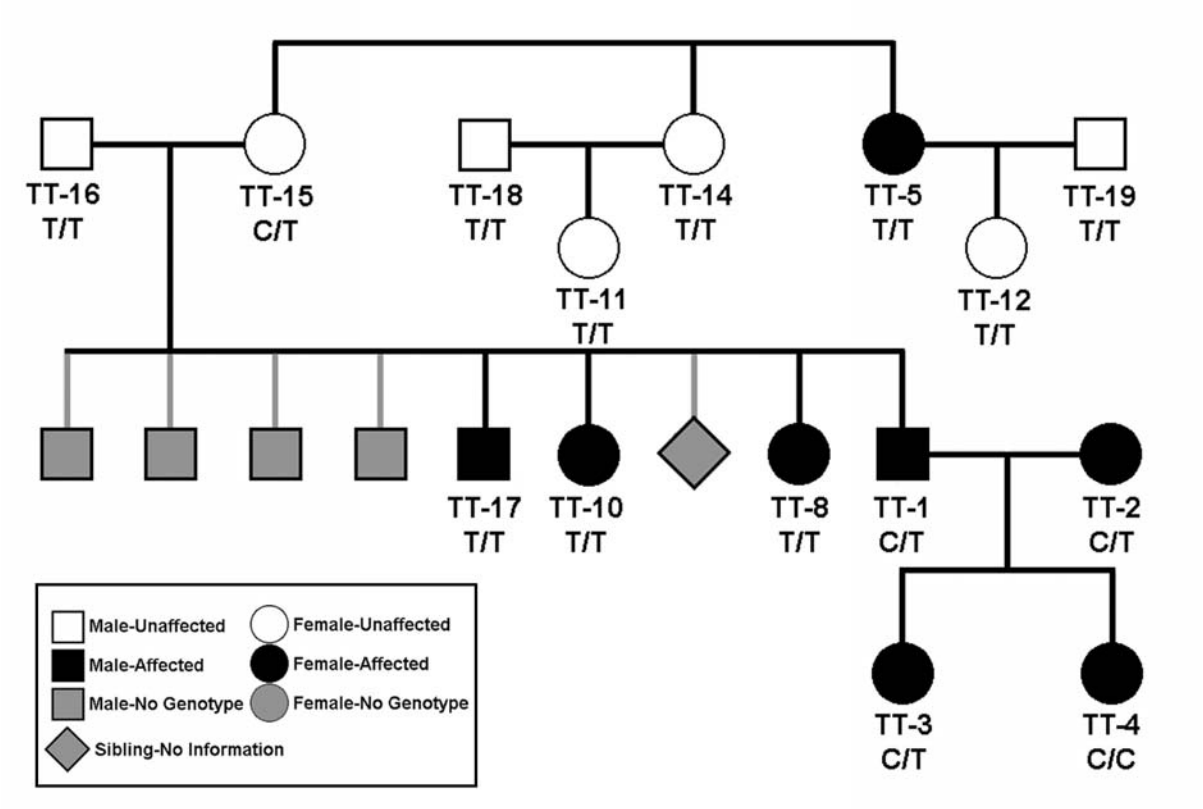

Figure 7-8: Tibetan Terrier pedigree with genotype data. Of the 19 dogs screened, 10 were clinically diagnosed as NCL affected and 9 were unaffected. Of those, 15 were closely related as depicted in this pedigree. The data show that the disease phenotype and TPP1 genotype sort separately, indicating they are not genetically linked.

PM4334T→C is located in exon 11 and changes the second base of a valine codon, creating a V427→A amino acid change.

To determine whether the polymorphism at position 4334 was responsible for the CCL phenotype in Tibetan Terriers, and to determine whether a particular allele of the gene was associated with the disease phenotype, we performed pyrosequencing reactions on a panel of related NCL affected and unaffected animals. Of the 19 dogs screened, 10 were clinically diagnosed as affected with NCL and 9 were confirmed unaffected. The pyrosequencing results in Figure 7-7 show that all three genotypes for the PM4334T→C polymorphism (C/C, C/T and T/T) are present in the affected dog population and all but the C/C genotype are present in the unaffected population. Figure 7-8 shows a pedigree including 15 of the 19 Tibetan Terriers screened by pyrosequencing. Only animals for which we had full disease status and genotype data (shown on the pedigree in bold) were included in the study. The pedigree shows that the distribution of disease phenotype is consistent with the Tibetan Terrier form of NCL being an autosomal recessive genetic disease. However, the pedigree also reveals that neither the T nor the C allele at position 4334 co-segregates with the affected phenotype.

GFAP is the Major Protein Component of Storage Material in Tibetan Terrier NCL

Autofluorescent storage material was isolated from brain tissue of an NCL affected Tibetan Terrier and analyzed by polyacrylamide gel electrophoresis. The initial gel showed a single major, soluble protein band running at ~50kDa. (see Figure 7-9a) This band was excised from the gel and the protein subjected to trypsin digestion. The resulting peptides were analyzed by MS and MS/MS using an Applied Biosystems 4700 MALDI TOF-TOF instrument. Mass spectral results were used in a combined (MS plus MS/MS) NCBInr database query limited to mammals and conducted using GPS Explorer software with integrated MASCOT search engine. The gel band was identified as a canine predicted protein similar GFAP isoform 2 (gi|73965502) with a MASCOT protein score of 997 (a MASCOT protein score >78 indicated a match at the 95% confidence level). A total of 39 peptides were matched to GFAP and these matched peptides covered 76% of the protein. (see Figure 7-10) The eight most abundant peptides in the MS

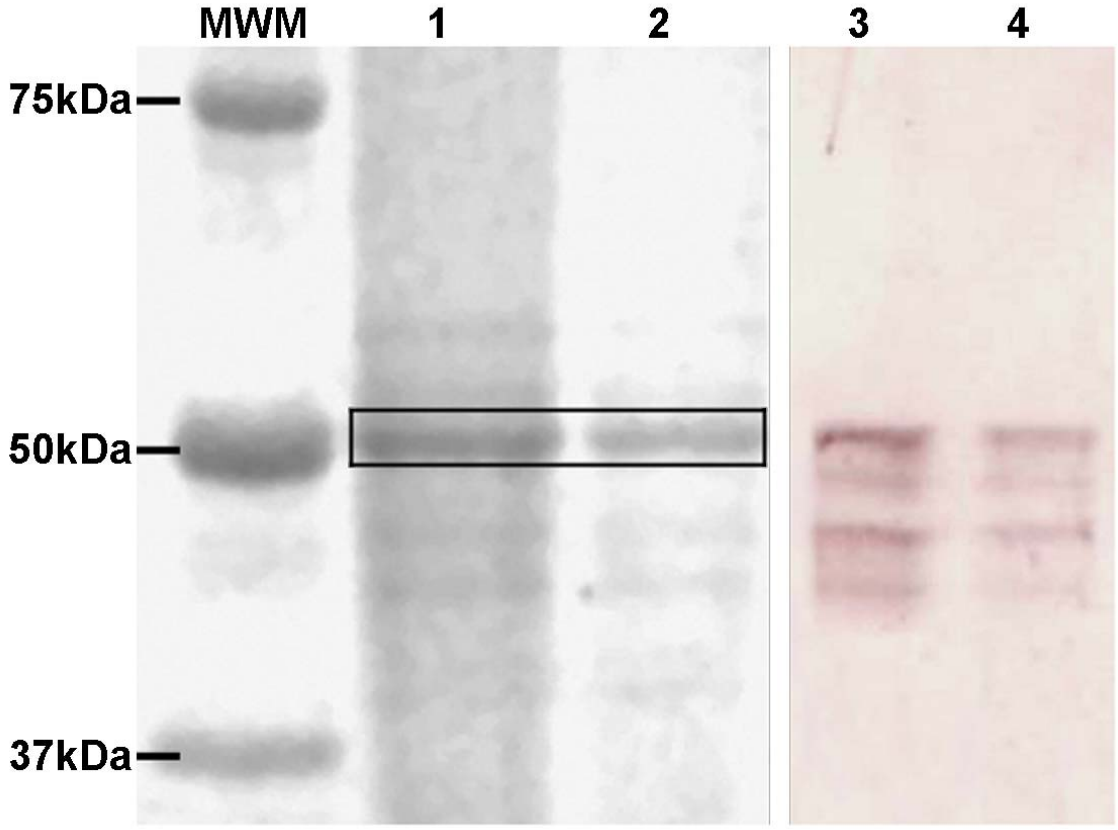

Figure 7-9: GFAP from Tibetan Terrier storage material. The soluble protein constituent from purified Tibetan Terrier storage bodies was separated by denaturing polyacrylamide gel electrophoresis and stained with Coomassie blue dye (Lanes 1 & 2). The boxed band at ~50kDa was the most abundant protein in TT storage material. Mass spectral analysis predicted that the band was GFAP, a commonly expressed protein in neural tissues. Western blot analysis with a GFAP-specific antibody (Lanes 3 & 4) confirmed this prediction.

A

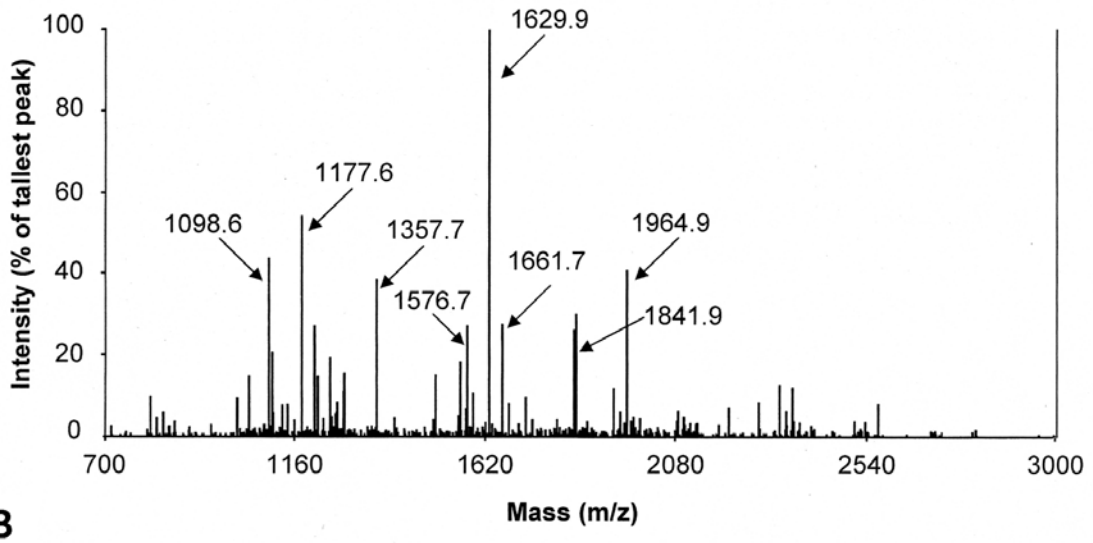

B

Precursor Mass	Best Peptide Sequence	Start	End	MASCOT Ion Score	Match Error (ppm)
1964.99	KIHDEEVQELQEQLAR	203	218	130.08	-3.85
1661.77	LEEEGQNLKDEMAR	332	345	110.78	-3.09
1576.79	QLQTLTCDLESLR	289	301	97.98	-3.87
1629.93	ITIPVQTFSNLQIR	378	391	91.65	-2.55
1177.61	LADVYQAELR	113	122	76.37	-6.32
1098.62	ALAAELNQLR	97	106	69.22	-7.89
1841.96	LEVERDNLAQDLGTLR	138	153	64.86	-3.78
1357.74	LRLDQLTANSAR	126	137	57.82	-7.10

Figure 7-10: Mass spectral analysis of the major protein band isolated from Tibetan Terrier lysosomal storage material. (A) MS spectrum of peptides from the trypsin-digested protein band. For clarity, only those peptides selected for MS/MS fragmentation are indicated. The eight most abundant peptides were automatically selected for MS/MS fragmentation based on their relative intensities in the MS spectrum. (B) Table of MS/MS fragmentation matches showing mass of the precursor ion, the peptide sequence, the position of the matched peptide in the protein sequence, the MASCOT ion score and the mass error associated with each peptide sequence. The low parts per million mass error indicates an almost exact match to the theoretical sequence.

Figure 7-11: The amino acid sequence of the protein identified by mass spectrometry. The top hit from a search of NCBInr limited to mammals was a predicted canine protein corresponding to glial fibrillary acidic protein, isoform 2 (gi|73965502). The red type indicates the sequence coverage by the 39 peptides observed in the MS spectrum of the trypsin digest. Peptide sequence was determined by mass matches (peptide mass fingerprinting) and/or by peptide fragmentation matches (amino acid sequencing). The under lined portion of the sequence indicates where isoforms 1 and 2 of canine GFAP differ.

spectrum were subjected to MS/MS fragmentation. All of these peptides were matched to GFAP with MASCOT ion scores ranging from 58 to 130 (a MASCOT ion score >42 indicated a match at the 95% confidence level). The amino acid sequences of the fragmented and matched peptides are shown in Figure 7-11 and the pertinent peaks are indicated on the MS spectrum. These MS/MS peptides alone covered 24% of the protein. Although peptide masses corresponding to the conserved regions of both isoforms 1 and 2 of canine GFAP were matched, the presence of the TVEMRDGEVIK peptide suggests that the protein present in the gel band is isoform 2. This peptide is from the variable C-terminal region of GFAP and it is only present in isoform 2.

A Western blot of storage material from brain tissue of a different NCL affected Tibetan Terrier with an α-GFAP antibody showed labeling of the ~50kDa band and several smaller bands, assumed to be breakdown products or modified proteins derived from the higher molecular weight band. (see Figure 7-9b) These results indicate that GFAP was correctly identified by mass spectrometry as the major, soluble protein component of Tibetan Terrier NCL lipofuscin storage material.

Examination of ATF2 Expression in a Neonatal Onset Form of Neurodegeneration

As part of our ongoing characterization of canine neurodegeneration models, we analyzed the tissues of a poodle that presented with neonatal onset neurodegeneration. This disease is associated with uncoordinated movement and seizures immediately after birth. Affected dogs usually die within 6 weeks. The animal we examined was kept alive by bottle feeding for 6 weeks, at which time its deteriorating health required that it be euthanized. Tissues were collected and frozen for later examination.

A defect in the ATF2 gene was identified by chromosomal mapping as the cause of this disease. In order to determine whether the genetic defect resulted in loss of protein expression we examined neural tissue from the brain of the affected dog and the brain of an age-matched control dog for the presence of the ATF2 protein by Western blot. Several isoforms of ATF2 arise by differential splicing. The stable, native, full length ATF2 (55kDa) is transcriptionally inactive as

a result of an inhibitory direct intramolecular interaction of its carboxy-terminal DNA binding domain with the amino-terminal transactivation domain. Following dimerization, ATF2 becomes a short-lived protein that undergoes ubiquination and proteolysis, seemingly in a protein phosphatase-dependent manner. Stimulation of the transcriptional activity of ATF2 occurs following cellular stress. This activation requires phosphorylation of two threonine residues in ATF2 by both JNK/SAP kinase and p38 MAP kinase. [172]

Our results show that several forms of the ATF2 protein are present in both control and affected samples from cerebrum and cerebellum, indicating that the genetic defect does not prevent transcription or translation of the ATF2 gene. (see Figure 7-12) However, the expression profiles differ between the affected and control samples. In particular, a very high molecular weight (~200kDa) isoform of the protein is present in the control sample but absent in the affected sample and the doublet located at ~70-75kDa in the control sample appears as a triplet in the affected sample. The genetic defect in this disease is a methionine to arginine missense mutation at position 51 in the protein. It is possible that the different protein profiles are caused by differences in molecular weight or by alternate proteolytic breakdown products of the protein caused by this amino acid change.

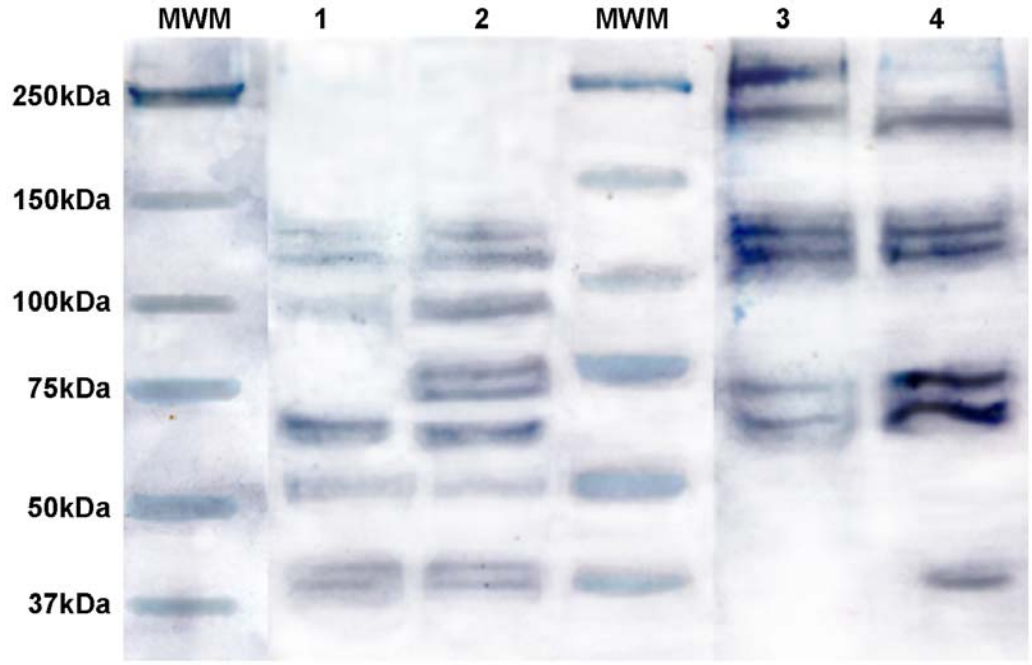

Figure 7-12: Western blot for canine ATF2 protein. Brain tissue from affected (Lanes 1 & 2) and age-matched unaffected control dogs (Lanes 3 & 4) both express several isoforms of ATF2, produced by differential splicing and post-translational modification. The isoform profiles differ between affected and unaffected dogs, but all samples display a band at ~55kDa, which corresponds to the active form of the protein. This indicates that the mutation in ATF2 in affected animals does not exert its phenotype by disrupting post-translational modification of the protein.

Isolation and Characterization of Canine Fibroblasts

In our studies of canine models of neuronal ceroid lipofuscinosis (NCL) we often rely heavily on the pet population for the samples we use to investigate the metabolic and genetic causes of the disease. While this reduces our costs and the necessity of keeping animals in laboratory confinement, it means that our access to animals is often limited. In order to facilitate our studies we developed a system for archiving canine skin fibroblasts which might be used for any number of experimental procedures. These cells can be cultured, frozen and kept even after animals of interest are no longer available to us. In addition, it relieves some of the burden on the pet owners who facilitate our research by reducing the number of times they are called upon to make their animals available for study. We envision the possibility of using these cells as models for dissecting the metabolic pathways which lead to neurodegeneration, as test subjects for various treatment protocols and as a renewable source of material for DNA, RNA and protein from affected, carrier and control animals.

In our analyses of canine models of NCL it is common practice to collect and archive DNA from animals of interest. These archived DNA samples are invaluable in identifying the genetic defects associated with the disease. However, since we often take samples from affected dogs who are being euthanized, the collected DNA is a limited commodity and the possibility exists that samples will be consumed before their usefulness is exhausted. As a first step in evaluating the usefulness of canine skin fibroblasts as a tool for NCL research, we examined their ability to serve as a long-term, renewable source of DNA.

Canine fibroblasts were cultured from the skin biopsy samples of several affected and normal dogs. In most cases, fibroblasts grew out from plated biopsy fragments within the initial two week culture period so that a single cell layer adhered to the plastic culture flask could be seen spreading from underneath the tissue. In some cases, fibroblasts failed to grow in culture from the skin biopsy. This failure to grow could be attributed to contamination of the culture by bacteria or fungi for some samples. In others, no discernible cause could be found for failure of the fibroblasts to proliferate. Neither age nor medical condition seemed to be responsible for lack

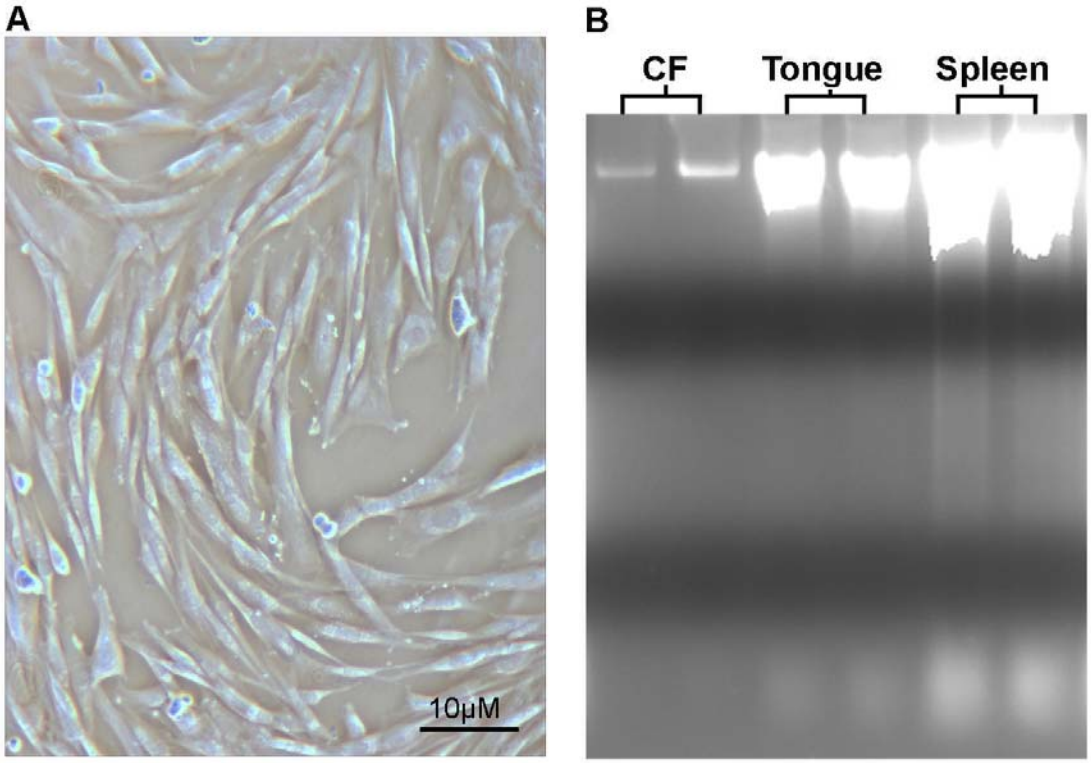

Figure 7-13: (A) Fibroblast cells in culture immediately before their first passage. When cultured at high density, fibroblasts doubled every 72 hours and could be passaged up to 6 times after isolation. (B) Genomic DNA derived from canine fibroblasts (CF), tongue and spleen. Exactly 0.2g of each sample was used for the isolation protocol. Tongue and spleen yielded a much greater concentration of DNA per unit of weight. However, fibroblast DNA was clean and adequate for most research purposes.

of growth, as neither factor was consistently associated with the non-growing samples. It is unlikely that differences in isolation success were the result of variations in the medium. All fibroblast culture medium was made from the same lot of fetal bovine serum over the course of these experiments and the recipe remained constant. Medium was made fresh for each new sample we obtained and never used for longer than two weeks.

One possible source of variability is the tissue biopsy itself. In some cases larger biopsies were used (> 1cm^2). These were usually obtained at euthanasia with a scalpel. In other cases very small skin-punch type biopsies were obtained (usually from live dogs at the time of another clinical procedure). At the time of culture, biopsy size was not recorded, but it is possible that obtaining more tissue area or deeper tissue biopsies (like those obtained by necropsy) resulted in better yields. In future experiments, the size of the biopsy will be recorded at the time of dissection and plating to investigate the contribution of biopsy size to the success of fibroblast isolation.

Canine fibroblasts which proliferated initially could easily be cultured for at least 4 passages. When thawed after storage at -80°C for several months, they continued to grow well in culture for many more passages. To confirm that these cultured cells could be used as a renewable source of DNA, whole genomic DNA was isolated from canine cells and the yield compared to genomic DNA extracted from a similar volume of frozen canine tissue (tongue and spleen). (see Figure 7-13) The DNA yield for cultured fibroblasts was lower than that of a similar volume of canine spleen or tongue tissue. However, the cultured cells did provide usable levels of genomic DNA which appeared identical to control DNA following agarose gel electrophoresis.

Isolation and Characterization of Putative Canine Mesenchymal Stem Cells

Putative canine mesenchymal stem cells (cMSCs) were isolated from bone marrow and characterized for growth properties and morphology. Initial cultures exhibited a mixed population of cells with varying morphologies. For approximately the first 30 days of incubation cell numbers in the culture slowly declined. During this time period, the heterogeneity of the cells within the flask decreased, yielding a mixed culture primarily composed of three types of cells. The most

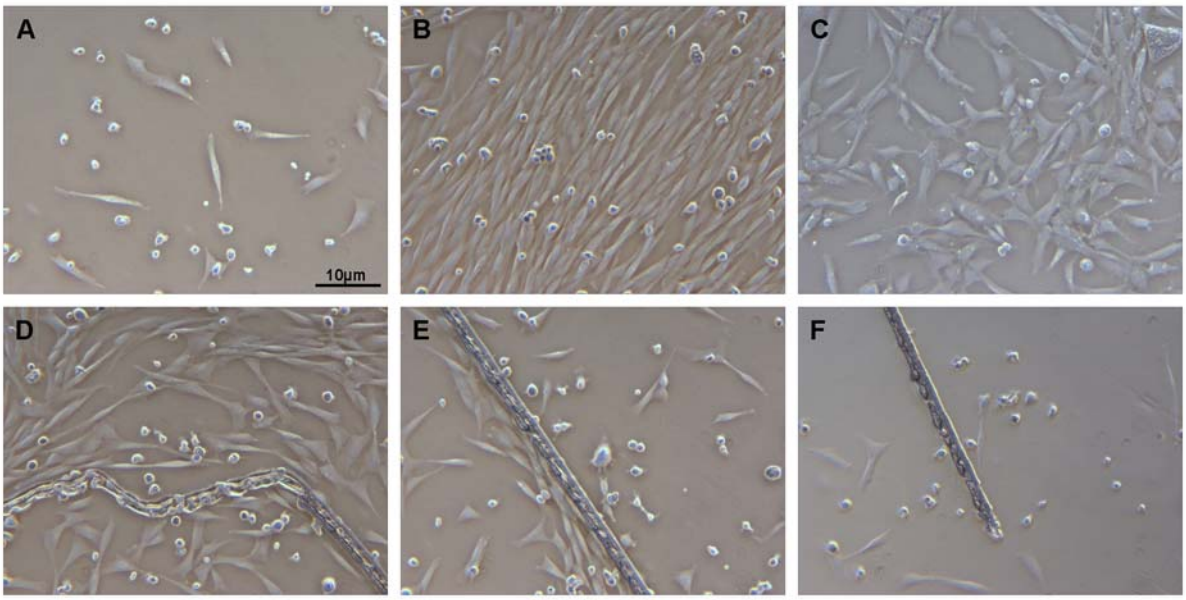

Figure 7-14: Canine MSCs in culture 24 hours after isolation (A), 30 days after isolation (B) and at passage 12 (C). During the initial stages of isolation, before the first passage, both murine and canine MSC cultures often developed long cellular strands (D-F) formed by cells oriented in a linear pattern and closely associated with what appears to be a thread-like deposit of extracellular matrix material. The three examples pictured here are from the same strand, which measured 2.7 cm from the non-linear section in D to the end of the long arm in F. Strands were always linear in areas of low density (E & F), but sometimes meandered in areas of higher cell density (D). Strands were not observed in cultures after the first or second passage.

abundant were fibroblast-like cells with a non-symmetrical geometry. The other two types of cells, small round cells and large, flattened, lymphocyte-like cells, composed only a small fraction of the culture at 30 days. After this transition, cell numbers in the culture began to increase and cultures usually reached confluency around day 40-45. This mixed cell population continued through passage 4, after which spindle-shaped, fibroblast-like cells became predominant, large, flat cells disappeared and small round cells, though still present, made up a much smaller proportion of the population. (see Figure 7-14a-c)

Measurements of doubling time were recorded after cultures had reached passage 1 (p1). Doubling time for the first 5-6 passages was relatively long, usually 5-15 days. At p8, cMSCs were doubling about every 36-48 hours and this rate remained steady for the culture thereafter. cMSCs frozen at p3 and thawed several months later displayed the same pattern of growth rate change as cells continuously cultured, with doubling times stabilizing at approximately 36 hours around p8. (see Figure 7-15) These results are nearly identical to results obtained for isolation and characterization of murine mesenchymal stem cells (mMSCs) under the same culture conditions. Further characterization of these putative cMSCs, similar to that performed on our mMSC population, is ongoing. Inducing terminal differentiation into several mesenchymal lineages will allow us to definitively determine whether the isolated cells can be classified as true mesenchymal stem cells.

Formation of Cellular Strands and Cellular Migration in Low Density Culture

On several occasions, when isolating a new line of MSCs, we observed the formation in culture of long strands composed of both compact cells and what appeared to be a fiber of extracellular matrix material. (see Figure 7-14d-f) All cells were aligned on a single side of the fiber, leaving the other side open. All lining cells were directly adjacent to, and appeared to be in direct contact with, their neighbors. These fibers appeared only during low density culture in mixed populations of cells (before a pure population of MSCs had emerged). In general, these conditions occurred during the first two weeks of MSC isolation and were not present in cultures thereafter, so we

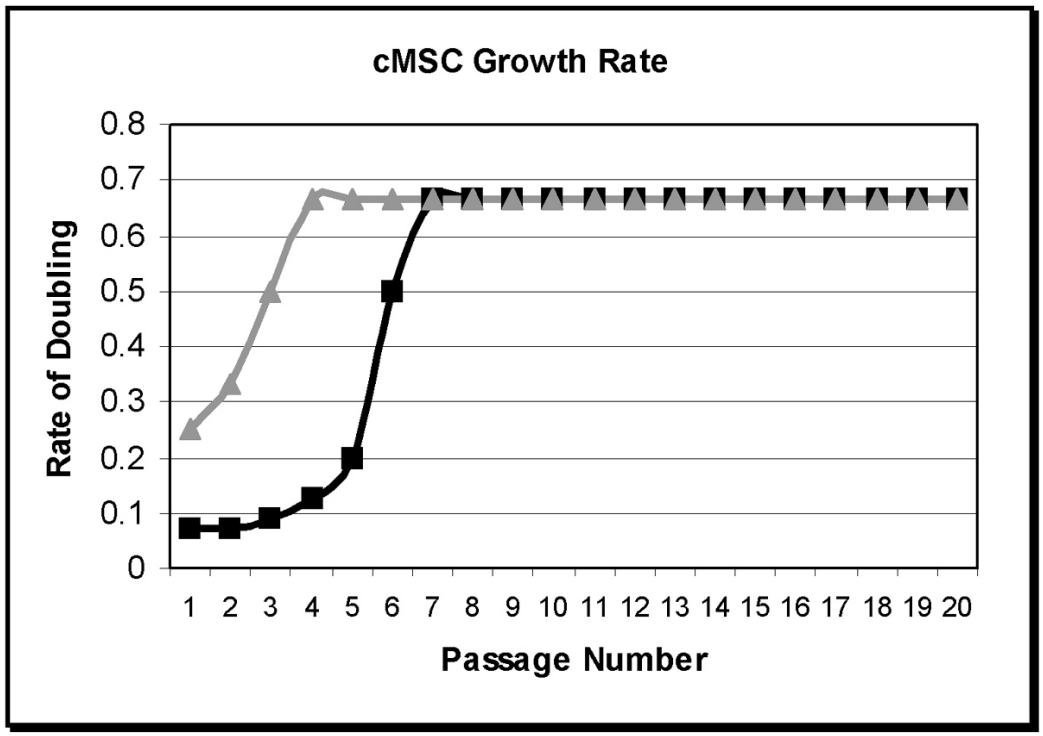

Figure 7-15: The growth rate of canine MSCs was examined for both freshly isolated (black squares) and frozen/thawed (grey triangles) cells. Rate of doubling is measured in passages per day. Both populations eventually reached a stable rate of doubling of ~0.67 per day. Frozen/thawed cells display a rate of doubling similar to unfrozen cells of the same passage number. This behavior is identical to that which we observed for MSCs derived from mice.

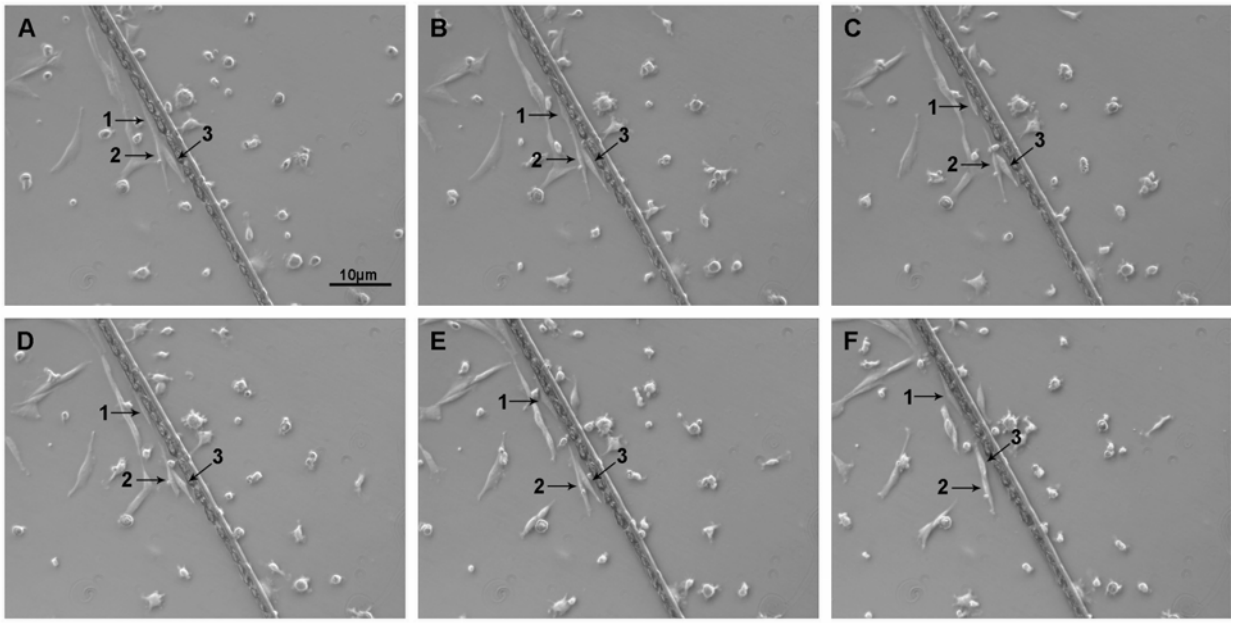

Figure 7-16: Canine MSCs move along strands of extracellular matrix in the early stages of *in vitro* culture. Pictures of the same frame were recorded over a two hour period (A = 0 minutes, B = 20 minutes, C = 40 minutes, D = 60 minutes, E = 90 minutes, F = 120 minutes). Three cells (labeled 1, 2 and 3) are closely associated with each other in A. In later frames, cell 1 moves along the strand toward the top of the frame, away from cell 2, which remains stationary throughout the observation period. Cell 3 remains stationary for the first hour (A-C) and then moves in the same direction as cell 1 in later frames (D-F). This is the same cell fiber pictured in Figure 6-5. The cells in this figure are moving toward the area of high cell density pictured in Figure 6-5D, which is about 1 cm away.

were not able to observe whether the pure population of MSCs obtained at later passage numbers retained their ability to form these structures.

Time lapse photography allowed us to observe the movement of cells along these fibers. (see Figure 7-16) Cells closely associated with the lining cells of a fiber were observed to move up to 10 microns over the course of two hours. Movement appeared to be in the direction of areas of higher cell density. Other adherent cells in the area which were not closely associated with the fiber were not observed to move at all during this same period of time. Cells were not observed to move along the side of the fiber with the bare extracellular matrix strand exposed. Moving cells had the fibroblastic morphology generally associated with MSCs.

Fluorescence Immunohistochemistry Analysis of Undifferentiated cMSCs

Passage 4 cMSCs were plated in 6-well plates as described for mMSC IHC. The expression of GFAP, MAP2, Nestin, Neurofilament M, Oct4 and PCNA were assessed by fluorescently labeled antibody. (see Figure 7-17) Cell nuclei were counterstained with DAPI. Labeling revealed that undifferentiated cMSCs were negative for Nestin, Oct4 and Neurofilament M.

Nestin is expressed in neural precursor cells of the subventricular zone, but is also present in undifferentiated embryonic stem cells and some researchers have also reported finding it expressed in undifferentiated MSCs and HSCs. Although we detected low levels of Nestin protein with the same antibody in our undifferentiated mMSC samples, we found no detectable protein expression for Nestin in our undifferentiated cMSCs.

Oct4 is a homeodomain transcription factor of the POU family. This protein is critically involved with self-renewal of undifferentiated embryonic stem cells. As such, it is frequently used as a marker for undifferentiated cells. We detected Oct4 expression in a small percentage of our undifferentiated mMSCs. However, using the same antibody we found no detectable Oct4 expression in our cMSCs.

A very small proportion of the cells labeled positive for PCNA. PCNA interacts with DNA polymerase and is involved in DNA synthesis and repair functions. It is expressed during the

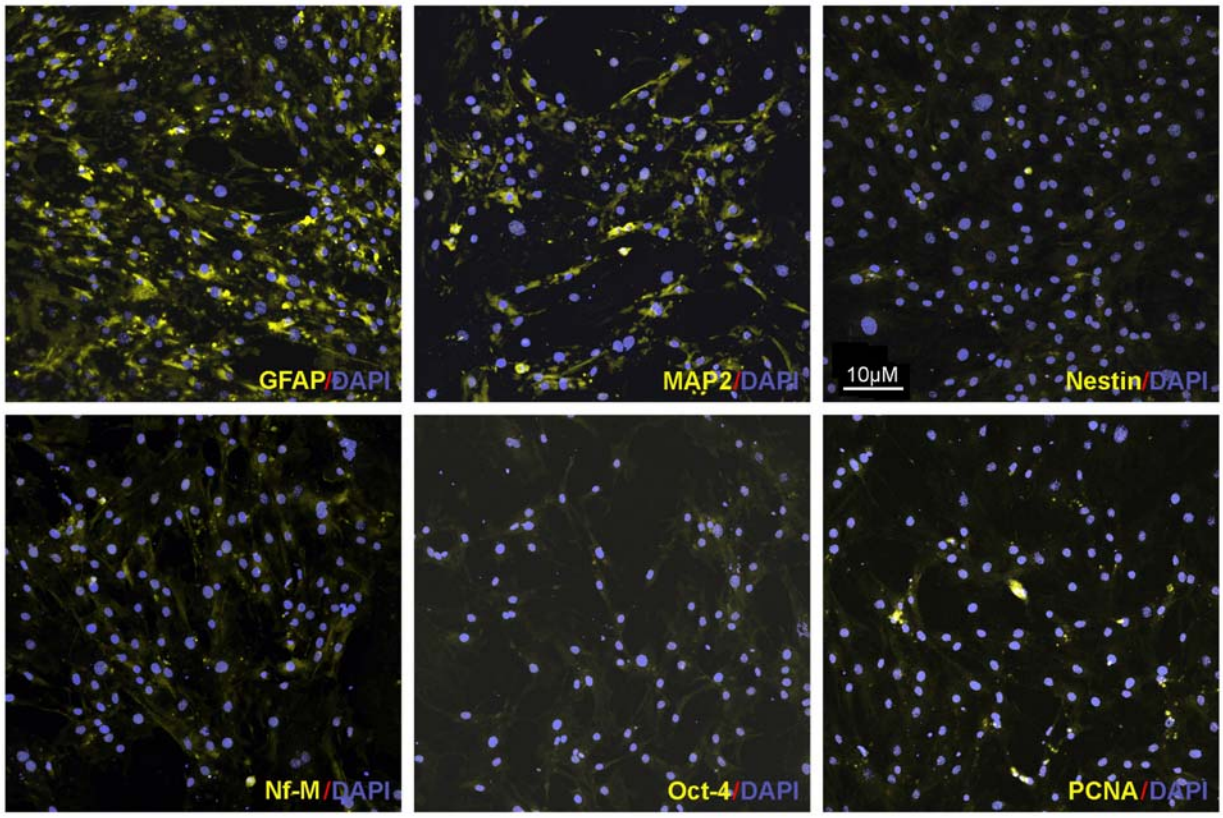

Figure 7-17: Results for immunohistochemical analysis of undifferentiated, passage 4 canine MSCs. Cells were labeled with Cy5-conjugated antibodies as indicated (yellow) and counterstained with DAPI (blue). GFAP and MAP2 labeled undifferentiated cMSCs strongly. A small number of cells also showed expression of PCNA in the nucleus. Nestin, Neurofilament M and Oct4 were not detected.

DNA replication phase of the cell cycle. The cells in this experiment were fixed and labeled during the logarithmic phase of their growth cycle when the largest number of cells in culture are actively dividing. Since MSC cultures are known to be largely composed of cells in cycle arrest at the G_0/G_1 phase, with only about 10% of the cells actively dividing at any one time, sporadic expression of PCNA in undifferentiated cells is expected. Our results are consistent with this pattern of expression. Similar results were observed for mMSCs.

Neurofilament M (NF-M) is an intermediate filament found in high concentrations in the axons of mature vertebrate neurons. Our observation that undifferentiated cMSCs express no detectable levels of NF-M agrees with our expectations and indicates that no neuronal differentiation is taking place within the culture.

Undifferentiated cMSC cells labeled strongly positive for both GFAP and MAP2. While GFAP and MAP2 are ostensibly glial and neuronal proteins respectively, several previous experiments have established that both murine and human MSCs express neural proteins both while resident in the BM stroma and in culture, before any neural differentiation has occurred. We also observed this pattern of expression in our mMSCs. Thus, we were not surprised to see positive expression of GFAP and MAP2 for our canine cells. However, these results indicate that expression of these two proteins will not be a reliable measure of neural differentiation to use for cMSCs.

4. Discussion

In addition to the experiments covered in this chapter, our laboratory has done additional work in an effort to characterize occurrences of NCL in several breeds of canine. As a result of this work and work in other laboratories, we currently know the genes responsible for the NCL phenotype in four dog models of NCL. These are Border Collies (*CLN5*), American Bulldogs (*Cathepsin D*), Dachshund (*TPP1*) and English Setters (*CLN8*). [173][174][169][8] The results we report here have eliminated one candidate gene for the cause of NCL in Tibetan Terriers (the canine *TPP1* gene) and further experiments are being performed in conjunction with our collaborators to map the location of the affected gene.

We also reported on our progress in culturing canine MSCs for future experiments evaluating their effectiveness as a therapy in a dog model of NCL. Moving from mice to dogs for some experiments has several benefits, most of which originate in the size differences between the two models. Because we are working with MSCs which we hope will take up residence in tissue and cross-correct other cells in the area, it is important to know how far cells will travel after implantation and how many cells are necessary to treat a given volume of tissue. Because variables such as protein diffusion, cellular motility and enzymatic absorption do not scale with the size of the host, the use of a small animal model, like a mouse, does not always give results which are completely translatable to human patients. In this case, size does matter. The murine eye is, on average, less than 3mm in diameter (~2.1µl), about one tenth the size of a human eye. A canine eye, on the other hand, is much closer to the size of a human eye (~60-70% by volume, depending upon the breed). If a single injection is performed into the vitreal space of a murine eye, the injected cells have a very short distance to travel in order to disperse across the whole retina. In a human eye, the distance could be 10 times larger. We would obviously inject a higher number of cells into a larger eye, but if the cells are still implanted with a single injection, the distance the cells would have to travel from the injection site to cover the entire retina is much larger. The same holds true of intravenous or intracranial transplantation. In both cases, the increase in size when transferring the procedure from mice to humans may not be entirely compensated for by simply increasing the number of cells used. In addition to making transplant procedures into the bone marrow, eye, brain and circulatory system technically easier, having an animal model of intermediate size will allow us to more closely evaluate the impact of the size of the transplanted host and develop means of adjusting our treatment to maximize its effectiveness in human patients.

Another benefit, for our intraocular transplants, of utilizing the dog model is that the eyesight and retinal function is physiologically much more similar between dogs and humans than between mice and humans. Mice are primarily nocturnal animals and their retina has adapted to this lifestyle. Rodent retinas are dominated by rod photoreceptors. In addition, rodents are known to

be far-sighted (also an adaptation to nocturnal vision). [175] While canine retinal function is not identical to humans, their visual acuity and light perception abilities are much more comparable, which will allow us to achieve greater specificity in our measurements of the effect of MSC transplant on retinal function in NCL-affected animals.

The canine model we plan to use for future MSC therapy experiments (the TPP1-deficient Dachshund model) has already been well characterized by other people in our laboratory. [169] We show here that we can isolate MSCs from both affected and unaffected dogs of this breed and that these MSCs are similar in many respects (as measured by growth rate, morphology and expression of certain proteins) to the MSCs we isolated from mice. We also report that canine MSCs appear to move under their own power in adherent culture toward areas of higher cell density. This may be related to the ability of MSCs to express trophic factors, which often act as or are accompanied by expression of chemotactic factors as well. The stronger growth characteristics of MSCs at higher densities may also be related to this phenomenon. Future experiments will focus on characterizing these canine cells by FACScan analysis, immunohistochemistry and differentiation toward specific cell types, including osteocytes, adipocytes, glia and neurons. In addition, we plan to eventually use these cells for intraocular and intramarrow transplant experiments in the Dachshund model of LINCL.

References

1. Bennett, M. and S. Hofmann, *The neuronal ceroid lipofuscinoses (Batten disease): A new class of lysosomal storage diseases.* Journal of Inherited Metabolic Diseases, 1999. **22**: p. 535-544.

2. Hosain, S., *et al.*, *Diagnoses of neuronal ceroid lipofuscinosis by immunochemical methods.* American Journal of Medical Genetics, 1995. **57**: p. 239-245.

3. Cooper, J.D., *Progress towards understanding the neurobiology of Batten disease or neuronal ceroid lipofuscinosis.* Current Opinion in Neurology, 2003. **16**: p. 121-128.

4. Jolly, R., R. Martinus, and D. Palmer, *Sheep and other animals with ceroid lipofuscinosis: Their relevance to Batten disease.* American Journal of Medical Genetics, 1992. **42**: p. 609-614.

5. Junaid, M.A., G. Wu, and R.K. Pullarkat, *Purification and characterization of bovine brain lysosomal pepstatin-insensitive proteinase, the gene product deficient in the human late-infantile neuronal ceroid lipofuscinosis.* Journal of Neurochemistry, 2000. **74**: p. 287-294.

6. Bronson, R., *et al.*, *Neuronal ceroid lipofuscinosis (ncl), a new disorder of the mouse linked to chromosome 9.* American Journal of Medical Genetics, 1998. **77**: p. 289-297.

7. Chang, B., *et al.*, *Retinal degeneration in motor neuron degeneration: A mouse model of ceroid lipofuscinosis.* Investigative Ophthalmology and Visual Science, 1994. **35**(3): p. 1071-1076.

8. Katz, M.L., *et al.*, *A mutation in the CLN8 gene in English Setter dogs with neuronal ceroid-lipofuscinosis.* Biochemical and Biophysical Research Communications, 2005. **327**: p. 541-547.

9. Katz, M.L., *et al.*, *Assessment of retinal function and characterization of lysosomal storage body accumulation in the retinas and brains of Tibetan Terriers with ceroid-lipofuscinosis.* American Journal of Veterinary Research, 2005. **66**(1): p. 67-76.

10. Riis, R., *et al.*, *Tibetan terrier model of canine ceroid lipofuscinosis.* American Journal of Medical Genetics, 1992. **42**: p. 615-621.

11. Lake, B.D., *et al.*, *Bone marrow transplantation in Batten disease (neuronal ceroid lipofuscinosis). Will it work? Preliminary studies on coculture experiments and on bone marrow transplant in late infantile batten disease.* American Journal of Medical Genetics, 1995. **57**: p. 369-373.

12. Santavuori, P. and T. Westermarck, *Antioxidant therapy in neuronal ceroid lipofuscinosis.* Medical Biology, 1984. **62**: p. 152-153.

13. Westlake, V.J., *et al.*, *Hematopoietic cell transplantation in fetal lambs with ceroid lipofuscinosis.* American Journal of Medical Genetics, 1995. **57**: p. 365-368.

14. Griffey, M., *et al.*, *Adeno-associated virus 2-mediated gene therapy decreases autofluorescent storage material and increase brain mass in a murine model of infantile neuronal ceroid lipofuscinosis.* Neurobiology of Disease, 2004. **16**: p. 360-369.

15. Taupin, P. and F.H. Gage, *Adult neurogenesis and neural stem cells of the central nervous system in mammals.* Journal of Neuroscience Research, 2002. **69**: p. 745-749.

16. Hughes, S., *Cardiac stem cells.* Journal of Pathology, 2002. **197**: p. 468-478.

17. Johnson, J., *et al.*, *Germ line stem cells and follicular renewal in the postnatal mammalian ovary.* Nature, 2004. **428**: p. 145-1062.

18. Grove, J.E., E. Bruscia, and D.S. Krause, *Plasticity of bone marrow-derived stem cells.* Stem Cells, 2004. **22**: p. 487-500.

19. Bjornson, C.R., *et al.*, *Turning brain into blood: A hematopoietic fate adopted by adult neural stem cells in vivo.* Science, 1999. **283**: p. 534-537.

20. Tondreau, T., *et al.*, *Bone marrow-derived mesenchymal stem cells already express specific neural proteins before any differentiation.* International Society of Differentiation, 2004. **72**: p. 319-326.

21. Pacary, E., *et al.*, *Synergistic effects of CoCL2 and Rock inhibition on mesenchymal stem cell differentiation into neuron-like cells.* Journal of Cell Science, 2006. **119**: p. 2667-2678.

22. Mezey, E., *et al.*, *Transplanted bone marrow generates new neurons in human brains.* PNAS, 2003. **100**(3): p. 1364-1369.

23. Blondheim, N.R., *et al.*, *Human mesenchymal stem cells express neural genes, suggesting a neural predisposition.* Stem Cells and Development, 2006. **15**(2006): p. 141-164.

24. Pierret, C., *et al.*, *Neural crest as the source of adult stem cells.* Stem Cells and Development, 2006. **15**(2006): p. 286-291.

25. Labat, M.L., *et al.*, *On the track of a human circulating mesenchymal stem cell of neural crest origin.* Biomedicine and Pharmacotherapy, 2000. **54**: p. 146-62.

26. Crane, J.F. and P.A. Trainor, *Neural crest stem and progenitor cells.* Annual Review of Cell Developmental Biology, 2006. **22**: p. 267-286.

27. Zhang, J., *et al.*, *Identification of hematopoietic stem cell niche and control of the niche size.* Nature, 2003. **425**: p. 836-841.

28. Moore, K.A. and I.R. Lemischka, *Stem cells and their niches.* Science, 2006. **311**: p. 1880-1885.

29. Kolf, C.M., E. Cho, and R.S. Tuan, *Biology of adult mesenchymal stem cells: regulation of niche, self-renewal and differentiation.* Arthritis Research & Therapy, 2007. **9**(1): p. 204-214.

30. Yin, T. and L. Li, *The stem cell niches in bone.* The Journal of Clinical Investigation, 2006. **116**(5): p. 1195-1201.

31. Potten, C.S., *et al.*, *Identification of a putative intestinal stem cell and early lineage marker; musashi-1.* Differentiation, 2003. **71**: p. 78-41.

32. Cotsarelis, G., T.-t. Sun, and R.M. Lavker, *Label-retaining cells reside in the bulge area of pilosebaceous unit: Implications for follicular stem cells, hair cycle, and skin carcinogenesis.* Cell, 1990. **61**: p. 1329-1337.

33. Tondreau, T., *et al.*, *Mesenchymal stem cells derived from CD133-positive cells in mobilized peripheral blood and cord blood: Proliferation, Oct4 expression and plasticity.* Stem Cells, 2005. **23**: p. 1105-1112.

34. Kuznetsov, S.A., *et al.*, *Circulating skeletal stem cells.* The Journal of Cell Biology, 2001. **153**(5): p. 1133-1193.

35. Neuss, S., *et al.*, *Functional expression of HGF and HGF receptor/c-met in adult human mesenchymal stem cells suggests a role in cell mobilization, tissue repair and wound healing.* Stem Cells, 2004. **22**(2005): p. 405-414.

36. Becker, A., E. McCulloch, and J. Till, *Cytological demonstration of the clonal nature of spleen colonies derived from transplanted mouse marrow cells.* Nature, 1963. **197**: p. 452-454.

37. Friedenstein, A., *et al.*, *Precursors for fibroblasts in different populations of hematopoietic cells as detected by the in vitro colony assay method.* Experimental Hematology, 1974. **2**(2): p. 83-92.

38. Gronthos, S., *et al.*, *Molecular and cellular characterization of highly purified stromal stem cells derived from human bone marrow.* Journal of Cell Science, 2003. **116**: p. 1827-1835.

39. Pochampally, R.R., *et al.*, *Serum deprivation of human marrow stromal cells (hMSCs) selects for a subpopulation of early progenitor cells with enhanced expression of OCT-4 and other embryonic genes.* Blood, 2004. **103**(5): p. 1647-1652.

40. Battula, V.L., *et al.*, *Human placenta and bone marrow derived MSC cultured in serum-free, b-FGF-containing medium express cell surface frizzled-9 and SSEA-4 and give rise to multilineage differentiation.* Differentiation, 2007. **75**: p. 279-291.

41. Lee, R.H., *et al.*, *A subset of human rapidly self-renewing marrow stromal cells preferentially engraft in mice.* Blood, 2006. **107**(5): p. 2153-2161.

42. Gang, E.J., *et al.*, *SSEA-4 identifies mesenchymal stem cells from bone marrow.* Blood, 2007. **109**: p. 1743-1751.

43. Jiang, Y., *et al.*, *Pluripotency of mesenchymal stem cells derived form adult marrow.* Nature, 2002. **418**: p. 41-49.

44. Lagar'kova, M.A., *et al.*, *Characteristics of human bone marrow mesenchymal stem cells isolated by immunomagnetic selection.* Cell Technologies in Biology and Medicine, 2006. **2**(1): p. 3-7.

45. Reyes, M. and C.M. Verfaillie, *Characterization of multipotent adult progenitor cells, a subpopulation of mesenchymal stem cells.* Journal of Neuroscience, 2004. **24**(47): p. 10642-102651.

46. Schrepfer, S., *et al.*, *Simplified protocol to isolate, purify and culture expand mesenchymal stem cells.* Stem Cells and Development, 2007. **16**: p. 105-107.

47. Baddoo, M., *et al.*, *Characterization of mesenchymal stem cells isolated from murine bone marrow by negative selection.* Journal of Cellular Biochemistry, 2003. **89**(2003): p. 1235-1249.

48. Horwitz, E.M., *et al.*, *Transplantability and the therapeutic effects of bone marrow-derived mesenchymal cells in children with osteogenesis imperfecta.* Nature Medicine, 1999. **5**(3): p. 309-313.

49. Horwitz, E.M., *et al.*, *Isolated allogeneic bone marrow-derived mesenchymal cells engraft and stimulate growth in children with osteogenesis imperfecta: Implications for cell therapy of bone.* PNAS, 2002. **99**(13): p. 8932-8937.

50. USDRS, U.S.R.D.S., *2006 ADR Reference Tables.* www.usrds.org/reference.htm, 2006.

51. St. Peter, W.L., *et al.*, *Chronic kidney disease: The distribution of health care dollars.* Kidney International, 2004. **66**: p. 313-321.

52. American Heart Association., *Heart disease and stroke statistics - 2007 update: A report from the American Heart Association Statistics Committee and Stroke Statistics Subcommittee.* Circulation, 2007. **115**: p. 69-171.

53. Morigi, M., *et al.*, *Mesenchymal stem cells are renotropic, helping to repair the kidney and improve function in acute renal failure.* Journal of the American Society of Nephrology, 2004. **15**: p. 1794-1804.

54. Zimmermann, W.-H., *et al.*, *Engineered heart tissue graft improve systolic and diastolic function in infracted rat hearts.* Nature Medicine, 2006. **12**(4): p. 452-458.

55. Miyahara, Y., *et al.*, *Monolayered mesenchymal stem cells repair scarred myocardium after myocardial infraction.* Nature Medicine, 2006. **12**(4): p. 459-465.

56. Minguell, J.J. and E. Alejandro, *Mesenchymal stem cells and the treatment of cardiac disease.* Experimental Biology and Medicine, 2006. **231**: p. 39-49.

57. Fukuda, K. and J. Fujita, *Mesenchymal, but not hematopoietic, stem cells can be mobilized and differentiate into cardiomyocytes after myocardial infarction in mice.* International Society Of Nephrology, 2005. **68**(2005): p. 1940-1943.

58. Sasaki, M., *et al.*, *Transplantation of an acutely isolated bone marrow fraction repairs demyelinated adult rat spinal cord axons.* Glia, 2001. **35**: p. 26-34.

59. Tohill, M., *et al.*, *Rat bone marrow mesenchymal stem cells express glial markers and stimulate nerve regeneration.* Neuroscience Letters, 2004. **362**: p. 200-203.

60. Coronel, M.F., L. Musolino, and M.J. Villar, *Selective migration and engraftment of bone marrow mesenchymal stem cells in rat lumber dorsal root ganglia after sciatic nerve constriction.* Neuroscience Letters, 2006. **405**(2006): p. 5-9.

61. Munoz-Elias, G., *et al.*, *Adult bone marrow stromal cells in the embryonic brain: Engraftment, migration, differentiation and long-term survival.* The Journal of Neuroscience, 2004. **24**(19): p. 4585-4595.

62. Lu, D., *et al.*, *Adult bone marrow stromal cells administered intravenously to rats after traumatic brain injury migrate into brain and improve neurological outcome.* NeuoReport, 2001. **12**(3): p. 559-563.

63. Zhao, L.-R., *et al.*, *Human bone marrow stem cells exhibit neural phenotypes and ameliorate neurological deficits after grafting into the ischemic brain of rats.* Experimental Neurology, 2002. **174**: p. 11-20.

64. Jin, H.K., *et al.*, *Intracerebral transplantation of mesenchymal stem cells into acid sphingomyelinase-deficient mice delays the onset of neurological abnormalities and extends their life span.* The Journal of Clinical Investigation, 2002. **109**(9): p. 1183-1191.

65. Jin, H.-K. and E.H. Schuchman, *Ex vivo gene therapy using bone marrow-derived cells: Combined effects of intracerebral and intravenous transplantation in a mouse model of Niemann-Pick disease.* Molecular Therapy, 2003. **8**(6): p. 876-881.

66. Bae, J.-s., *et al.*, *Neurodegeneration augments the ability of bone marrow-derived mesenchymal stem cells to fuse with Purkinje neurons in Niemann-Pick type c mice.* Human Gene Therapy., 2005. **16**(2005): p. 1006-1011.

67. Sakurai, K., *et al.*, *Brain transplantation of genetically modified bone marrow stromal cells corrects CNS Pathology and cognitive function in MPS VII mice.* Gene Therapy, 2004. **11**: p. 1475-1481.

68. Hellmann, M.A., *et al.*, *Increase survival and migration of engrafted mesenchymal bone marrow stem cells in 6-hydroxydopamine-lesiones rodents.* Neuroscience Letters, 2002. **395**(2006): p. 124-128.

69. Koc, O.N., *et al.*, *Allogeneic mesenchymal stem cell infusion for treatment of metachromatic leukodystrophy (MLD) and Hurler syndrome (MPS-IH).* Bone Marrow Transplantation, 2002. **30**: p. 215-222.

70. Kicic, A., *et al.*, *Differentiation of marrow stromal cells into photoreceptors in the rat eye.* The Journal of Neuroscience, 2003. **23**(21): p. 7742-7749.

71. Tomita, M., *et al.*, *Bone marrow-derived stem cells can differentiate into retinal cells in injured rat retina.* Stem Cells, 2002. **20**: p. 279-283.

72. Thorpe, S., Porteous, *Optimising gene repair strategies in cell culture.* Gene Therapy, 2002. **9**: p. 700-702.

73. Gruenert, B., Novelli, Colosimo, Dallapiccola, Sangiuolo, Goncz, *Sequence-specific modification of genomic DNA by small DNA fragments.* The Journal of Clinical Investigation, 2003. **112**(5): p. 637-641.

74. Parekh-Olmedo, H., D. Krainc, and E.B. Kmiec, *Targeted gene repair and its application to neurodegenerative disorders.* Neuron, 2002. **33**: p. 495-498.

75. Colosimo, A., *et al.*, *Targeted correction of a defective selectable marker gene in human epithelial cells by small DNA fragments.* Molecular Therapy, 2001. **3**(2): p. 178-184.

76. Tsuchiya, H., H. Harashima, and H. Kamiya, *Factors affecting SFHR gene correction efficiency with single-stranded DNA fragment.* Biochemical and Biophysical Research Communications, 2005. **336**: p. 1194-1200.

77. Goncz, K., *et al.*, *Targeted replacement of normal and mutant CFTR sequences in human airway epithelial cells using DNA fragments.* Human Molecular Genetics, 1998. **7**(12): p. 1913-1919.

78. Goncz, K., *et al.*, *Expression of ΔF508 CFTR in normal mouse lung after site-specific modification of CFTR sequences by SFHR.* Gene Therapy, 2001. **8**: p. 961-965.

79. Sangiuolo, F., *et al.*, *In vitro restoration of functional SMN protein in human trophoblast cells affected by spinal muscular atrophy by small fragment homologous replacement.* Human Gene Therapy, 2005. **16**: p. 869-880.

80. Zayed, H., *et al.*, *In vitro functional correction of the mutation responsible for murine severe combined immune deficiency by small fragment homologous replacement.* Human Gene Therapy, 2006. **17**: p. 158-166.

81. Kapsa, Q., Vadolas, Steeper, Ioannou, Byrne, Kornberg, *Targeted gene correction in the mdx mouse using short DNA fragments: towards application with bone marrow-derived cells for autologous remodeling of dystrophic muscle.* Gene Therapy, 2002. **9**: p. 695-699.

82. Dezawa, M., M. Hishino, and C. Ide, *Treatment of neurodegenerative diseases using adult bone marrow stromal cell-derived neurons.* Expert Opinion on Biological Therapy, 2005. **5**(4): p. 427-435.

83. Tang, Y.L., *et al.*, *Paracrine action enhances the effects of autologous mesenchymal stem cell transplantation on vascular regeneration in rat model of myocardial infarction.* Annals of Thoracic Surgery, 2005. **80**: p. 229-237.

84. Liu, C.H. and S.H. Hwang, *Cytokine interactions in mesenchymal stem cells from cord blood.* Cytokine, 2005. **32**(6): p. 270-279.

85. Gregory, C.A., J. Ylostalo, and P.D. J., *Adult bone marrow stem/progenitor cells (MSCs) are preconditioned by microenvironmental "niches" in culture: A two-stage hypothesis for regulation of MSC fate.* Science, 2005. **294**: p. 1-4.

86. Martin, M.J., *et al.*, *Human embryonic stem cells express an immunogenic nonhuman sialic acid.* Nature Medicine, 2005. **11**(2): p. 228-232.

87. Stute, N., *et al.*, *Autologous serum for isolation and expansion of human mesenchymal stem cells for clinical use.* Experimental Hematology, 2004. **32**: p. 1212-1225.

88. Meuleman, N., *et al.*, *Human marrow mesenchymal stem cell culture: serum-free medium allows better expansion than classical alpha-MEM medium.* European Journal of Haematology, 2006. **76**: p. 309-316.

89. Blixt, Y., *Exchange of the cellular growth medium supplement from fetal bovine serum to Ultroser G increases the affinity of adenovirus for HeLa cells.* Archives of Virology, 1993. **129**: p. 251-263.

90. Aggarwal, S. and M.F. Pittenger, *Human mesenchymal stem cells modulate allogeneic immune cell responses.* Blood, 2005. **105**(4): p. 1815-1822.

91. Stroms, R.W., *et al.*, *Isolation of primitive human hematopoietic progenitors on the basis of aldehyde dehydrogenase activity.* Cell Biology, 1999. **96**: p. 9118-9123.

92. Wislet-Gendebien, S., *et al.*, *Regulation of neural markers Nestin and GFAP expression by cultivated bone marrow stromal cells.* Journal of Cell Science, 2003. **116**: p. 3295-3302.

93. Epiting, C.L., *et al.*, *Stem cell antigen-1 necessary for cell-cycle withdrawal and myoblast differentiation in C2C12 cells.* Journal of Cell Science, 2004. **117**: p. 6185-6195.

94. Wilson, A., *et al.*, *c-Myc controls the balance between hematopoietic stem cell self-renewal and differentiation.* Genes & Development, 2004. **18**: p. 2747-2763.

95. Guo, Y., M. Lubbert, and M. Engelhardt, *CD34 hematopoietic stem cells: Current concepts and controversies.* Stem Cells, 2003. **21**: p. 15-20.

96. Choong, M.L., B. Luo, and H.F. Lodish, *Microenvironment-driven changes in the expression profile of haematopoietic cobblestone area-forming cells.* Annals of Hematology, 2004. **83**: p. 160-169.

97. Woodbury, D., K. Reynolds, and I.B. Black, *Adult bone marrow stroma stem cells express germ line, ectodermal, endodermal and mesodermal genes prior to neurogenesis.* Journal of Neuroscience Research, 2002. **96**(2002): p. 908-917.

98. Beck, H.N., *et al.*, *Bone morphogenetic protein-5 (BMP-5) promotes dendritic growth in cultured sympathetic neurons.* BMC Neuroscience, 2001. **2**: p. 1471-2202.

99. Barry, F., *et al.*, *The SH-3 and SH-4 antibodies recognize distinct epitopes on CD73 from human mesenchymal stem cells.* Biochemical and Biophysical Research communications, 2001. **289**: p. 519-524.

100. Bianco, P. and P.G. Robey, *Marrow stromal stem cells.* The Journal of Clinical Investigation, 2000. **105**(12): p. 1663-1668.

101. Phinney, D.G., *et al.*, *Plastic adherent stromal cells from the bone marrow of commonly used strains of inbred mice: Variations in yield, growth and differentiation.* Journal of Cellular Biochemistry, 1999. **72**(1999): p. 570-585.

102. Wislet-Gendebien, S., *et al.*, *Nestin-positive mesenchymal stem cells favour the astroglial lineage in neural progenitors and stem cells by releasing active BMP4.* BMC Neuroscience, 2004. **5**(33): p. 1-12.

103. Zeng, Z., *et al.*, *Manipulation of proliferation and differentiation of human bone marrow-derived neural stem cells in vitro and in vivo.* Journal of Neuroscience Research, 2007. **85**: p. 310-320.

104. Minguell, J.J., A. Ericers, and P. Conget, *Mesenchymal stem cells.* Experimental Biology and Medicine, 2001. **226**(6): p. 507-520.

105. Scintu, F., *et al.*, *Differentiation of human bone marrow stem cells into cells with a neural phenotype: Diverse effects of two specific treatments.* BMC Neuroscience, 2006. **7**(14): p. 1-12.

106. Potten, C.S., G. Owen, and D. Booth, *Intestinal stem cells protect their genome by selective segregation of template DNA strands.* Journal of Cell Science, 2002. **115**: p. 2381-2388.

107. Bentwich, I., *et al.*, *Identification of hundreds of conserved and nonconserved human microRNAs.* Nature Genetics, 2005. **37**(7): p. 766-770.

108. Alarcon, C.M., M. Pedram, and J.E. Donelson, *Leaky transcription of variant surface glycoprotein gene expression sites in bloodstream African trypanosomes.* Journal of Biological Chemistry, 1999. **274**(24): p. 16884-16893.

109. Peister, A., *et al.*, *Adult stem cells from bone marrow (MSCs) isolated from different strains of inbred mice vary in surface epitopes, rates of proliferation, and differentiation potential.* Gene Therapy, 2004. **103**(5): p. 1662-1668.

110. Woodbury, D., *et al.*, *Adult rat and human bone marrow stromal cells differentiate into neurons.* Journal of Neuroscience Research, 2000. **61**: p. 364-370.

111. Sanchez-Ramos, J., *et al.*, *Adult bone marrow stroma cells differentiate into neural cells in vitro.* Experimental Neurology, 2000. **164**: p. 247-256.

112. Song, H., C.F. Stevens, and F.H. Gage, *Astroglia induce neurogenesis from adult neural stem cells.* Nature, 2002. **417**: p. 39-44.

113. Joannides, A., *et al.*, *Postnatal astrocytes promote neural induction from adult human bone marrow-derived stem cells.* Journal of Hematotherapy and Stem Cell Research, 2003. **12**(6): p. 681-688.

114. Chen, Y., F.Y.H. Teng, and T. B.L., *Coaxing bone marrow stromal mesenchymal stem cells toward neuronal differentiation : progress and uncertainties.* Cellular and Molecular Life Sciences, 2006. **63**(2006): p. 1649-1657.

115. Bertani, N., *et al.*, *Neurogenic potential of human mesenchymal stem cells revisited: analysis by immunostaining, timelapse video and microarray.* Journal of Cell Science, 2005. **118**(3925-3936).

116. Neuhuber, B., *et al.*, *Reevaluation of in vitro differentiation protocols for bone marrow stromal cells: disruption of actin cytoskeleton induces rapid morphological changes and mimics neuronal phenotype.* Journal of Neuroscience Research, 2004. **77**(192-204).

117. Lu, P., A. Blesch, and M.H. Tuszynski, *Induction of bone marrow stromal cells to neurons: differentiation, transdifferentiation or artifact?* Journal of Neuroscience Research, 2004. **77**: p. 174-191.

118. Benninger, F., *et al.*, *Functional integration of embryonic stem cell-derived neurons in hippocampal slice cultures.* The Journal of Neuroscience, 2003. **23**(18): p. 1075-1083.

119. Hung, S.H., *et al.*, *In vitro differentiation of size-sieved stem cells into electrically active neural cells.* Stem Cells, 2002. **20**: p. 522-529.

120. Kohyama, J., *et al.*, *Brain from bone: efficient 'meta-differentiation' of marrow stroma-derived mature osteoblasts to neurons with Noggin or a demethylating agent.* Differentiation, 2001. **68**: p. 235-244.

121. Locatelli, F., *et al.*, *Neuronal differentiation of murine bone marrow Thy-1 and Sca-1 positive cells.* Journal of Hematotherapy and Stem Cell Research, 2003. **12**: p. 727-734.

122. Hermann, A., *et al.*, *Efficient generation of neural stem cell-like cells from adult human bone marrow stromal cells.* Journal of Cell Science, 2004. **117**: p. 4411-4422.

123. Qian, L. and W.M. Saltzman, *Improving the expansion and neuronal differentiation of mesenchymal stem cells through culture surface modification.* Biomaterials, 2003. **25**(2004): p. 1331-1337.

124. Zyuz'kov, G.N., *et al.*, *Role of stem cells in adaptation of hypoxia and mechanisms of neuroprotective effects of granulocytic colony-stimulating factor.* Cell Technology in Biology and Medicine, 2005. **1**(4): p. 606-611.

125. Martin, B.J. and M.F. Pitterger, *Mesenchymal stem cells and their potential as cardiac therapeutics.* Circulation Research, 2004. **95**: p. 9-20.

126. Baxter, M.A., *et al.*, *Retrovirally mediated correction of bone marrow- derived mesenchymal stem cells from patients with mucopolysaccharidosis type I.* Blood, 2002. **99**(5): p. 1857-1859.

127. Oshima, Y., *et al.*, *Behavior of transplanted bone marrow-derived GFP mesenchymal cells in osteochondral defect as a simulation of autologous transplantation.* Journal of Histochemistry & Cytochemistry, 2005. **53**(2): p. 207-216.

128. Zhang, X.-Y., V.F. La Russa, and J. Reiser, *Transduction of bone marrow-derived mesenchymal stem cells by using Lentivirus vectors pseudotyped with modified RD114 envelope glycoproteins.* Journal of Virology, 2004. **78**(3): p. 1219–1229.

129. Aluigi, M., *et al.*, *Nucleofection is an efficient nonviral transfection technique for human bone marrow-derived mesenchymal stem cells.* Stem Cells, 2006. **24**(2): p. 454-461.

130. Peister, A., *et al.*, *Stable transfection of MSCs by electroporation.* Gene Therapy, 2004. **11**: p. 224-228.

131. Haltia, M., *The neuronal ceroid lipofuscinoses.* Journal of Neuropathology and Experimental Neurology, 2003. **62**(1): p. 1-13.

132. Mole, S.E., H.M. Mitchison, and P.B. Munroe, *Molecular basis of the neuronal ceroid lipofuscinoses: Mutations in CLN1, CLN2, CLN3 and CLN5.* Human Mutation, 1999. **14**: p. 199-215.

133. Mole, S.E., *The genetic spectrum of human neuronal ceroid lipofuscinoses.* Brain Pathology, 2004. **14**: p. 70-76.

134. Kapsa, R., *et al.*, *In vivo and in vitro correction of the mdx dystrophin gene nonsense mutation by short-fragment homologous replacement.* Human Gene Therapy, 2001. **12**: p. 629-642.

135. Tsuchiya, H., H. Harashima, and H. Kamiya, *Increased SFHR gene correction efficiency with sense single-stranded DNA.* The Journal of Gene Medicine, 2005. **7**: p. 486-493.

136. Ohlemiller, K., *et al.*, *Retinal function is improved in a murine model of a lysosomal storage disease following bone marrow transplantation.* Experimental Eye Research, 2000. **71**: p. 469-481.

137. Grove, J.E., *et al.*, *Marrow-derived cells as a vehicle for delivery of gene therapy to pulmonary epithelium.* Cell Mol. Bio., 2002. **27**: p. 645-651.

138. Shihabuddin, L.S., *et al.*, *Intracerebral transplantation of adult mouse neural progenitors cells into the Niemann-Pick-S mouse leads to a marked decrease in lysosomal storage pathology.* The Journal of Neuroscience, 2004. **24**(47): p. 10642-10651.

139. Kinnaird, T., *et al.*, *Marrow-derived stromal cells express genes encoding a broad spectrum of arteriogenic cytokines and promote in vitro and in vivo arteriogenesis through paracrine mechanisms.* Circulation Research, 2004. **94**: p. 678-685.

140. Haynesworth, S.E., M.A. Baber, and A.I. Caplan, *Cytokine expression by human marrow-derived mesenchymal progenitor cells in vitro: effects of dexamethasone and IL-1a.* Journal of Cellular Physiology, 1996. **166**: p. 585-592.

141. Caplan, A.I. and J.E. Dennis, *Mesenchymal stem cells as trophic mediators.* Journal of Cellular Biochemistry, 2006. **98**: p. 1076-1084.

142. Silva, W.A., *et al.*, *The profile of gene expression of human marrow mesenchymal stem cells.* Stem Cells, 2003. **21**: p. 661-669.

143. Crigler, L., *et al.*, *Human mesenchymal stem cell subpopulations express a variety of neuro-regulatory molecules and promote neuronal cell survival and neuritogeneis.* Experimental Neurology, 2006. **198**: p. 54-64.

144. Pittenger, M.F. and M.B. J., *Mesenchymal stem cells and their potential as cardiac therapeutics.* Circulation Research, 2004. **95**: p. 9-20.

145. Zhao, R.C., L. Lio, and Q. Han, *Mechanisms of and perspectives on the mesenchymal stem cell in immunotherapy.* Journal of Laboratory and Clinical Medicine, 2004. **143**(5): p. 284-291.

146. Dazzi, F., *et al.*, *The role of mesenchymal stem cells in haemopoiesis.* Blood Reviews, 2005. **20**(2006): p. 161-171.

147. Gupta, P., *et al.*, *Disruption of PPT1 or PPT2 causes neuronal ceroid lipofuscinosis in knockout mice.* PNAS, 2001. **98**(24): p. 13566-13571.

148. Lei, B., *et al.*, *Ocular phenotype in a mouse gene knockout model for infantile neuronal ceroid lipofuscinosis.* Journal of Neuroscience Research, 2006. **84**: p. 1139-1149.

149. Wendt, K.D., *et al.*, *Behavioral assessment in mouse models of neuronal ceroid lipofuscinosis using a light-cued T-maze.* Behavioral Brain Research, 2005. **161**: p. 175-182.

150. Alers, J.C., *et al.*, *Effect of bone decalcification procedures on DNA in situ hybridization and comparative genomic hybridization. EDTA is highly preferable to a routinely used acid decalcifier.* Journal of Histochemistry & Cytochemistry, 1999. **47**(5): p. 703-710.

151. Yamamoto-Fukud, T., *et al.*, *Effects of various decalcification protocols on detection of DNA strand breaks by terminal dUTP nick end labeling.* Histochemical Journal, 2000. **32**(11): p. 697-702.

152. Meyer, J.S., *et al.*, *Embryonic stem cell-derived neural progenitors incorporate into degenerating retina and enhance survival of host photoreceptors.* Stem Cells, 2006. **24**: p. 274-283.

153. Beck, M., *New therapeutic options for lysosomal storage disorders: enzyme replacement, small molecules and gene therapy.* Human Genetics, 2007. **121**(1): p. 1-22.

154. Uruyama, A., *et al.*, *Developmentally regulated mannose 6-phosphate receptor-mediated transport of a lysosomal enzyme across the blood-brain barrier.* Proceedings of the National Academy of Sciences, 2004. **101**(34): p. 12658-12663.

155. Hara, H., *et al.*, *Limited engraftment capacity of bone marrow-derived mesenchymal cells in xenogeneic bone marrow transplantation.* Transplantation Proceedings, 2003. **35**: p. 504-505.

156. Koc, O.N., *et al.*, *Bone marrow-derived mesenchymal stem cells remain host-derived despite successful hematopoietic engraftment after allogeneic transplantation in patients with lysosomal and peroxisomal storage diseases.* Experimental Hematology, 1999. **27**(1999): p. 1675-1681.

157. Devine, S.M., *Mesenchymal stem cells: Will they have a role in the clinic.* Journal of Cellular Biochemistry Supplement, 2002. **38**: p. 38-73.

158. Devine, S.M., *et al.*, *Mesenchymal stem cells distribute to a wide range of tissues following systemic infusion into nonhuman primates.* The American Society of Hematology, 2003. **101**(8): p. 2999-3001.

159. Van Marion, A.M.W., *et al.*, *Morphology of bone marrow after stem cell transplantation.* Histopathology, 2006. **48**: p. 329-342.

160. Ikehara, S., *Intra-bone marrow-bone marrow transplantation: A new strategy for treatment of stem cell disorders.* Annals of the New York Academy of Sciences ., 2005. **1051**: p. 626-634.

161. Muguruma, Y., *et al.*, *Reconstruction of the function of human hematopoietic microenvironment derived from human mesenchymal stem cells in the murine bone marrow compartment.* Blood, 2006. **107**(5): p. 1878-1887.

162. Descamps, F.J., *et al.*, *Gelatinase B/matrix metalloproteinase-9 provokes cataracts by cleaving lens BB1 crystallin.* FASEB Journal, 2004. **19**: p. 29-35.

163. Fruehauf, S., T. Seeger, and J. Topaly, *Innovative strategies for PBPC mobilization.* Cyotherapy, 2005. **7**(5): p. 438-446.

164. Vila, C., *et al.*, *Multiple and ancient origins of the domestic dog.* Science, 1997. **276**: p. 1687-1689.

165. Ostrander, E.A. and E. Giniger, *Semper Fidelis: What man's best friend can teach us about human biology and disease.* American Journal of Human Genetics, 1997. **61**: p. 475-480.

166. Breen, M., *et al.*, *Chromosome-specific single-locus FISH probes allow anchorage of an 1800-marker integrated radiation-hybrid/linkage map of the domestic dog genome to all chromosomes.* Genome Research, 2001. **11**: p. 1784-1795.

167. Kirchhoff, C., *The dog as a model to study human epididymal function at a molecular level.* Molecular Human Reproduction, 2002. **8**(8): p. 695-701.

168. Haines, J.L., *et al.*, *Genome-wide search for CLN2, the gene causing late-infantile neuronal ceroid lipofuscinosis (LINCL).* American Journal of Medical Genetics, 1995. **57**: p. 344-347.

169. Awano, T., *et al.*, *A frame shift mutation in canine TPP1 (the ortholog of human CLN2) in a juvenile dachshund with neuronal ceroid lipofuscinosis.* Molecular Genetics and Metabolism, 2006. **89**: p. 254-260.

170. Koppang, N., *English Setter model and juvenile ceroid lipofuscinosis in man.* American Journal of Medical Genetics, 1992. **42**: p. 599-604.

171. Golabek, A.A., *et al.*, *Maturation of human tripeptidyl-peptidase 1 in vitro.* The Journal of Biological Chemistry, 2004. **279**(30): p. 31058-31067.

172. Pearson, A.G., *et al.*, *Activating transcription factor 2 expression in the adult human brain: Association with both neurodegeneration and neurogenesis.* Neuroscience, 2005. **133**: p. 437-451.

173. Melville, S.A., *et al.*, *A mutation in canine CLN5 causes neuronal ceroid lipofuscinosis in Border collie dogs.* Genomics, 2005. **86**(3): p. 287-294.

174. Evans, J., *et al.*, *A variant form of neuronal ceroid lipofuscinosis in American bulldogs.* Journal of Veterinary Internal Medicine, 2005. **19**(1): p. 44-51.

175. Jeon, C.-J., E. Strettoi, and R.H. Masland, *The major cell populations of the mouse retina.* Journal of Neuroscience, 1998. **18**(21): p. 8936-8946.

176. Kim, S-J., Zhang, Z., Hitomi, E., Lee, Y-C., Mukherjee, A.B., *Endoplasmic reticulum stress-induced caspase-4 activation mediates apoptosis and neurodegeneration in INCL.* Human Molecular Genetics, 2006. **15**(11): p. 1826-1834.

177. Siakotos, A., Blair, P., Savill, J., Katz, M., *Altered mitochondrial function in canine ceroid-lipofuscinosis.* Neurochemical Research, 1998. **23**(7): p. 983-989.

178. Wisniewski, K., Kaczmarski, W., Golabek, A., Kida, E., *Rapid detection of subunit c of mitochondrial ATP synthase in urine as a diagnostic screening method for neuronal ceroid lipofuscinoses.* American Journal of Medical Genetics, 1995. **57**(2): p. 246-249.

179. Siintola, E., Topcu, M., Aula, N., Lohi, H., Minassian, BA., Paterson, AD., Liu, X-Q., Wilson, C., Lahtinen, U., Anttonen, A-K., Lehesjoki, A-E., *The novel neuronal ceroid lipofuscinosis gene MFSD8 encodes a putative lysosomal transporter.* American Journal of Human Genetics, 2007. **81**: p.136-146.

180. Steinfeld, R., Reinhardt, K., Schreiber, K., Hillebrand, M., Kraetzner, R., Bruck, W., Saftig, P., Gartner, J., *Cathepsin D deficiency is associated with a human neurodegenerative disorder.* American Journal of Human Genetics, 2006. **78**: p. 988-998.

181. Siintola, E., Lehesjoki, A-E., Mole, SE., *Molecular genetics of the NCLs – status and perspectives.* Biochimica et Biophysica Acta, 2006. **1762**: p.857-864.

182. Heine, C., Quitsch, A., Storch, S., Martin, Y., Lonka, L., Lehesjoki, A-E., Mole, SE., Braulke, T., *Topology and endoplasmic reticulum retention signals of the lysosomal storage disease-related membrane protein CLN6.* Molecular Membrane Biology, 2007. **24**(1): p. 74-87.

183. Lonka, L., Aalto, A., Kopra, O., Kuronen, M., Kokaia, Z., Saarma, M., Lehesjoki, A-E., *The neuronal ceroid lipofuscinosis Cln8 gene expression is developmentally regulated in mouse brain and up-regulated in the hippocampal kindling model of epilepsy.* BMC Neuroscience, 2005. **6**(1): p. 27-38.

184. Mole, SE., Michaux, G., Codlin, S., Wheeler, R., Sharp, J., Cutler, D., *CLN6, which is associated with a lysosomal storage disease, is an endoplasmic reticulum protein.* Experimental Cell Research, 2004. **298**: p. 399-406.

Appendix I: pPNT Vector Information

The following is a letter from the creator of the pPNT vector issued to several labs requesting information about the vector and its construction.

October 1995

Gene targeters:

A couple of years ago I compiled the sequences of the PGKneo and PGKtk cassettes that make up pPNT [ref: Tybulewicz et al. Cell vol 65 p1153- 1163 (1991)]. This compilation contained quite a bit of unpublished sequence data and vector construction info that I got from a number of labs (the PGK promoter and terminator sequences that are in GenBank contain errors). At any rate, there were a number of requests for copies of it so I ended up e-mailing it out to a bunch of knock-out labs. For practical purposes this document is now kind of generic in form in that it contains the sequence of pPNT, the sequences of 2 additional pPNT based vectors: pPN2T [ref: Paszty et al. Nature Genetics vol 11 p33-39 (1995)] and pPN2T-hGHterm [ref: Zhu et al. Blood vol 93 p2404-2410 (1999)], as well as some general things to keep in mind when deciding on a targeting strategy and when building targeting vectors. Please pass this document on to any interested colleagues.

Chris Paszty, Ph.D.
Human Genome Center
Lawrence Berkeley Laboratory
Berkeley, CA 94720...U.S.A.

Address as of February 1998
Amgen Inc.
Dept. of Molecular Genetics
One Amgen Center, MS 14-1-B
Thousand Oaks, CA 91320-1789
U.S.A.
tel: (805) 447-2082
fax: (805) 447-1982
e-mail: cpaszty@amgen.com

Some general info:

pPNT is a pUC/Bluescript based vector.

The most effective way to use pPNT and pPNT-derivatives is to clone the short arm (1-2 kb) in-between the PGKneo cassette and the PGKtk cassette, and then to clone the long arm (6-11 kb) in-between the other side of the PGKneo cassette (PGK promoter side) and the unique Not I site. For electroporation the resulting targeting vector can then be linearized at the unique Not I site.

In an effort to increase the effectiveness of positive-negative selection I've introduced a second same orientation PGKtk cassette into the single HindIII site of pPNT to create pPN2T. The apparent negative selection enrichment obtained with an alpha globin targeting vector (pPN2T-alphaKO) based on pPN2T was 3-5 fold higher than that obtained with a variety of different single PGKtk based targeting vectors that had been electroporated and selected under identical conditions as those used for pPN2T-alphaKO ie. same lab, same E.S. cells, same feeder cells, same reagents and same protocols. Although this has not been rigorously tested it is likely that the additional PGKtk cassette present in pPN2T-alphaKO is responsible for the high apparent enrichment values obtained with this targeting vector.

Creating a null allele knock-out for small genes is usually not too difficult as one can just delete the whole gene or most of it to guarantee achieving complete loss of gene function. However, for larger genes, particularly those who's genomic structure has not been well mapped out, creating this type of whole gene deletion can be time consuming and difficult. The targeting strategy we've been using for such large genes is to create as extensive a deletion as is practical in the 5' region of the gene. The deletion is designed so as to include the presumed translational initiator codon and at least 1 kb of sequence upstream from the ATG in an effort to delete the promoter and thereby shut down transcription. Permanently shutting down transcription is an extremely effective way to achieve complete loss of gene function. In situations where transcription isn't shut down and a full length but mutated mRNA is produced one runs the risk that the mutagenic (translational stop codons in 3 frames etc...) neo cassette might be removed by normal or alternative splicing pathways. This may result in a "leaky" mutation rather than a null mutation or, even worse, a dominant negative mutation. Because some genes have multiple promoters which may be quite a distance upstream of the ATG, deleting a 1 kb region upstream of the ATG, even if it does inactivate one of the promoters, might not cause a complete shut down of transcription. An additional "tool" for shutting down transcription is transcriptional termination. For this reason it is desirable to end up with a targeting event that results in the insertion of a polyA-signal/terminator in the same orientation as the transcription of the gene in question. For pPNT and pPN2T if one's long arm is 5' of one's short arm within the gene to be inactivated then the structure of the final targeting event puts the PGKneo cassette in the same transcriptional orientation as that of the gene's. In this case, transcripts originating from the gene's promoter(s) will terminate at the PGK polyA-signal/terminator that is part of the PGKneo cassette. This leaves any downstream exons untranscribed and thus increases the probability of creating a null allele. However, for pPNT and pPN2T, if one's short arm is 5' of one's long arm within the gene to be inactivated then the structure of the final targeting event will put the PGKneo cassette in reverse transcriptional orientation with respect to that of the gene's. Thus the extra protection against the production of a "leaky" allele that is afforded by the premature termination of any transcripts originating from the gene's promoter(s) is lost. To retain the feature of transcriptional termination for this configuration of long and short arms we've introduced the polyA-signal/terminator from the human growth hormone N gene into pPN2T to create pPN2T-hGHterm. Although this is a human and not a murine polyA-signal/terminator, it is highly homologous to other mammalian growth hormone polyA-signal/terminators, has been extensively used in adenovirus based gene therapy vectors in mice and thus should work well for terminating transcription at a targeted locus.

The standard null allele type knock-out is usually the most straight forward to generate, however other approaches that should be considered are: 1) The inclusion of a reporter gene, such as lacZ (for example: Le Mouellic et al 1992 Cell vol 69, p246-251; Mountford et al 1994 PNAS vol 91 p4303-4307) in one's targeting vector. This allows one to examine the spatial and temporal pattern of gene expression of the targeted gene and also to follow cell fate. 2) A conditional knock-out using Cre-loxP (Gu et al 1994 Science vol 265 p103-106; Kuhn et al 1995 Science vol 269, p1427-1429) and/or FLP-frt (Fiering et al 1995 Genes and Development vol 9, p2203-2213). Cell fate can also be followed using these recombinase systems.

Other variations on the basic knock-out theme will undoubtedly be developed in the future, so it's wise to check the latest literature. The particular approach one decides on is based on what information one is interested in, as well as how much of a hurry one is in. The standard null allele type is still the simplest and quickest to make. For many genes a fair amount of information can be gotten from a null allele knock-out. If one is still intrigued then a subsequent fancier knock-out can be generated.

Reference points for the pPNT sequence (bprs):

- bp7-23 T3 promoter in pBluescript SK(+)
- bp54-61 Single NotI site in pPNT
- bp71-78 Single Sse8387I site in pPNT
- bp81-587 EcoRI(destroyed)-TaqI fragment of PGK-1 promoter
- bp589-1418 PstI-HinclI(destroyed) neo gene containing frag from pKJ1DB (derived from pKJ1 which was derived from pMC1neo).
- bp600-602 Neo^r start codon
- bp1401-1403 Neo^r stop codon
- bp1419-1883 PvuII(destroyed)-HindIII(filled) frag of PGK-1 terminator
- bp1914-1919 Single EcoRI site in pPNT
- bp1914-2421 EcoRI-TaqI fragment of PGK-1 promoter
- bp2423-4253 PstI-PvuII(destroyed) frag from HSV-1 containing the tk gene.
- bp2519-2521 HSVtk start codon
- bp3647-3649 HSVtk stop codon
- bp4257-4714 PstI-HindIII fragment of PGK-1 terminator
- bp4714-7348 pUC18/Bluescript SK+ vector backbone

pPNT sequence:

```
BASE COUNT    1578 a   2058 c   2010 g   1702 t    0 others

        1 gctcgaaatt aaccctcact aaagggaaca aaagctggag ctccaccgcg gtggcggccg
       61 ctcgagggcc cctgcaggtc aattctaccg ggtaggggag gcgcttttcc caaggcagtc
      121 tggagcatgc gctttagcag ccccgctggc acttggcgct acacaagtgg cctctggcct
      181 cgcacacatt ccacatccac cggtagcgcc aaccggctcc gttctttggt ggccccttcg
      241 cgccaccttc tactcctccc ctagtcagga agttcccccc cgccccgcag ctcgcgtcgt
      301 gcaggacgtg acaaatggaa gtagcacgtc tcactagtct cgtgcagatg gacagcaccg
      361 ctgagcaatg gaagcgggta ggcctttggg gcagcggcca atagcagctt tgctccttcg
      421 ctttctgggc tcagaggctg ggaaggggtg ggtccggggg cgggctcagg ggcgggctca
      481 ggggcggggc gggcgcgaag gtcctcccga ggcccggcat tctcgcacgc ttcaaaagcg
      541 cacgtctgcc gcgctgttct cctcttcctc atctccgggc ctttcgacct gcagccaata
      601 tgggatcggc cattgaacaa gatggattgc acgcaggttc tccggccgct tgggtggaga
      661 ggctattcgg ctatgactgg gcacaacaga caatcggctg ctctgatgcc gccgtgttcc
      721 ggctgtcagc gcaggggcgc ccggttcttt ttgtcaagac cgacctgtcc ggtgccctga
      781 atgaactgca ggacgaggca gcgcggctat cgtggctggc cacgacgggc gttccttgcg
      841 cagctgtgct cgacgttgtc actgaagcgg gaagggactg gctgctattg ggcgaagtgc
      901 cggggcagga tctcctgtca tctcaccttg ctcctgccga gaaagtatcc atcatggctg
      961 atgcaatgcg gcggctgcat acgcttgatc cggctacctg cccattcgac caccaagcga
     1021 aacatcgcat cgagcgagca cgtactcgga tggaagccgg tcttgtcgat caggatgatc
     1081 tggacgaaga gcatcagggg ctcgcgccag ccgaactgtt cgccaggctc aaggcgcgca
     1141 tgcccgacgg cgatgatctc gtcgtgaccc atggcgatgc ctgcttgccg aatatcatgg
     1201 tggaaaatgg ccgcttttct ggattcatcg actgtggccg gctgggtgtg gcggaccgct
     1261 atcaggacat agcgttggct acccgtgata ttgctgaaga gcttggcggc gaatgggctg
     1321 accgcttcct cgtgctttac ggtatcgccg ctcccgattc gcagcgcatc gccttctatc
     1381 gccttcttga cgagttcttc tgaggggatc gatccgtcct gtaagtctgc agaaattgat
     1441 gatctattaa acaataaaga tgtccactaa aatggaagtt tttcctgtca tactttgtta
     1501 agaagggtga gaacagagta cctacatttt gaatggaagg attggagcta cgggggtggg
     1561 ggtggggtgg gattagataa atgcctgctc tttactgaag gctctttact attgctttat
     1621 gataatgttt catagttgga tatcataatt taaacaagca aaaccaaatt aagggccagc
     1681 tcattcctcc cactcatgat ctatagatct atagatctct cgtgggatca ttgtttttct
     1741 cttgattccc actttgtggt tctaagtact gtggtttcca aatgtgtcag tttcatagcc
     1801 tgaagaacga gatcagcagc ctctgttcca catacacttc attctcagta ttgttttgcc
     1861 aagttctaat tccatcagaa gctgactcta gaggatcccc gggtaccgag ctcgaattct
     1921 accgggtagg ggaggcgctt ttcccaaggc agtctggagc atgcgcttta gcagccccgc
     1981 tggcacttgg cgctacacaa gtggcctctg gcctcgcaca cattccacat ccaccggtag
     2041 cgccaaccgg ctccgttctt tggtggcccc ttcgcgccac cttctactcc tcccctagtc
     2101 aggaagttcc cccccgcccc gcagctcgcg tcgtgcagga cgtgacaaat ggaagtagca
```

2161 cgtctcacta gtctcgtgca gatggacagc accgctgagc aatggaagcg ggtaggcctt
2221 tggggcagcg gccaatagca gctttgctcc ttcgctttct gggctcagag gctgggaagg
2281 ggtgggtccg ggggcgggct caggggcggg ctcaggggcg gggcgggcgc gaaggtcctc
2341 ccgaggcccg gcattctcgc acgcttcaaa agcgcacgtc tgccgcgctg ttctcctctt
2401 cctcatctcc gggcctttcg acctgcagcg acccgcttaa cagcgtcaac agcgtgccgc
2461 agatcttggt ggcgtgaaac tcccgcacct cttcggccag cgccttgtag aagcgcgtat
2521 ggcttcgtac ccctgccatc aacacgcgtc tgcgttcgac caggctgcgc gttctcgcgg
2581 ccataacaac cgacgtacgg cgttgcgccc tcgccggcaa caaaaagcca cggaagtccg
2641 cctggagcag aaaatgccca cgctactgcg ggtttatata gacggtcccc acgggatggg
2701 gaaaaccacc accacgcaac tgctggtggc cctgggttcg cgcgacgata tcgtctacgt
2761 acccgagccg atgacttact ggcgggtgtt gggggcttcc gagacaatcg cgaacatcta
2821 caccacacaa caccgcctcg accagggtga gatatcggcc ggggacgcgg cggtggtaat
2881 gacaagcgcc cagataacaa tgggcatgcc ttatgccgtg accgacgccg ttctggctcc
2941 tcatatcggg ggggaggctg ggagctcaca tgccccgccc ccggccctca ccctcatctt
3001 cgaccgccat cccatcgccg ccctcctgtg ctacccggcc gcgcgatacc ttatgggcag
3061 catgaccccc caggccgtgc tggcgttcgt ggccctcatc ccgccgacct tgcccggcac
3121 aaacatcgtg ttgggggccc ttccggagga cagacacatc gaccgcctgg ccaaacgcca
3181 gcgccccggc gagcggcttg acctggctat gctggccgcg attcgccgcg tttatgggct
3241 gcttgccaat acggtgcggt atctgcaggg cggcgggtcg tggcgggagg attggggaca
3301 gctttcgggg gcggccgtgc cgccccaggg tgccgagccc cagagcaacg cgggcccacg
3361 accccatatc ggggacacgt tatttaccct gtttcgggcc cccgagttgc tggcccccaa
3421 cggcgacctg tataacgtgt ttgcctgggc tttggacgtc ttggccaaac gcctccgtcc
3481 catgcatgtc tttatcctgg attacgacca atcgcccgcc ggctgccggg acgccctgct
3541 gcaacttacc tccgggatgg tccagaccca cgtcaccacc ccaggctcca taccgacgat
3601 ctgcgacctg gcgcgcacgt ttgcccggga gatgggggag gctaactgaa acacggaagg
3661 agacaatacc ggaaggaacc cgcgctatga cggcaataaa aagacagaat aaaacgcacg
3721 ggtgttgggt cgtttgttca taaacgcggg gttcggtccc agggctggca ctctgtcgat
3781 accccaccga gaccccattg ggaccaatac gcccgcgttt cttccttttc cccaccccaa
3841 cccccaagtt cgggtgaagg cccagggctc gcagccaacg tcggggcggc aagccctgcc
3901 atagccacgg gccccgtggg ttagggacgg ggtcccccat ggggaatggt ttatggttcg
3961 tgggggttat tattttgggc gttgcgtggg gtcaggtcca cgactggact gagcagacag
4021 acccatggtt tttggatggc ctgggcatgg accgcatgta ctggcgcgac acgaacaccg
4081 ggcgtctgtg gctgccaaac acccccgacc cccaaaaacc accgcgcgga tttctggcgc
4141 cgccggacga actaaacctg actacggcat ctctgccccc tcttcgctgg tacgaggagc
4201 gcttttgttt tgtattggtc accacggccg agtttccgcg ggaccccggc caggacctgc
4261 agaaattgat gatctattaa acaataaaga tgtccactaa aatggaagtt tttcctgtca
4321 tactttgtta agaagggtga gaacagagta cctacatttt gaatggaagg attggagcta
4381 cgggggtggg ggtggggtgg gattagataa atgcctgctc tttactgaag gctctttact
4441 attgctttat gataatgttt catagttgga tatcataatt taaacaagca aaaccaaatt
4501 aagggccagc tcattcctcc cactcatgat ctatagatct atagatctct cgtgggatca
4561 ttgtttttct cttgattccc actttgtggt tctaagtact gtggtttcca aatgtgtcag
4621 tttcatagcc tgaagaacga gatcagcagc ctctgttcca catacacttc attctcagta
4681 ttgttttgcc aagttctaat tccatcagaa gcttggcact ggccgtcgtt ttacaacgtc
4741 gtgactggga aaaccctggc gttacccaac ttaatcgcct tgcagcacat ccccctttcg
4801 ccagctggcg taatagcgaa gaggcccgca ccgatcgccc ttcccaacag ttgcgcagcc
4861 tgaatggcga atggcgcctg atgcggtatt ttctccttac gcatctgtgc ggtatttcac
4921 accgcatatg gtgcactctc agtacaatct gctctgatgc cgcatagtta agccagcccc
4981 gacacccgcc aacacccgct gacgcgccct gacgggcttg tctgctcccg gcatccgctt
5041 acagacaagc tgtgaccgtc tccgggagct gcatgtgtca gaggttttca ccgtcatcac
5101 cgaaacgcgc gagacgaaag ggcctcgtga tacgcctatt tttataggtt aatgtcatga
5161 taataatggt ttcttagacg tcaggtggca cttttcgggg aaatgtgcgc ggaacccCta
5221 tttgtttatt tttctaaata cattcaaata tgtatccgct catgagacaa taaccctgat
5281 aaatgcttca ataatattga aaaaggaaga gtatgagtat tcaacatttc cgtgtcgccc
5341 ttattccctt ttttgcggca ttttgccttc ctgtttttgc tcacccagaa acgctggtga
5401 aagtaaaaga tgctgaagat cagttgggtg cacgagtggg ttacatcgaa ctggatctca
5461 acagcggtaa gatccttgag agttttcgcc ccgaagaacg ttttccaatg atgagcactt
5521 ttaaagttct gctatgtggc gcggtattat cccgtattga cgccgggcaa gagcaactcg
5581 gtcgccgcat acactattct cagaatgact tggttgagta ctcaccagtc acagaaaagc
5641 atcttacgga tggcatgaca gtaagagaat tatgcagtgc tgccataacc atgagtgata
5701 acactgcggc caacttactt ctgacaacga tcggaggacc gaaggagcta accgcttttt
5761 tgcacaacat gggggatcat gtaactcgcc ttgatcgttg ggaaccggag ctgaatgaag
5821 ccataccaaa cgacgagcgt gacaccacga tgcctgtagc aatggcaaca acgttgcgca
5881 aactattaac tggcgaacta cttactctag cttcccggca acaattaata gactggatgg

```
5941 aggcggataa agttgcagga ccacttctgc gctcggccct tccggctggc tggtttattg
6001 ctgataaatc tggagccggt gagcgtgggt ctcgcggtat cattgcagca ctggggccag
6061 atggtaagcc ctcccgtatc gtagttatct acacgacggg gagtcaggca actatggatg
6121 aacgaaatag acagatcgct gagataggtg cctcactgat taagcattgg taactgtcag
6181 accaagttta ctcatatata ctttagattg atttaaaact tcatttttaa tttaaaagga
6241 tctaggtgaa gatccttttt gataatctca tgaccaaaat cccttaacgt gagttttcgt
6301 tccactgagc gtcagacccc gtagaaaaga tcaaaggatc ttcttgagat cctttttttc
6361 tgcgcgtaat ctgctgcttg caaacaaaaa aaccaccgct accagcggtg gtttgtttgc
6421 cggatcaaga gctaccaact ctttttccga aggtaactgg cttcagcaga gcgcagatac
6481 caaatactgt ccttctagtg tagccgtagt taggccacca cttcaagaac tctgtagcac
6541 cgcctacata cctcgctctg ctaatcctgt taccagtggc tgctgccagt ggcgataagt
6601 cgtgtcttac cgggttggac tcaagacgat agttaccgga taaggcgcag cggtcgggct
6661 gaacgggggg ttcgtgcaca gcccagct tggagcgaac gacctacacc gaactgagat
6721 acctacagcg tgagctatga gaaagcgcca cgcttcccga agggagaaag gcggacaggt
6781 atccggtaag cggcagggtc ggaacaggag agcgcacgag ggagcttcca gggggaaacg
6841 cctggtatct ttatagtcct gtcgggtttc gccacctctg acttgagcgt cgatttttgt
6901 gatgctcgtc agggggggcgg agcctatgga aaaacgccag caacgcggcc tttttacggt
6961 tcctggcctt ttgctggcct tttgctcaca tgttctttcc tgcgttatcc cctgattctg
7021 tggataaccg tattaccgcc tttgagtgag ctgataccgc tcgccgcagc cgaacgaccg
7081 agcgcagcga gtcagtgagc gaggaagcgg aagagcgccc aatacgcaaa ccgcctctcc
7141 ccgcgcgttg gccgattcat taatgcagct ggcacgacag gtttcccgac tggaaagcgg
7201 gcagtgagcg caacgcaatt aatgtgagtt agctcactca ttaggcaccc caggctttac
7261 actttatgct tccggctcgt atgttgtgtg gaattgtgag cggataacaa tttcacacag
7321 gaaacagcta tgaccatgat tacgccaa
```

For additional information, see:

Tybulewicz, V. L. J., C. E. Crawford, et al. (1991). "*Neonatal lethality and lymphopenia in mice with a homozygous disruption of the c-abl proto-oncogene*." Cell **65**(7): 1153-1163.

Appendix II

Canine NCL Questionnaire

CANINE NCL- DNA RESEARCH Breed _____
Individual Dog Information Family ID code:_____
Blood – Tissue – other _____

Registered Name _____ Call name _____

Reg# _____ Birth Date _____ Sex? M – F Neutered/Spayed? Y – N

Sample Submission Date: _____ Color _____

Sample submitted for which research project? ____**Neuronal Ceroid Lipofuscinosis**_____

Owner: name _____ breeder's name _____

address _____ address _____

_____ _____

phone (day) _____ phone _____

phone (eve) _____ _____

fax _____ _____

e-mail _____ e-mail _____

Does this dog exhibit any of the following conditions? (*Please attach history for any Yes answer*)

Y - N Allergies
Y – NArthritis
Y - N Autoimmune Disorders
Y - N Bite or Tooth Abnormalities
Y - N Cancer / Tumors
Y - N Cataracts / Vision Problems
Y - N Deafness / Hearing Impaired
other (please list):

Y - N Digestive difficulties
Y - N Heart Problems
Y - N Hernia (where? _____)
Y - N Reproductive Problems
Y - N Seizures
Y - N Skin / Coat Problems
Y - N Skeletal Abnormalities (Hip Dysplasia, etc.)
Y - N Temperament Problems (shy, aggressive, etc.)

Testing done on this dog:

OFA/PennHip Y - N age at test: _____ result:_____ #_____

CERF Y - N age last tested:_____ result:_____
#_____

Thyroid Y - N age last tested:_____ result:_____

other (please list):

ATTACH PEDIGREE COPY TO THIS FORM

Please circle your response to the following;

- I am / am not willing to provide additional blood samples if needed for research.

- I will / will not consider donation of a tissue sample upon the death of this dog, and will discuss this decision with my veterinarian so that a notation is placed in my file.

I submit this sample and pedigree for the purpose of DNA research; I understand that the identity of dogs and owners participating in the research will not be revealed; and I have supplied complete and accurate information, to the best of my knowledge.

Signed: _____ date _____

Canine NCL-specific Questionaire

Has this dog been diagnosed as likely to be affected with NCL? Yes No

Have any relatives of this dog been diagnosed with NCL? Yes No Don't Know
If yes, which relatives? Sire Dam Sibling Offspring Other _____
Paternal Grandsire Paternal Grand-dam Maternal Grandsire Maternal Grand-dam

When is the best time to reach you by phone? _____

Veterinary Contact Information

Primary Care
Vet Name _____
Clinic Name _____
Address _____
City,St,Zip _____
Phone # _____

Ophthalmologist
Name _____
Clinic Name _____
Address _____
City,St,Zip _____
Phone # _____

Neurologist
Vet Name _____
Clinic Name _____
Address _____
City,St,Zip _____
Phone # _____

Other Specialist
Name _____
Clinic Name _____
Address _____
City,St,Zip _____
Phone # _____

May we have your permission to contact your veterinarians to request records and discuss your dog's health history, diagnostic testing, and possible treatment options? Yes No

Signed: _____ date: _____

Behavior and Activity survey follows – please complete for all sampled dogs

CHANGES IN *BEHAVIOR*
Compare this dog's current behavior to its earlier behavior. Please circle the correct answer.
If you need additional space to describe changes, please use back of form or attach additional pages.

Changes	**Normal** - or - **Degree of Change**				**Describe**
1. Housetraining	normal	mild	moderate	severe	_____
2. Interest in food (eating habits)	normal	mild	moderate	severe	_____
3. Appears nervous	normal	mild	moderate	severe	_____
4. Interaction/socialization with other dogs	normal	mild	moderate	severe	_____
5. Aggressiveness to other dogs	normal	mild	moderate	severe	_____
6. Aggressiveness to people	normal	mild	moderate	severe	_____
7. Tolerance to grooming or bathing	normal	mild	moderate	severe	_____
8. Tolerance to being alone	normal	mild	moderate	severe	_____
9. Ability to recognize/respond to commands	normal	mild	moderate	severe	_____
10. Ability to recognize or respond to name	normal	mild	moderate	severe	_____
11. Recognizes you or other familiar people	normal	mild	moderate	severe	_____
13. Responses to noise/loud sounds	normal	mild	moderate	severe	_____
14. Development of compulsive behavior	normal	mild	moderate	severe	_____
15. Circling	normal	mild	moderate	severe	_____
16. Wakes you more at night	normal	mild	moderate	severe	_____
17. Inappropriate or persistent vocalization	normal	mild	moderate	severe	_____

CHANGES IN *PHYSICAL ACTIVITY*

Compare this dog's current physical activity to its earlier activity and ability. Please circle the option that best describes the change observed in the relevant behavior. If you need additional space to describe changes, please use back of form or attach additional pages.

Changes	**Normal** - or - **Degree of Change**				**Describe**
18. Climbing up or down stairs	normal	mild	moderate	severe	_____
19. Tremors or shaking	normal	mild	moderate	severe	_____
20. Seizures	normal	mild	moderate	severe	_____
21. Increased stiffness or weakness	normal	mild	moderate	severe	_____
22. Difficulty in movement or coordination	normal	mild	moderate	severe	_____
23. Changes in posture ("roached" back)	normal	mild	moderate	severe	_____
24. Tail carriage when alert & interested	normal	mild	moderate	severe	_____
25. Ability to see during the day	normal	mild	moderate	severe	_____
26. Ability to see at night in dim light	normal	mild	moderate	severe	_____
27. Head movements	normal	mild	moderate	severe	_____
28. Trance-like behavior	normal	mild	moderate	severe	_____
29. Bumps into objects, clumsy	normal	mild	moderate	severe	_____

Please describe any other health problems or behavioral abnormalities:

_____

_____

_____

VITA

Douglas Newton Sanders was born on November 11, 1973 in Nevada, Missouri. He graduated from the University of Missouri – Columbia with a B.S. in Biological Sciences in 1997 and entered the Ph.D. graduate program at UMC in the Molecular Microbiology & Immunology department in fall of the same year. After completing his comprehensive exams he transferred to the Pathobiology Area Program at UMC in 2000, supervised by Dr. Martin L. Katz in the University Hospital's Ophthalmology department. He earned a Ph.D. in Pathobiology in August of 2007.